L O N D O N U N I V E R S I T Y

CITY AND GUILDS COLLEGE

Interface Problems at Dielectric Discontinuities in Wave Guides.

Thesis presented for the Ph.D. Degree in Electrical Engineering.

by

Robert E. Collin.

November, 1953.

Acknowledgement

The author wishes to acknowledge his indebtedness to Professor Willis Jackson, F.R.S. for providing the facilities for this work in his department. Many thanks are also due to Mr. John Brown of this department for numerous valuable suggestions and general guidance regarding this work.

Thanks are also given to the British Government for the award of an Athlone Fellowship which enabled the author to study in this country. The author would like also to acknowledge the financial assistance awarded him by the Canadian Defence Research Board for the completion of this work.

Abstract

This thesis is primarily concerned with the theoretical evaluation of the parameters of the equivalent circuit used to represent the discontinuity effect existing at the junction between an empty and an inhomogenously filled rectangular wave guide, followed by an application of the results to the design of quarter-wave matching sections. The input admittance and impedance at the junction are obtained from variational expressions. These variational expressions are shown to be equivalent to minimizing the volume integral of the difference between the stored magnetic and electric energy at the junction. After developing the basic theory required it is applied to specific problems. Thus in chapters 4 and 5 the H-plane and E-plane dielectric step discontinuities are discussed. Chapter 6 begins with a discussion of the properties of ideal quarter-wave transformers. The analysis of their properties is carried considerably further than has been done before. In particular it is shown that by a suitable choice of parameters it is possible to make the reflection coefficient go to zero at as many different frequencies as there are quarter-wave sections. As these zeros coalesce together at one frequency the resulting transformer so obtained is the usual binomial transformer. With the above more general design a considerable increase in bandwidth is obtained. A detailed design procedure and performance curves for the optimum bandwidth two section transformer are included. This is followed by an analysis of the H-plane dielectric step transformers in a rectangular wave guide. Theoretical and experimental bandwidth curves are given.

Chapter 7 is devoted to the design of a free space to dielectric matching section for matching a plane dielectric surface to free space.

During this work on dielectric interface discontinuities a new type of phase changer was developed. The outstanding feature of this phase changer is its linear characteristics. This phase changer is fully discussed in the concluding chapter and design data and performance curves are given.

Contents

		Page
Chapter 1 -	Introduction	1
Chapter 2 -	Basic Theory	
2.1 -	Orthogonality conditions and expandibility of fields	7
2.2 -	Variational principle for the electromagnetic field	13
2.3 -	Relation between junction admittance and stored reactive energy	16
2.4 -	Variational expressions for junction admittance and impedance	19
2.5 -	Approximation to the aperture fields	25
2.6 -	Application of the Ritz method	29
2.7 -	The equivalent circuit	32
Chapter 3 -	Experimental Technique	
3.1 -	Description of apparatus	34
3.2 -	Method of measurement	35
3.3 -	Equivalent circuit of a symmetrical structure	38
Chapter 4 -	H-Plane Dielectric Step Discontinuities	
4.1 -	The asymmetrical step	42
4.2 -	Numerical work	48
4.3 -	The symmetrical step	58
4.4 -	Numerical work	61
Chapter 5 -	E-Plane Dielectric Step in a Rectangular Wave Guide	
5.1 -	Theoretical solution	66
5.2 -	Numerical work	73
Chapter 6 -	Properties of Quarter-Wave Transformers	
6.1 -	Ideal transformers	79
6.2 -	Single section quarter-wave transformer	80
6.3 -	Two section quarter-wave transformer	81
6.4 -	Design procedure and universal bandwidth curves	87
6.5 -	The three section transformer	91
6.6 -	H-plane dielectric step transformers in a rectangular wave guide	99

		Page
Chapter 7 -	Free Space Matching Section	
7.1 -	Theoretical solution	111
7.2 -	Numerical work	115
7.3 -	Experimental work	118
Chapter 8 -	A Rectangular Wave Guide Phase Changer	
8.1 -	Theory	124
8.2 -	Errors	128
8.3 -	A Working Model	131
Appendix 1 -	A Note on Weisafloch's Method for Finding Equivalent Circuits.	
Appendix 2 -	Some Properties of Expansions in terms of Complete sets of Orthonormal Functions.	
Appendix 3 -	Application of the Ritz Method for Finding the Approximate Eigenvalues and Eigenfunctions.	
Appendix 4 -	Solutions of the Wave Equation when Guide Wavelength equals Free Space Wavelength.	
Appendix 5 -	Theoretical solution for E-plane dielectric step.	
Bibliography :		

CHAPTER 1.

Introduction

Inhomogenously filled waveguides have been used quite extensively both for laboratory equipment and for practical applications. However there seems to be little or no available published literature on the discontinuity effects existing at the junction between an empty guide and an inhomogenously filled guide. To date there is no general method of obtaining a rigorous solution in closed form for this type of boundary value problem so one must be content with approximate solutions.

Variational methods have been used a great deal by mathematical physicists to obtain very good approximation to solutions of the Schrödinger wave equation and also to nuclear and other scattering problems. During the last decade these methods have been carried over into the field of electromagnetic scattering and diffraction problems. J. Schwinger has used variational methods for the solution of a wide range of waveguide problems and several other workers have followed in his footsteps (1.1, 1.2, 1.3, 1.4)* The type of problems considered by the above authors were usually of the metallic discontinuity type. For such problems the fields are expanded into a series consisting of the normal modes that can be excited in the empty guide. These modes are relatively easy to work with since they satisfy simple orthogonality conditions and by suitable approximation can be summed in a closed form in several cases. For inhomogenously filled guides none

* (The bracketed numbers refer to references collected together at the end of the thesis.)

of the field components for two distinct modes are in general orthogonal. However ny means of a more general orthogonality relation it is still possible to expand an arbitrary field into a series consisting of the proper modes existing in the inhomogenously filled guide. The number of available modes must of course form a complete set. This will be discussed in greater detail in chapter two.

Previous authors have used variational methods purely as a mathematical tool for the solution of a given problem with no physical interpretation of the principles involved. In this thesis it is shown that the variational expression set up for the junction admittance between an empty and an inhomogenously filled guide is equivalent to minimizing the volume integral of the difference between the magnetic and electric energy stored in the higher order modes at the junction. If the magnetic energy exceeds the electric energy the junction is considered as inductive and as capacitive if the stored electric energy is the greater. It should be noted that evanescent H modes store more magnetic energy while evanescent E modes store an excess of electric energy. Thus a knowledge of the type of modes excited determines whether a junction is inductive or capacitive. The presence of stored reactive energy causes a phase change in the transmitted and reflected waves at the junction. In general there is also a change in impedance level at the junction.

The behaviour of a waveguide discontinuity is most conveniently expressed by means of an equivalent lumped electric circuit. The waveguide is replaced by transmission lines and the discontinuity by

a four terminal network. Although this equivalent circuit does not have the usual frequency dependence it does give all the required information needed about the propagating mode at any one frequency. If more than one mode propagates then one transmission line is introduced for each propagating mode. (1.5.) From a consideration of the effect of the higher order modes it is readily seen that a very natural equivalent circuit for a lossless structure is two lengths of transmission line connected together by an ideal transformer. The two lengths of transmission line represents the phase shift produced in the transmitted and reflected waves while the transformer takes care of any change in impedance level. Furthermore the parameters of this circuit are readily obtained experimentally. A full discussion of this equivalent circuit will be found in appendix 1.

The input impedance at any point on the axis in the waveguide is taken as the ratio of the transverse electric field to the transverse magnetic field. An arbitrary load impedance in the output guide is transformed into an equivalent impedance in the input guide. This impedance transformation can be expressed as a bilinear transformation with three arbitrary constants. Thus

$$Z_{in} = \frac{a Z_L + b}{c Z_L + d}$$

where a, b, c, and d are the parameters of the transformation and Z_L is the load impedance. For a guide with no intervening discontinuity the above transformation reduces to the usual transmission line formula for the input impedance of a load Z_L seen through a length of

transmission line. By a proper choice of the constants this transformation can be reduced to the form $Z_{in} = N^2 Z_L$ where N^2 is a real quantity. This corresponds to a suitable choice of reference planes at one of which Z_{in} is measured and to the other of which Z_L is referred. These two reference planes are called the characteristic planes and have the property that an arbitrary impedance Z_L located at one plane is transformed by a real quantity N^2 to an impedance $N^2 Z_L$ at the other plane. That these characteristic planes exist follows from an inspection of the equivalent circuit analysed in appendix 1, since referring Z_{in} and Z_L to these planes reduces the equivalent circuit to an ideal transformer which has the above transformation property. If the constants c and b are zero in the above transformation one set of characteristic planes is obtained. Another set is obtained by choosing a and d to be zero since this reduces the transformation to

$$Z_{in} = \frac{b}{c} \frac{1}{Z_L}$$

and Z_{in} or Z_L can be referred to a plane a quarter of a wavelength further along the guide since a quarter wave transformer inverts the impedance with respect to the characteristic impedance of the line squared, thus $Z_{in}' = \frac{c}{b} Z_1^2 Z_L$ or $\frac{b}{c} Z_2^2 Z_L$.

In the above discussion it was assumed that the discontinuity was lossless. This type of equivalent circuit is used throughout this work on the junction admittance existing between an empty and an inhomogenously filled guide.

The great utility of the variational method comes from the stationary nature of the junction admittance with respect to any first order variations of the aperture fields. The junction admittance is correct to the second order for an assumed aperture field distribution correct to only the first order. Furthermore by terminating the output guide in a short circuit an analytical expression for Weissfloch's technique of obtaining the equivalent circuit is obtained. It is also then possible to obtain upper and lower bounds to the junction admittance and hence an estimate of the maximum error involved.

The interest in the discontinuity effect existing at the junction between an empty and an inhomogenously filled waveguide arises because of the application to the design of quarter-wave matching sections. Such quarter-wave matching sections are used for matching dielectric strip phase changers, empty guides to completely or partially filled guides and so forth. To date these quarter-wave matching sections have been designed largely by trial and error methods. This latter statement is based on the fact that there appears to be no published theoretical design data. There seems to have been a more or less general assumption that the binomial transformer represented an optimum design as far as bandwidth requirements were concerned. A more thorough analysis of their properties disproved this claim and showed that considerable bandwidth increases could be obtained by a more suitable choice of the design parameters. This analysis and results are contained in chapter 6.

A specific application of quarter-wave matching sections is made in chapter 8 where a new type of rectangular waveguide phase changer

is discussed.

Although most of the theory in chapter 2 is formulated for H_{on} modes in rectangular waveguides it is still quite general and can be easily extended to cover any uniform cylindrical guide supporting all possible types of modes. The main reason for this formulation is to enable the direct carry over of many of the derived expressions to the problems that were worked out in detail. The derivation of Maxwell's equations and the method of solution for the modes existing in a waveguide are not discussed since these are fully covered in many standard texts (1.5, 1.6, 1.7). Throughout this work the time factor $e^{j\omega t}$ is omitted.

CHAPTER 2.

Basic Theory

2.1. Orthogonality Conditions and Expandibility of Fields.

For empty waveguides and also for guides homogenously filled with a lossless dielectric the following orthogonality relations hold (1.5)

$$\iint_A \varphi_{Tn}\, \varphi_{Tm}\, da = 0$$

$$\iint_A \varphi_{zn}\, \varphi_{zm}\, da = 0$$

where φ_{Tn} and φ_{Tm} may be the transverse electric field components or the transverse magnetic field components of two distinct modes. The subscript z denotes longitudinal components. The φ_j are functions of the transverse co-ordinates only since variation along the axis of propagation is taken as $e^{-\gamma_j z}$. In all cases the integration is over the cross section of the guide. The usual method of proving these relations is by an application of Green's theorems to the wave equation of which the φ_j are solutions.

When a waveguide is inhomogenously filled the above orthogonality relations do not in general hold. In some cases they do hold for some of the field components while in other cases they do not hold for any of the components. For a guide inhomogenously filled as in figure 2.1-1 where $\epsilon_i \mu_i$ have a constant but arbitrary value over any cross sectional area A_i, these orthogonality relations hold only for those field components that are continuous with a continuous normal derivative across all boundaries C_i and with either φ_j or $\frac{\partial \varphi_j}{\partial n}$

vanishing on the outer perfectly conducting boundary C_o. The proof is as follows :

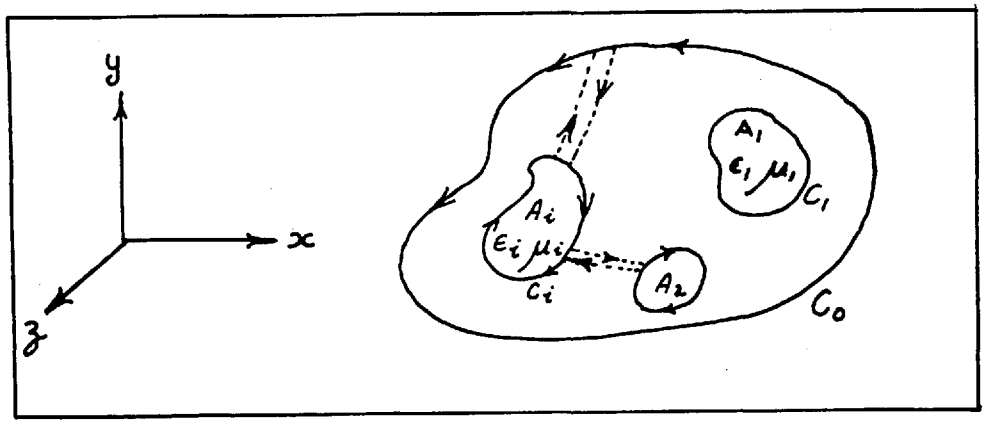


Fig. 2.1. - 1.

The wave equation satisfied by φ_n in A_i is

$$\nabla_t^2 \varphi_{ni} + (\gamma_n^2 + k_i^2)\varphi_{ni} = 0$$

where $k_i^2 = \omega^2 \epsilon_i \mu_i$. For any one mode γ_n^2 must be the same in all A_i in order to satisfy the boundary condition along the axis of propagation. When the above equation is multiplied by φ_{mi} and subtracted from the similar equation obtained by interchanging the subscripts n and m there is obtained

$$\varphi_{ni} \nabla_t^2 \varphi_{mi} - \varphi_{mi} \nabla_t^2 \varphi_{ni} = (\gamma_n^2 - \gamma_m^2)\varphi_{ni}\varphi_{mi} .$$

Now integrate over the cross sectional area A_i, thus

$$\iint_{A_i} \varphi_{ni}\varphi_{mi}\, da = \frac{1}{\gamma_n^2 - \gamma_m^2} \iint_{A_i} (\varphi_{ni} \nabla_t^2 \varphi_{mi} - \varphi_{mi} \nabla_t^2 \varphi_{ni})\, da$$

$$= \frac{1}{\gamma_n^2 - \gamma_m^2} \int_{C_i} \left(\varphi_{ni} \frac{\partial \varphi_{mi}}{\partial n} - \varphi_{mi} \frac{\partial \varphi_{ni}}{\partial n}\right) dl$$

by an application of Green's second theorem. The integral over the whole guide cross section is the sum of the above typical term for all i.

It is readily seen that if φ_{ki} and $\frac{\partial \varphi_{ki}}{\partial n}$ are continuous across all C_i and one or the other vanishes on C_o then the total integral vanishes also. This is due to the fact that by the introduction of suitable cuts when carrying out the boundary integrals all boundaries C_i are traversed twice but in opposite senses and hence the line integrals all cancel except the integral over C_o which however is zero anyway by virtue of the boundary condition. Unfortunately the φ_{ki} and $\frac{\partial \varphi_{ki}}{\partial n}$ are not as a rule both continuous across all boundaries C_i. However there is a much more general and important orthogonality relation that does hold for any inhomogenously filled waveguide. The dielectric may also have losses without violating this more general relation (2.1-1).

The following more general orthogonal principle will now be proved.

$$\iint_A \vec{i}_z \cdot \vec{E}_{Tn} \times \vec{H}_{Tm} \, da = 0$$

and for lossless structures

$$\iint_A \vec{i}_z \cdot \vec{E}_{Tn} \times \vec{H}^*_{Tm} \, da = 0 \qquad \text{also.}$$

$\vec{E}_{Tn}$ and $\vec{H}_{Tm}$ refer to the transverse components of the electric and magnetic fields for two distinct non-degenerate modes. $\vec{E}_{Tn}$ and $\vec{H}_{Tm}$ are assumed to be functions of x and y only. Let $\vec{E}_n, \vec{H}_n$ and $\vec{E}_m, \vec{H}_m$ be two linearly independent solutions of Maxwell's equations.

Then $\nabla \times \vec{E}_n = -j\omega\mu \vec{H}_n$, $\nabla \times \vec{E}_m = -j\omega\mu \vec{H}_m$.
Scalar multiply these equations by $\vec{H}_m$ and $\vec{H}_n$ respectively and subtract to get

$$\vec{H}_m \cdot \nabla \times \vec{E}_n - \vec{H}_n \cdot \nabla \times \vec{E}_m = 0$$

Scalar multiplying Maxwell's curl equation for $\vec{H}_n$ and $\vec{H}_m$ by $\vec{E}_m$ and $\vec{E}_n$ respectively and subtracting gives a similar result but with the role of $\vec{E}$ and $\vec{H}$ interchanged, thus

$$\vec{E}_m \cdot \nabla \times \vec{H}_n - \vec{E}_n \cdot \nabla \times \vec{H}_m = 0$$

By adding these equations together it is readily seen that

$$\nabla \cdot (\vec{E}_n \times \vec{H}_m - \vec{E}_m \times \vec{H}_n) = 0$$

since $\vec{H}_m \cdot \nabla \times \vec{E}_n - \vec{E}_n \cdot \nabla \times \vec{H}_m = \nabla \cdot \vec{E}_n \times \vec{H}_m$.

Now $\vec{E}_k$ and $\vec{H}_k$ depend on z only as $e^{-\gamma_k z}$ and hence this last relation reduces to

$$\nabla_t \cdot (\vec{E}_n \times \vec{H}_m - \vec{E}_m \times \vec{H}_n) = (\gamma_n + \gamma_m) \vec{i}_z \cdot (\vec{E}_{Tn} \times \vec{H}_{Tm} - \vec{E}_{Tm} \times \vec{H}_{Tn})$$

where all quantities are now taken as functions of x and y only and ∇_t is the transverse operator $\vec{i}_x \frac{\partial}{\partial x} + \vec{i}_y \frac{\partial}{\partial y}$.
By the divergence theorem it follows that

$$\iint_{A_i} \nabla_t \cdot (\vec{E}_n \times \vec{H}_m - \vec{E}_m \times \vec{H}_n)\, da = \int_{C_i} \vec{n} \cdot (\vec{E}_n \times \vec{H}_m - \vec{E}_m \times \vec{H}_n)\, dl$$

$$= \int_{C_i} (\vec{n} \times \vec{E}_n \cdot \vec{H}_m - \vec{n} \times \vec{E}_m \cdot \vec{H}_n)\, dl = (\gamma_n + \gamma_m) \iint_{A_i} \vec{i}_z \cdot (\vec{E}_{Tn} \times \vec{H}_{Tm} - \vec{E}_{Tm} \times \vec{H}_{Tn})\, da$$

Now $\vec{n} \times \vec{E}_n$ selects the tangential electric field component and the dot product with $\vec{H}_m$ selects only the tangential magnetic

field components so the sum of all the integrals around C_i vanish by a similar argument as used before. The tangential field components are by construction continuous across all C_i and the tangential electric field vanishes on the perfectly conducting boundary C_o. It therefores follows that

$$(\gamma_n + \gamma_m) \iint_A \vec{i}_z \cdot (\vec{E}_{Tn} \times \vec{H}_{Tm} - \vec{E}_{Tm} \times \vec{H}_{Tn})\, da = 0$$

Since $(-\vec{E}_{Tm}, H_{Tm}, -\gamma_m)$ is another solution the following result also holds

$$(\gamma_n - \gamma_m) \iint_A \vec{i}_z \cdot (\vec{E}_{Tn} \times \vec{H}_{Tm} + \vec{E}_{Tm} \times \vec{H}_{Tn})\, da = 0$$

If $\gamma_n \pm \gamma_m \neq 0$ then by adding the above equations one obtains

$$\iint_A \vec{i}_z \cdot (\vec{E}_{Tn} \times \vec{H}_{Tm})\, da = 0$$

which completes the proof. The proof for the alternate relations also valid for lossless structures is similar and so will not be given here.

When the modes which can exist in an inhomogenously filled guide form a complete set of eigenfunctions then by means of the above orthogonality relations any arbitrary field configuration can be expanded into an infinite series consisting of these eigenfunctions. Thus if the total transverse electric field is $\vec{E}_T$, then

$$\vec{E}_T = \sum_1^\infty c_n \vec{E}_{Tn}$$ where

$C_n = \iint_A \vec{E}_T \cdot \vec{E}_{Tn}\, da$ if the following orthogonality relation holds

$$\iint_A \vec{E}_{Tn} \cdot \vec{E}_{Tm}\, da = 0 .$$

If this orthogonality relation does not hold then C_n is given by

$$C_n = \iint_A \vec{i}_z \cdot \vec{E}_T \times \vec{H}_{Tn}\, da .$$

Usually it is convenient to normalize the eigenfunctions so that

$$\iint_A \vec{E}_{Tn} \cdot \vec{E}_{Tm}\, da = \delta_{nm}$$

or

$$\iint_A \vec{i}_z \cdot \vec{E}_{Tn} \times \vec{H}_{Tm}\, da = \delta_{nm}$$

where δ_{nm} is by definition equal to unity for $n = m$ and equal to zero for $n \neq m$.

For the H-plane dielectric strip discussed in chapter four the transverse electric and transverse magnetic field components are orthogonal over the cross sectional area of the guide. This follows at once when it is recognized that $\frac{\partial E_y}{\partial n}$ is proportional to the tangential longitudinal magnetic field which is continuous along with E_y across the discontinuity interface. Since H_x is proportional to E_y it also forms an orthogonal set over the guide cross section. For the E-plane dielectric strip the more general orthogonality relation must be used for expanding any arbitrary field into a series.

2.2. Variational Principle for the Electromagnetic Field.

All problems of wave motion and in fact most problems in mathematical physics can be formulated as an equivalent variational problem. The variational problem does not depend on any particular co-ordinate system and hence it expresses general principles. It also makes the transformation from one co-ordinate system to another relatively easy. When a solution to a given problem cannot be obtained by other means it is still possible to get a good approximation to the correct solution by means of the equivalent variational problem.

For the electromagnetic field the difference between the magnetic and electric energy is taken as the Lagranian function in the variational integral (2.2-1). The electromagnetic field is characterized by the condition that

$$\delta \int_{t_1}^{t_2} \int_V \frac{1}{2} (\mu \vec{H} \cdot \vec{H} - \epsilon \vec{E} \cdot \vec{E}) \, dv \, dt = 0 .$$

Now $\vec{E}$ and $\vec{H}$ are not independent since the following condition must not be violated

$$\nabla \times \vec{H} - \epsilon \frac{\partial \vec{E}}{\partial t} = 0 .$$

However in the variational problem they can be considered as independent if a vector Lagranian multiplier $\vec{A}$ is introduced. Alternately a scalar multiplier for each component could be introduced. The integral whose first variation must vanish now becomes

$$\int_{t_1}^{t_2} \int_V \left[\frac{1}{2} \mu \vec{H} \cdot \vec{H} - \frac{1}{2} \vec{E} \cdot \vec{E} + \vec{A} \cdot \left(\nabla \times \vec{H} - \epsilon \frac{\partial \vec{E}}{\partial t} \right) \right] dt \, dv .$$

The modified Lagranian function is taken as

$$L \equiv \frac{\mu \vec{H}\cdot\vec{H} - \epsilon \vec{E}\cdot\vec{E}}{2} + \vec{A}\cdot\left(\nabla\times\vec{H} - \epsilon\frac{\partial \vec{E}}{\partial t}\right)$$

where $\vec{A}\cdot\nabla\times\vec{H}$ may be written in determinental form as

$$\begin{vmatrix} A_x & A_y & A_z \\ \frac{\partial}{\partial x} & \frac{\partial}{\partial y} & \frac{\partial}{\partial z} \\ H_x & H_y & H_z \end{vmatrix}$$

When the Euler-Lagrange* equations are applied to this function it follows that

$$\frac{\partial L}{\partial \vec{H}} - \frac{\partial}{\partial x}\frac{\partial L}{\partial \frac{\partial \vec{H}}{\partial x}} - \frac{\partial}{\partial y}\frac{\partial L}{\partial \frac{\partial \vec{H}}{\partial y}} - \frac{\partial}{\partial z}\frac{\partial L}{\partial \frac{\partial \vec{H}}{\partial z}} - \frac{\partial}{\partial t}\frac{\partial L}{\partial \frac{\partial \vec{H}}{\partial t}} = 0$$

gives

$$\mu(H_x + H_y + H_z) - \frac{\partial}{\partial x}(A_z - A_y) - \frac{\partial}{\partial y}(A_x - A_z) - \frac{\partial}{\partial z}(A_y - A_x) = 0$$

which can be easily recognised as

$$\mu\vec{H} - \nabla\times\vec{A} = 0.$$

* To minimize an integral such as

$$\int_V F\left(u(x_1,\cdots x_n), \frac{\partial u}{\partial x_1}\cdots\cdots\frac{\partial u}{\partial x_n}\right) dx_1,\cdots dx_n$$

the function F must be determined so as to satisfy the following partial differential equation:

$$\frac{\partial F}{\partial u} - \sum_{i=1}^{n}\frac{\partial}{\partial x_i}\frac{\partial F}{\partial \frac{\partial u}{\partial x_i}} = 0.$$

This is the basic Euler-Lagrange equation of the variational calculus.

The $(A_z - A_y)$ etc. are the components of $\vec{A}$ that prepmultiply the $\frac{\partial}{\partial x}$ etc. in the expansion of the determinant. The condition imposed on $\vec{E}$ by the minimization of the above energy integral is found to be

$$\vec{E} = -\frac{\partial \vec{A}}{\partial t} .$$

It is seen that $\vec{A}$ is identical to the usual vector potential introduced into electromagnetic theory.

When the above values of $\vec{E}$ and $\vec{H}$ are substituted into the above energy integral it becomes

$$\delta \int_{t_1}^{t_2} \int_V \left(\nabla \times \vec{A} \cdot \nabla \times \vec{A} - \epsilon\mu \frac{\partial \vec{A}}{\partial t} \cdot \frac{\partial \vec{A}}{\partial t} \right) dv\, dt = 0$$

Applying the Euler-Lagrange equations to this integral gives

$$\nabla^2 \vec{A} - \nabla \nabla \cdot \vec{A} - \epsilon\mu \frac{\partial^2 \vec{A}}{\partial t^2} = 0 .$$

In a homogenous charge free medium $\nabla \cdot \vec{E} = 0$ and consequently $\nabla \cdot \vec{A} = 0$ also. Thus the final result is the usual homogenous wave equation

$$\nabla^2 \vec{A} - \epsilon\mu \frac{\partial^2 \vec{A}}{\partial t^2} = 0 .$$

When this wave equation cannot be solved then a minimization of the original integral with only an approximately correct value of the electric and magnetic fields can give a closer approximation to the correct solution. This principle is used later on to obtain the approximate eigenfunctions and eigenvalues of the wave equation.

2.3 Relation between Junction Admittance and Stored Reactive Energy.

It is easy to show that the reactance component of the impedance of any network at low frequencies depends solely on the difference between the capacitive and inductive energy stored. When the two are equal a condition of resonance exists. The same principles carry over into the impedance or admittance representation of discontinuities in waveguides.

From Maxwell's equiatons

$$\nabla \cdot \vec{E} \times \vec{H}^* = \vec{H}^* \cdot \nabla \times \vec{E} - \vec{E} \cdot \nabla \times \vec{H}^* = -j\omega(\mu \vec{H} \cdot \vec{H}^* - \epsilon \vec{E} \cdot \vec{E}^*)$$

where $\vec{E}$ and $\vec{H}$ are complex vector functions depending on the time coordinate only as $e^{j\omega t}$. The star denotes the complex conjugate. The volume integral of the divergence of the complex Poynting vector is equivalent to the surface integral of the normal component of the complex Poynting vector and hence $\int_S \vec{E} \times \vec{H}^* \cdot \vec{n}\, ds =$

$$j\omega \int_V (\mu \vec{H} \cdot \vec{H}^* - \epsilon \vec{E} \cdot \vec{E}^*) dv + \sigma \int_V \vec{E} \cdot \vec{E}^* dv = 4j\omega(W_H - W_E) + 2P$$

where $\vec{n}$ is the unit inward normal to the surface S bounding the volume V and W_H, W_E and P are the average stored magnetic energy, electric energy and the total dissipated power respectively.

Consider now an H_{01} wave incident on a general discontinuity or termination in a rectangular waveguide. The transverse electric field is

$$E_y = \sin \frac{\pi x}{a} \left(e^{-\Gamma z} + R e^{\Gamma z} \right)$$

and the transverse magnetic field is

$$H_x = \frac{j\Gamma}{\omega\mu} \sin\frac{\pi x}{a}\left(e^{-\Gamma z} - R e^{\Gamma z}\right)$$

where R is the reflection coefficient and is equal to $\rho e^{j\theta}$. If some of the energy is transmitted past the discontinuity then the output guide can be replaced by a resistive termination that absorbs the same equivalent power as far as the input impedance is concerned. Thus

$$\int_S \vec{E}\times\vec{H}^*\cdot\vec{n}\,ds = (1+R)(1-R^*)\frac{\beta_1}{\omega\mu}\int_S \sin^2\frac{\pi x}{a}\,dy\,dx$$

at a point in the guide where $|\Gamma_1|z = \beta_1 z = 2n\pi$ since $\vec{E}$ tan. vanishes on the guide walls. The incident energy W_i is equal to

$$\frac{1}{2}\frac{\beta_1}{\omega\mu}\int_S \sin^2\frac{\pi x}{a}\,dy\,dx.$$

It then follows that (1.5)

$$(1+R)(1-R^*) = \frac{2j\omega(W_H - W_E)}{W_i} + \frac{P}{W_i} \qquad \text{or}$$

$$1 - RR^* = 1-\rho^2 = \frac{P}{W_i} \quad \text{and} \quad \text{Imag. } R = \omega\frac{W_H - W_E}{W_i}.$$

To obtain expressions for $\frac{1+R}{1-R}$ and $\frac{1-R}{1+R}$, the input impedance and admittance respectively it is noted that at $\beta_1 z = 2n\pi$

$$E_y = \frac{-j\omega\mu}{\Gamma_1}\,\frac{1+R}{1-R}\,H_x$$

or alternatively

$$H_x = \frac{j\Gamma}{\omega\mu}\,\frac{1-R}{1+R}\,E_y.$$

Thus $\int_S E_y H_x^*\,ds = \frac{j\omega\mu}{\Gamma_1}\,\frac{1+R}{1-R}\int_S H_x H_x^*\,ds$ and

hence $$\frac{1+R}{1-R} = \frac{4j\omega(W_H - W_E) + 2P}{\frac{\omega\mu}{\beta_1}\int_S H_x H_x^*\,ds}.$$

Similarly

$$\frac{1-R}{1+R} = \frac{-4j\omega(W_H - W_E) + 2P}{\frac{\beta_1}{\omega\mu}\int_S E_y E_y^*\,ds}.$$

It is seen that the input admittance and impedance is directly related to the stored reactive energy and absorbed power. The term $2P$

may be considered as being due to power transmitted past a discontinuity.

As a simple application of these results the input impedance at z for a short circuited guide with a short at $z=0$ will be worked out. The fields in the guide are given by the following expressions

$$E_y = C \sin\frac{\pi x}{a}\left(e^{-\Gamma z} + Re^{\Gamma z}\right), \quad H_x = -C\frac{\beta_1}{\omega\mu}\sin\frac{\pi x}{a}\left(e^{-\Gamma z} - Re^{\Gamma z}\right),$$

$$H_z = C\frac{j\pi}{\omega\mu a}\cos\frac{\pi x}{a}\left(e^{-\Gamma z} + Re^{\Gamma z}\right)$$

where R is equal to $\rho e^{j\theta}$. The difference between the average stored magnetic and electric energy is $W_H - W_E = \frac{ab}{8}CC^*\epsilon\int_0^z\left\{\left(\frac{\pi^2}{\omega^2\mu\epsilon a^2}-1\right)\right.$

$$\left.(1+\rho^2+2\rho\cos\overline{2\beta_1 z+\theta}) + \frac{\beta_1^2}{\omega^2\mu\epsilon}(1+\rho^2-2\rho\cos\overline{2\beta_1 z+\theta})\right\}dz =$$

$$\frac{ab\rho\beta_1}{4\omega^2\mu}CC^*(\sin\theta - \sin\overline{2\beta_1 z+\theta}).$$

It is seen that over half a wavelength the electric and magnetic energy stored is equal. If θ is positive then for $\sin\overline{2\beta_1 z+\theta} < \sin\theta$ the stored magnetic energy exceeds the stored electric energy.

For a short circuited guide $R=-1$ so $\rho=1$ and $\theta=\pi$.

Thus $W_H - W_E = CC^*\frac{ab\beta_1}{4\omega^2\mu}\sin 2\beta_1 z = CC^*\frac{ab\beta_1}{2\omega^2\mu}\sin\beta_1 z\cos\beta_1 z$.

For $z < \frac{\lambda_g}{4}$ the stored magnetic energy exceeds the electric energy and the input impedance is inductive. For $\frac{\lambda_g}{4} < z < \frac{\lambda_g}{2}$ the input impedance is capacitive since $W_E > W_H$. The input impedance at z is $\frac{1+R}{1-R} = \frac{4j\omega(W_H-W_E)}{\frac{\omega\mu}{\beta_1}\int_s H_x H_x^* ds}$ since P is zero for a short circuited guide. The $\int_s H_x H_x^* ds$ is equal to $\frac{ab\beta_1^2}{\omega^2\mu^2}2\cos^2\beta_1 z$ and therefore

$$Z_{in} = \frac{1+R}{1-R} = \frac{4j\omega ab\beta_1\sin\beta_1 z\cos\beta_1 z}{2\omega^2\mu\,\frac{\omega\mu}{\beta_1}\,\frac{ab\beta_1^2}{\omega^2\mu^2}2\cos^2\beta_1 z} = j\tan\beta_1 z$$

which is the usual expression for the input impedance of a short circuited transmission line. It should be noted that the reflection

coefficient R in the expression for Z_{in} is the equivalent reflection coefficient at the plane z such that at this plane $\frac{E_y}{H_x} = -\frac{\omega\mu}{\beta_1}\frac{1+R}{1-R}$. At the points where $\tan \beta_1 z$ becomes zero i.e. $z = \frac{\lambda_g}{2}$, a condition of resonance exists and $W_H = W_E$.

2.4. Variational Expressions for Junction Admittance and Impedance.

A general plane junction between two inhomogenously filled rectangular waveguides supporting H_{on} modes will now be considered. The inhomogenity is assumed constant for all values of z except at the junction $z = 0$ where there is a sharp discontinuity as in figure 2.4-1. The inhomogenous filling to be considered is a lossless dielectric. A similar analysis would apply if the dielectric was lossy by replacing the dielectric constant by its complex value $\epsilon(1 - j\tan\delta)$ where ϵ is the real part and δ is the loss angle.

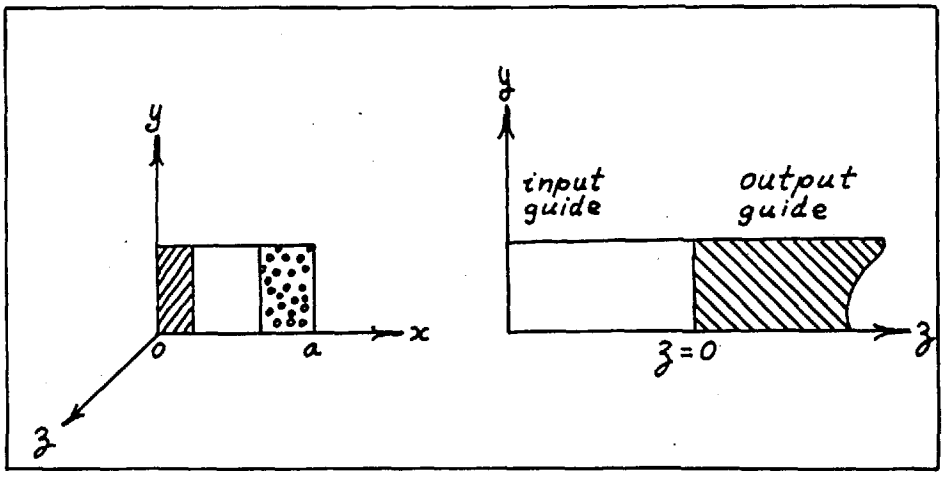


Fig. 2.4-1.

It has been shown that the reactance depends on $W_H - W_E$ and also that $\delta \int_V (w_H - w_E)\, dv = 0$ so it seems reasonable to expect that a variational expression for the junction impedance would exist. Rather than deriving this variational expression from basic principles it will be obtained by the usual process of direct mathematical manipulation on the continuity equations relating the fields at the aperture $z = 0$ and then later will be shown to be equivalent to minimizing the volume integral of the difference between the magnetic and electric energy stored in the evanescent modes at the junction.

For the present it will be assumed that it has been possible to solve the wave equation for the complete set of eigenfunctions existing in the input and output guides illustrated in figure 2.4-1. Let the eigenfunctions representing the y component of the electric field in the input guide be $\sum_1^\infty \phi_n e^{\pm \Gamma_n z}$ and $\sum_1^\infty F_m e^{\pm \gamma_m z}$ in the output guide. For the type of discontinuity being studied here it is obvious that these functions form an orthogonal set over the guide cross section (see section 2.1). Also it will be assumed that these functions have been normalized so that

$$\int_0^a F_n(x)\, F_m(x)\, dx = \int_0^a \phi_n(x)\, \phi_m(x)\, dx = \delta_{nm}.$$

Further it will be assumed that only one mode propagates in the guides although it would be a simple matter to consider the case of more than one propagating mode.

The incident and reflected wave in the input guide is given by

$$E_y = \phi_1 (e^{-\Gamma_1 z} + R e^{+\Gamma_1 z})$$

$$j\omega\mu H_x = -\Gamma_1 \phi_1 (e^{-\Gamma_1 z} - R e^{+\Gamma_1 z})$$

where R is the reflection coefficient and equal to $\rho e^{j\theta}$. At the junction higher order modes will be excited and are given by

$$E_y = \sum_2^\infty D_n \varphi_n e^{\Gamma_n z}$$

$$j\omega\mu H_x = \sum_2^\infty D_n \Gamma_n \varphi_n e^{\Gamma_n z}$$

In the output guide there will be a transmitted wave plus higher order modes generated. These are given by

$$E_y = \sum_1^\infty A_m F_m e^{-\gamma_m z}$$

$$j\omega\mu H_x = -\sum_1^\infty A_m \gamma_m F_m e^{-\gamma_m z}.$$

At the junction or plane $z=0$ the tangential fields must be continuous. The continuity of the transverse field components is sufficient to ensure the continuity of the longitudinal magnetic field component also. These continuity conditions give

$$(1+R)\varphi_1 + \sum_2^\infty D_n \varphi_n = \sum_1^\infty A_m F_m, \qquad (1)$$

$$(1-R)\Gamma_1 \varphi_1 - \sum_2^\infty D_n \Gamma_n \varphi_n = \sum_1^\infty A_m \gamma_m F_m. \qquad (2)$$

Now if the total electric field at the junction or aperture is $G_0(x)$ where $G_0(x)$ is a complex function of the real variable x, it follows by Fourier analysis that the coefficients D_n and A_m are given by

$$1+R = \int_0^a G_0 \varphi_1 \, dx, \qquad D_n = \int_0^a G_0 \varphi_n \, dx,$$

$$A_m = \int_0^a G_0 F_m \, dx.$$

Replace the coefficients in (2) by their integral representations and introduce $1+R$ on the left hand side, thus

$$\frac{1-R}{1+R}\Gamma_1 \varphi_1 = \sum_2^\infty \Gamma_n \varphi_n \int G_0 \varphi_n \, dx + \sum_1^\infty \gamma_m F_m \int G_0 F_m \, dx. \qquad (3)$$

As it stands this expression is an identity for the correct values of R and G_0 and consequently both sides can be multiplied by an arbitrary function and integrated over the aperture without violating the equality. Let this arbitrary function be $G_0(x)$, then after dividing by $\Gamma_1\left(\int G_0 \varphi_1 \, dx\right)^2$ one obtains

$$\frac{1-R}{1+R} = \frac{\sum_{2}^{\infty} \Gamma_n \left(\int G_0 \Phi_n dx\right)^2 + \sum_{1}^{\infty} \gamma_m \left(\int G_0 F_m dx\right)^2}{\Gamma_1 \left(\int G_0 \Phi_1 dx\right)^2} \qquad (4)$$

which is a variational expression for the input junction admittance $\frac{1-R}{1+R}$. To show that $\frac{1-R}{1+R}$ is stationary for first order variations δG_0 of G_0 the first variation of the above expression is taken with respect to G_0, thus $\frac{1-R}{1+R} \Gamma_1 2 \int G_0 \Phi_1 dx \int \delta G_0 \Phi_1 dx + \Gamma_1 \left(\int G_0 \Phi_1 dx\right)^2 \delta\left(\frac{1-R}{1+R}\right)$

$$= 2 \sum_{2}^{\infty} \Gamma_n \int G_0 \Phi_n dx \int \delta G_0 \Phi_n dx + 2 \sum_{1}^{\infty} \gamma_m \int G_0 F_m dx \int \delta G_0 F_m dx$$

which may be written as $\Gamma_1 \left(\int G_0 \Phi_1 dx\right)^2 \delta \left(\frac{1-R}{1+R}\right) =$

$$2 \int \delta G_0 \left[\sum_{2}^{\infty} \Gamma_n \Phi_n \int G_0 \Phi_n dx + \sum_{1}^{\infty} \gamma_m F_m \int G_0 F_m dx - \frac{1-R}{1+R} \Gamma_1 \Phi_1 \int G_0 \Phi_1 dx \right] dx$$

where it has been assumed permissible to interchange the order of integration and summation. By virtue of (3) it is seen that the coefficient of δG_0 is identically zero and hence the first variation of $\frac{1-R}{1+R}$ vanishes. For a first order approximation of the aperture field G_0 a second order approximation to $\frac{1-R}{1+R}$ is obtained.

For numerical work it is more convenient to multiply (3) by the conjugate field distribution G_0^*, thus

$$\frac{1-R}{1+R} = \frac{\sum_{2}^{\infty} \Gamma_n \int G_0 \Phi_n dx \int G_0^* \Phi_n dx + \sum_{1}^{\infty} \gamma_m \int G_0 F_m dx \int G_0^* F_m dx}{\Gamma_1 \int G_0 \Phi_1 dx \int G_0^* \Phi_1 dx}.$$

This expression is easily shown to be stationary with respect to variations in G_0^* and also represents the stored reactive energy and transmitted power. A typical term such as $\Gamma_n \int G_0 \Phi_n dx \int G_0^* \Phi_n dx = \Gamma_n D_n D_n^*$ is proportional to the excess magnetic energy stored in an evanescent H_{on} mode since $4\omega(W_H - W_E) = \omega \int_V (\mu H \cdot H^* - \epsilon E \cdot E^*) dv = \int_S E_y H_x^* da$

$$= \frac{D_n D_n^* \Gamma_n}{\omega \mu} \int_0^a \int_0^b \Phi_n^2 \, dx \, dy$$ since the fields vanish as $e^{\Gamma_n z}$ for large negative values of z. Therefore $\Gamma_n D_n D_n^*$ is equal to

$\frac{4}{b}\omega^2\mu\,(W_H - W_E)$. The term $\gamma_1 A_1 A_1^*$ is proportional to the transmitted energy. This aspect of the problem is discussed in more detail in a later section.

Almost identical variational expressions for the junction impedance is obtained if the coefficients in equation ② are determined from the aperture tangential magnetic field distribution $H_0(x)$. By a smiilar process as used before it is found that

$$\frac{1+R}{1-R} = \frac{\sum_1^\infty \frac{1}{\Gamma_n}\int H_0 \Phi_n dx \int H_0^* \Phi_n dx + \sum_1^\infty \frac{1}{\gamma_m}\int H_0 F_m dx \int H_0^* F_m dx}{\frac{1}{\Gamma_1}\int H_0 \Phi_1 dx \int H_0^* \Phi_1 dx}.$$

For the examples worked out in this thesis it turns out that the average value of $\frac{1-R}{1+R}$ calculated from the above variational expressions is more accurate than either one by itself. It is difficult to justify this mathematically due to the complex nature of G_0 and H_0. However if the output guide is terminated in a short curcuit then the electric and magnetic fields are everywhere either in phase or 180° out of phase and G_0 and H_0 are real functions. Furthermore the modulus of R is unity and the input admittance or impedance is a pure imaginary quantity. It can then be shown that the stationary value of both variational expressions is an absolute minimum and consequently upper and lower bounds for the input admittance or impedance can be obtained. This absolute minimum property is proved in a following section.

With the output guide terminated in a short circuit there will be a transmitted and a reflected wave in the output guide given by

$$C_1 F_1 (e^{-\gamma_1 z} + \tau e^{\gamma_1 z})$$

with a transverse magnetic component

$$-\frac{j}{\omega\mu}\gamma_1 C_1 F_1 (e^{-\gamma_1 z} - \tau e^{\gamma_1 z})$$

where τ is the reflection coefficient and equal to $e^{j\alpha}$. For a short

circuit located at $z = \ell$ the electric field must vanish at $z = \ell$ and hence $e^{-\gamma_1 \ell} + e^{\gamma_1 \ell + j\alpha} = 0$ or $2C_1 e^{j\frac{\alpha}{2}} \cos(|\gamma_1|\ell + \frac{\alpha}{2}) = 0$. Thus $|\gamma_1|\ell + \frac{\alpha}{2} = \frac{\pi}{2}$ and $\tan\frac{\alpha}{2} = \tan(\frac{\pi}{2} - |\gamma_1|\ell)$. Consequently the transmitted and reflected wave can be taken as

$$A_1 F_1 \cos(|\gamma_1| z + \tfrac{\alpha}{2})$$

with a transverse magnetic component

$$\frac{j}{\omega\mu} A_1 |\gamma_1| F_1 \sin(|\gamma_1| z + \tfrac{\alpha}{2}).$$

At $z = 0$, the coefficient A_1 is given by

$$\cos^{-1}\tfrac{\alpha}{2} \int_0^a G_0 F_1 \, dx.$$

Since $R = e^{j\theta}$, $\frac{1-R}{1+R}$ can be replaced by $-j\tan\frac{\theta}{2}$ and hence $\frac{1-R}{1+R}\Gamma_1$ becomes $\beta_1 \tan\frac{\theta}{2}$ where $j\beta_1 = \Gamma_1$. By a similar analysis as used before it is found that

$$\cot\frac{\theta}{2} = \frac{\sum_2^\infty \frac{1}{\Gamma_n}\left(\int H_0 \phi_n dx\right)^2 + \sum_2^\infty \frac{1}{\gamma_m}\left(\int H_0 F_m dx\right)^2 + \frac{\cot\frac{\alpha}{2}}{|\gamma_1|}\left(\int H_0 F_1 dx\right)^2}{1/\beta_1 \left(\int H_0 \phi_1 dx\right)^2},$$

and

$$\tan\frac{\theta}{2} = \frac{\sum_2^\infty \Gamma_n \left(\int G_0 \phi_n dx\right)^2 + \sum_2^\infty \gamma_m \left(\int G_0 F_m dx\right)^2 + |\gamma_1| \tan\frac{\alpha}{2}\left(\int G_0 F_1 dx\right)^2}{\beta_1 \left(\int G_0 \phi_1 dx\right)^2}.$$

Since these expressions are both absolute minima for the correct aperture fields it follows that the value of $\tan\frac{\theta}{2}$ obtained from the first will be too large and that obtained from the second will be too small and an estimate of the maximum error involved is readily obtained.

At a position of a field minimum $R = -1$ so $\theta - 2\beta_1 d = \pi$ and hence $\frac{\theta}{2} = \beta_1 d + \frac{\pi}{2}$, where d is the position of a field minimum in the input guide measured from the junction. Thus $\tan\frac{\theta}{2}$ and $\tan\frac{\alpha}{2}$ in the above variational expressions can be replaced by the following

$$\tan\tfrac{\theta}{2} = \tan(\beta_1 d + \tfrac{\pi}{2}) = -\cot\beta_1 d,$$

$$\tan\tfrac{\alpha}{2} = -\tan(|\gamma_1|\ell - \tfrac{\pi}{2}) = \cot|\gamma_1|\ell.$$

These variational expressions are now the analytical equivalent of

Weissfloch's experimental technique for finding the equivalent circuit of a discontinuity.

2.5. Approximations to the Aperture Fields.

It is logical to assume an aperture field distribution consisting of a series of the proper eigenfunctions existing in the input guide. Thus take

$$G_0(x) = \sum_1^\infty D_n \phi_n(x).$$

As shown in appendix 2 the functions F_m are given by $\sum_1^\infty R_{nm}\phi_n$ where the factors R_{nm} are given by $\int_0^a \phi_n F_m \, dx$.

Substituting this aperture distribution into the variational expression for the input admittance gives

$$\frac{1-R}{1+R} = \frac{\sum_1^\infty \Gamma_n D_n D_n^* + \sum_{m=1}^\infty \gamma_m \sum_{n=1}^\infty R_{nm} D_n \sum_{n=1}^\infty R_{nm} D_n^*}{\Gamma_1 D_1 D_1^*}.$$

This is a homogenous quadratic function in the unknown coefficients D_n. It is independent of the value of D_1 since all the other D_n can be divided by D_1. To make this expression stationary with respect to arbitraty variations of G_0^* all the partial derivatives with respect to D_n^* for $n>1$ are set equal to zero. This gives the following set of infinite equations to be solved.

$$\sum_{n=2}^\infty \left\{ \Gamma_n D_n + \sum_{m=1}^\infty \gamma_m R_{nm} \sum_{i=1}^\infty R_{im} D_i = 0 \right\}$$

or

$$\sum_{n=2}^\infty \left\{ \Gamma_n D_n + \sum_{m=1}^\infty \gamma_m R_{nm}^2 D_n + \sum_{j=1}^\infty D_j \sum_{m=1}^\infty \gamma_m R_{nm} R_{jm}(1-\delta_{nj}) = 0 \right\}$$

where $1-\delta_{nj}$ equals zero for $n=j$ and equals unity for $n \neq j$. Usually the factors R_{nm} for $n \neq m$ converge to zero quite rapidly and R_{nn} converges to unity. In the above determinant the off diagonal terms are small in comparison to the diagonal terms and the terms for n and m large approach zero. Thus a first order approximation to the

solution of this determinant is obtained by neglecting all terms except the diagonal ones, thus $D_n = \dfrac{-\sum_{m=1}^{\infty} \gamma_m R_{1m} R_{nm} D_1}{\Gamma_n + \sum_{m=1}^{\infty} \gamma_m R_{nm}^2}$.

A second approximation can be obtained by substituting these values of D_n into the first off diagonal terms and solving for the new values D_n say D_n'. This process converges very rapidly and can be repeated until any desired degree of approximation is obtained.

To avoid an excess amount of numerical work one must be content with an approximation to the input admittance obtained from a two or three term approximation to the aperture fields. Thus if $G_o(x)$ is approximated by the following finite series $\sum_{n=1}^{N} D_n \phi_n$ the effect is to terminate the summations over n at $n = N$. This then gives the following finite set of equations to be solved

$$\sum_{n=2}^{N} \left\{ \left(\Gamma_n + \sum_{m=1}^{\infty} \gamma_m R_{nm}^2 \right) D_n + \sum_{j=1}^{N} D_j \sum_{m=1}^{\infty} R_{nm} R_{jm} \gamma_m (1 - \delta_{nj}) = 0 \right\}$$

To take full advantage of the stationary property of the input admittance these equations must be solved accurately for the $N-1$ unknowns D_n. Although the summation over m is not terminated, the factors R_{nm} usually converge so rapidly that terms beyond $m=N$ can be neglected without introducing appreciable error. This assumes that N is of the order of 3 or more. If N is less than 3 a value of m up to 3 or 4 must be used at any rate.

A similar set of equations to be solved is obtained for the input impedance with all Γ_n and γ_m replaced by $\frac{1}{\Gamma_n}$ and $\frac{1}{\gamma_m}$. For the case of the short circuited output guide it suffices to replace γ_1 by $|\gamma_1| \tan \frac{\alpha}{2}$ in the above equations.

It will now be shown that the variational expression obtained for the input admittance by multiplying by the conjugate electric field

distribution is equivalent to a minimization of the difference between the magnetic and electric energies stored in the higher order modes subject to the conditions that the tangential field components are continuous at the junction. The difference between the magnetic and electric energies stored is given by

$$\sum_{n=2}^{\infty} \left\{ \Gamma_n D_n D_n^* + \gamma_n \sum_{j=1}^{\infty} R_{jn} D_j \sum_{j=1}^{\infty} R_{jn} D_j^* \right\}$$

The conditions imposed on the coefficients D_n and D_n^* in order to ensure continuity of the tangential magnetic field at the aperture is obtained from equation (2) section 2.4 by multiplying both sides by φ_n and integrating over the aperture, thus

$$\Gamma_n D_n + \sum_{m=1}^{\infty} \gamma_m R_{nm} \sum_{j=1}^{\infty} R_{jm} D_j = 0, \quad n>2,$$

and similarly

$$\Gamma_n D_n^* + \sum_{m=1}^{\infty} \gamma_m^* R_{nm} \sum_{j=1}^{\infty} R_{jm} D_j^* = 0, \quad n>2 .$$

The continuity of the electric field is ensured since the A_m have been expanded in terms of the D_n . Now introduce $2n$ Lagrange multipliers λ_n and λ_n^* and the following expression is minimized

$$\sum_{n=2}^{\infty} \left\{ \Gamma_n D_n D_n^* + \gamma_n \sum_{j=1}^{\infty} R_{jn} D_j \sum_{j=1}^{\infty} R_{jn} D_j^* + \lambda_n \left(\Gamma_n D_n + \sum_{j=1}^{\infty} D_j \sum_{m=1}^{\infty} \gamma_m R_{nm} R_{jm} \right) \right.$$
$$\left. + \lambda_n^* \left(\Gamma_n D_n^* + \sum_{j=1}^{\infty} D_j^* \sum_{m=1}^{\infty} \gamma_m^* R_{nm} R_{jm} \right) \right\} .$$

Setting all $\frac{\partial}{\partial D_n}$ and $\frac{\partial}{\partial D_n^*}$ equal to zero gives

$$\Gamma_n D_n + \sum_{j=1}^{\infty} D_j \sum_{m=2}^{\infty} \gamma_m R_{nm} R_{jm} + \lambda_n^* \left(\Gamma_n + \sum_{m=1}^{\infty} \gamma_m^* R_{nm}^2 \right) = 0$$

for all $n>1$, with a similar expression for D_n^* . But from the conditions imposed on D_n it follows that

$$\Gamma_n D_n + \sum_{m=2}^{\infty} \gamma_m R_{nm} \sum_{j=1}^{\infty} R_{jm} D_j = -\gamma_1 R_{n1} \sum_{j=1}^{\infty} R_{j1} D_j$$

and consequently the value of the Lagrange multiplier λ_n^* must be

$$\lambda_n^* = \frac{\gamma_1 R_{n1} \sum_{j=1}^{\infty} R_{j1} D_j}{\Gamma_n + \sum_{m=1}^{\infty} \gamma_m^* R_{nm}^2},$$

with a similar expression for the λ_n. Substituting this value of λ_n^* into the above equation gives

$$\Gamma_n D_n + \sum_{m=1}^{\infty} \gamma_m R_{nm} \sum_{j=1}^{\infty} R_{jm} D_j = 0 \qquad \text{for} \quad n > 1,$$

which is recognized at once to be identical with the previously given equations. The conclusion is therefore that these variational expressions are equivalent to minimizing the difference between the magnetic and electric energies stored in the evanescent modes. As such it is equivalent with the variational principle discussed in section 2.2.

For the case of the short circuited output guide $\tan\frac{\theta}{2}$ is given by

$$\tan\frac{\theta}{2} = \frac{\sum_{n=2}^{\infty} \Gamma_n D_n^2 + \sum_{m=2}^{\infty} \gamma_m \left(\sum_{n=1}^{\infty} R_{nm} D_n\right)^2 + |\gamma_1| \tan\frac{\alpha}{2} \left(\sum_{n=1}^{\infty} R_{n1} D_n\right)^2}{\beta_1 D_1^2}.$$

Taylor's expansion theorem for a function of several variables can be written symbolically as (2.2-2)

$$\delta F(x_1, \cdots x_i \cdots) = \left(e^{\sum_i \frac{\partial}{\partial x_i} \Delta x_i} - 1\right) F(x_i)\Big|_{x_i = x_{oi}}.$$

When this expansion is applied to the above variational expression it gives

$$\delta \tan\frac{\theta}{2} = \sum_{n=2}^{\infty} \Delta_n \frac{\partial}{\partial D_n} \sum_{s=2}^{\infty} \Delta_s \left(\Gamma_s D_s + \sum_{m=2}^{\infty} \gamma_m R_{sm} \sum_{j=1}^{\infty} R_{jm} D_j + |\gamma_1| R_{s1} \tan\frac{\alpha}{2} \sum_{j=1}^{\infty} R_{j1} D_j\right)$$

$$= \sum_{n=2}^{\infty} \sum_{s=2}^{\infty} \left[\Delta_s \Delta_n \Gamma_s \delta_{sn} + \Delta_s \Delta_n \left(\sum_{m=2}^{\infty} \gamma_m R_{sm} R_{nm} + |\gamma_1| \tan\frac{\alpha}{2} R_{s1} R_{n1}\right)\right]$$

$$= \sum_{n=2}^{\infty} \Gamma_n \Delta_n^2 + \sum_{m=2}^{\infty} \gamma_m \left(\sum_{n=2}^{\infty} \Delta_n R_{nm}\right)^2 + |\gamma_1| \tan\frac{\alpha}{2} \left(\sum_{n=2}^{\infty} \Delta_n R_{n1}\right)^2$$

since the first variation is zero and where Δ_n is the variation in the coefficient D_n. An inspection of this expression shows that it is positive if all Γ_n, γ_m and $\tan\frac{\alpha}{2}$ is positive. Now Γ_n and γ_m

are positive and as long as $/\gamma_1/\tan\frac{\alpha}{2}\left(\sum_{n=2}^{\infty}\Delta_n R_{n1}\right)^2$ is not large enough negatively to render the whole expression negative, then the variation in $\tan\frac{\theta}{2}$ is positive and consequently for the correct aperture distribution it is an absolute minimum. Likewise it can be shown that $\cot\frac{\theta}{2}$ is also an absolute minimum. Any approximate aperture distribution will consequently give too large a value of $\tan\frac{\theta}{2}$ and $\cot\frac{\theta}{2}$. Taking the reciprocal of $\cot\frac{\theta}{2}$ then gives too small a value of $\tan\frac{\theta}{2}$ and thus an upper and a lower bound to the true value is obtained.

2.6. Application of the Ritz Method :

This section deals with the case when the input guide is empty which is the usual case in practice. To obtain the propagation constants γ_m for dielectric slabs in a rectangular waveguide one is led to the solution of a transcendental equation for the simplest case of one dielectric strip and to sets of simultaneous transcendental equations for more complicated cases. Also the process of determining the normalization constants P_m, the eigenfunctions $F_m(x)$ and the elements R_{nm} becomes very tedious. However by an application of theRitz method all this information can be determined to a good degree of approximation with much less labour. These approximate eigenfunctions when used in the variational expression for the input admittance then leads to an excellent approximation for $\frac{1-R}{1+R}$. This is reasonable since an application of the Ritz method does in fact minimize the difference in the magnetic and electric energies. The functions F_m are approximated by a finite series of the φ_n which are the proper functions existing in the empty guide, thus $F_m=\sum_{n=1}^{N}\alpha_{nm}\varphi_n$. To find the propagation constants γ_m and the coefficients α_{nm}

the following energy integral is minimized (2.5-1).

$$\int_V (\mu \vec{H}\cdot\vec{H} - \epsilon \vec{E}\cdot\vec{E})\, dv.$$

The transverse electric field is taken as

$$\sum_{n=1}^{N} \alpha_{nm} \sqrt{\frac{2}{a}} \sin\frac{n\pi x}{a}\; e^{-\gamma_m z}$$

with a transverse magnetic field component

$$-\sum_{n=1}^{N} \alpha_{nm} \sqrt{\frac{2}{a}}\, \frac{\gamma_m}{\omega\mu} \sin\frac{n\pi x}{a}\; e^{-\gamma_m z}$$

and a longitudinal magnetic component

$$+\sum_{n=1}^{N} \alpha_{nm}\, \frac{n\pi}{a}\, \frac{1}{\omega\mu} \sqrt{\frac{2}{a}} \cos\frac{n\pi x}{a}\, e^{-\gamma_m z}$$

If γ_m is imaginary it is replaced by $|\gamma_m|$ in the energy integral since it involves the modulus of the field components only.

The energy integral to be minimized is now $\frac{2}{a}\int_0^b \int_0^z \int_0^a \Big\{ \mu \Big[\Big(\sum_1^N \alpha_{nm} \frac{\gamma_m}{\omega\mu} \sin\frac{n\pi x}{a} \Big)^2$

$$+ \Big(\sum_1^N \alpha_{nm}\, \frac{n\pi}{a}\, \frac{1}{\omega\mu} \cos\frac{n\pi x}{a} \Big)^2 \Big] - \epsilon(x) \Big(\sum_1^N \alpha_{nm} \sin\frac{n\pi x}{a} \Big)^2 \Big\} e^{-2\gamma_m z}\, dv.$$

The factor $\int_0^b \int_0^z e^{-2\gamma_m z}\, dy\, dz$ is common to all terms. Since this integral is going to be minimized with respect to the coefficients α_{nm} a set of equations to be solved for the α_{nm} will be obtained. These equations will all contain this common factor which will cancel out and hence it can be deleted from the above energy integral. This is true only for the case when the structure is uniform in the z and y directions. The integral to be considered is now

$$\sum_{n=1}^{N} \alpha_{nm}^2 \Big(\gamma_m^2 + \frac{n^2\pi^2}{a^2} \Big) - k_0^2 \int_0^a K(x) \Big(\sum_1^N \alpha_{nm} \sqrt{\frac{2}{a}} \sin\frac{n\pi x}{a} \Big)^2 dx$$

where some of the integrations with respect to x have been carried

out and $k_o^2 = \omega^2 \mu_o \epsilon_o$.

Let $\int_o^a K(x) \left(\sum_1^N \alpha_{nm} \sqrt{\frac{2}{a}} \sin \frac{n\pi x}{a} \right)^2 dx =$

$$\sum_{n=1}^{N} \sum_{s=1}^{N} \alpha_{nm} \alpha_{sm} \chi_{sn}$$

and the final result is

$$\sum_{n=1}^{N} \alpha_{nm}^2 \left(\gamma_m^2 + \frac{n^2\pi^2}{a^2} \right) - k_o^2 \sum_{n=1}^{N} \sum_{s=1}^{N} \alpha_{nm} \alpha_{sm} \chi_{sn} .$$

Setting all $\frac{\partial}{\partial \alpha_{nm}}$ equal to zero gives the following set of simultaneous equations to be solved,

$$\sum_{n=1}^{N} \left\{ \alpha_{nm} \left(\gamma_m^2 + \frac{n^2\pi^2}{a^2} \right) - k_o^2 \sum_{s=1}^{N} \alpha_{sm} \chi_{sn} = 0 \right\}$$

In order for these equations to have a solution the determinant of the coefficients must vanish. The N roots of γ_m^2 so obtained are approximations from above to the first N eigenvalues γ_m^2 . For each root a set of coefficients α_{nm} can be obtained by solving for all the α_{nm} in terms of one of them, say α_{1m} . By subjecting the α_{nm} to the following normalization condition

$$\sum_{n=1}^{N} \alpha_{nm}^2 = 1$$

it can be shown that the N approximate eigenfunctions so obtained form an orthonormal set over the guide cross section. (See appendix 3)

An infinite number of terms in the above series approximation for F_m would give a correct value for F_m and hence it follows that

$$F_m = \sum_1^{\infty} \alpha_{nm} \phi_n = \sum_1^{\infty} R_{nm} \phi_n .$$

Thus the coefficients α_{nm} can be recognized as the approximate factors R_{nm} and can be used as such in the variational expression for the junction admittance. The above procedure has

the advantage that it terminates the summation over m at $m=N$ in the variational expression.

2.7. The Equivalent Circuit :

When the output guide is terminated in a short circuit located a distance l from the junction the variational expression gives the position of a field minimum in the input guide directly. Thus a position of a field minimum can be calculated for a series of values of l and $|\gamma_1|l+\beta_1 d$ plotted against $\beta_1 d$. This resultant curve is then analysed by the method discussed in appendix 1 to obtain the parameters of the equivalent circuit.

For the open circuited output guide the value of the reflection coefficient R is calculated from the value of $\frac{1-R}{1+R}$ obtained from the variational expression. Let this value be $\rho e^{j\theta}$. A characteristic plane in the input guide is located at a point where $\theta - 2\beta_1 d = n\pi$. The transformation constant for the impedance between the characteristic planes in the two guides is N^2 where N^2 is equal to $\frac{1 \pm \rho}{1 \mp \rho}$ and is greater or less than unity depending on whether n is even or odd. To locate the characteristic plane in the output guide a similar analysis could be carried through with a wave incident on the junction from the right. A check on the results would be obtained since the transformation constant for the impedance from a characteristic plane in guide two to a characteristic plane in guide one is the reciprocal of that from guide one to guide two. Alternatively and with much less work a good approximation to the phase of the transmitted wave can be obtained from the coefficients D_n for

$$A_1 = \sum_{n=1}^{\infty} R_{n1} D_n \quad \text{and} \quad D_1 = 1+R.$$

If the value of A_1 is $|A_1|e^{j\alpha}$ the transmitted wave will be $|A_1| F_1 e^{-\gamma_1 z + j\alpha}$. From the phase of the transmitted wave the characteristic plane in the output guide can be located. This is fully discussed in appendix I.

CHAPTER 3.

Experimental Technique

3.1. Description of Apparatus :

For the measurements made on the dielectric strips and quarter wave transformers a conventional 3cm. microwave bench was used. The standard equipment such as standing wave gear, movable short-circuiting plunger, oscillator, power supply and so forth were all of conventional design and commercially made. For the frequency range from 3.00 cm. to 3.20 cm. a CV-322 valve was used. For the range from 3.20 cm. to 3.65 cm. a CV-129 valve was used. The reflector and grid voltages were obtained from dry cell batteries and an electronically stabilized 1.5 K.V. power supply was used for the anode voltage. The oscillator wavelength was determined by a calibrated absorbtion type wave meter inserted between the standing wave gear and a 10 Db. attenuation pad used to isolate the oscillator from the rest of the waveguide set up. No frequency pulling of the oscillator was detectable with this 10 Db. attenuation pad. The crystal current from the standing wave gear probe was read on a 0-6 microamp meter.

The measurements on the free space lens matching section was made on a 10 cm. strip transmission line which had been built by the Electrical Engineering Workshop staff at City and Guilds College. A full description of this line will be found in a University of London Ph.D. thesis by Kharadhi. (3.1-1). On this line it is possible to measure reflection coefficients as small as .003 although the accuracy is only about 50% for these small values of reflected power. For much larger

values of reflection coefficients the accuracy increases to about 1% or so.

3.2. Method of Measurement :

In all cases the Weissfloch technique with minor modifications was used to obtain the equivalent circuits or the values of the reflection coefficients being sought. A full account off the basic method is found in appendix I.

For the asymmetrical dielectric strip the position of a field minimum was determined for various lengths of samples varying over half a wavelength in approximately .04 wavelength increments, thus giving about twelve points. One end of the sample was kept against a short circuiting plate in the waveguide. A movable short circuit was not used since the equivalent circuit of one discontinuity only was sought. It is possible to find the equivalent circuit of one junction by measurements made on one sample only, provided the structure is symmetrical along the longitudinal axis. This is discussed in section 3.3. However it was felt that the above method was more accurate.

For measurements on the quarter wave transformers a movable short-circuit was used since it was possible to determine the effective position of a short circuit in the dielectric when the position of a short in the empty guide was known. This equivalent position was obtained from the followinganalysis.

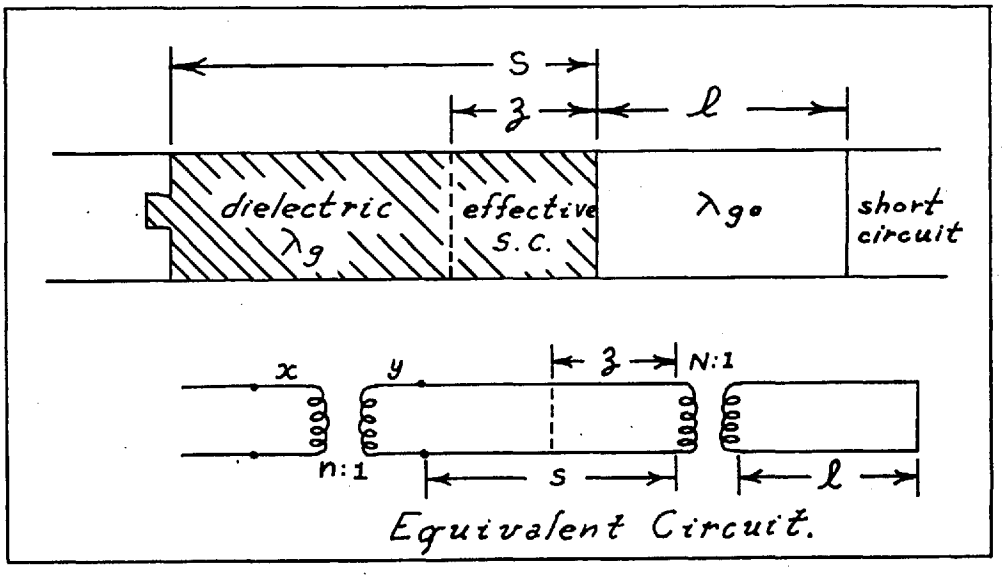


Fig. 3.2-1

The effect of the plane dielectric interface can be accounted for by an ideal transformer of turn ratio given by

$$N = \sqrt{Z_{go}/Z_g} \quad \text{where} \quad Z_{go}/Z_g = \lambda_{go}/\lambda_g = \sqrt{\frac{K-(\lambda_o/2a)^2}{1-(\lambda_o/2a)^2}}$$

where K is the dielectric constant, λ_o the free space wavelength and a is the waveguide width. The effective short is located in the dielectric at a position where the input impedance is zero i.e. where the electric field is zero, and is given by

$$\tan\beta_g z = -\left(Z_{go}/Z_g\right)\tan\beta_{go}\ell \,.$$

When z is known then the equivalent circuit of the transformer section is readily obtained by the usual method as detailed in appendix I. At the matching frequency $x = y = 0$ and $n^2 = \frac{Z_{go}}{Z_g}$ so that

$$\tan\beta_{go} d = -\tan\beta_g(s-z) \,.$$

Thus

$$\frac{\tan\beta_g s - \tan\beta_g z}{1+\tan\beta_g s\tan\beta_g z} = \frac{\tan\beta_g s + \frac{Z_{go}}{Z_g}\tan\beta_{go}\ell}{1-\frac{Z_{go}}{Z_g}\tan\beta_g s\tan\beta_{go}\ell}$$

and it

follows that

$$\tan\beta_{go}d - \frac{z_{go}}{z_g}\tan\beta_{go}d\tan\beta_g S\tan\beta_{go}l = -\tan\beta_g S - \frac{z_{go}}{z_g}\tan\beta_{go}l$$

$$\text{or} \quad \tan(\beta_{go}d + \beta_g S) = -\frac{z_{go}}{z_g}\tan\beta_{go}l = \tan\beta_g z .$$

Therefore

$$\beta_g z = \beta_{go}d + \beta_g S$$ at the matching frequency.

In all cases a position of a field minimum was determined by averaging the two readings obtained for current readings of approximately 1/10 full scale on either side of the minimum. It was estimated that a position of a minimum could be determined to $\pm$ .005 cm. The position of a short circuit was determined to about the same degree of accuracy. The maximum error for the width W of the curve $\beta_{go}d+\beta_g l$ *vs* $\beta_{go}d$ was then of the order of $\pm$ .03 radians which corresponds to approximately .0225% of reflected power, an amount which is 36.5 Db. below the incident power. Since the width of the curve is based on the average of several points it is reasonable to expect an overall accuracy greater than this. For the quarter wave transformers only the magnitude of the reflection coefficient was measured.

The same technique was used to obtain the modulus of the reflection coefficient for the free space matching section with the exception that the short circuit was fixed and the sample was moved instead. The reason was simply that a movable short circuit was not available.

3.3. Equivalent Circuit of a Symmetrical Structure.

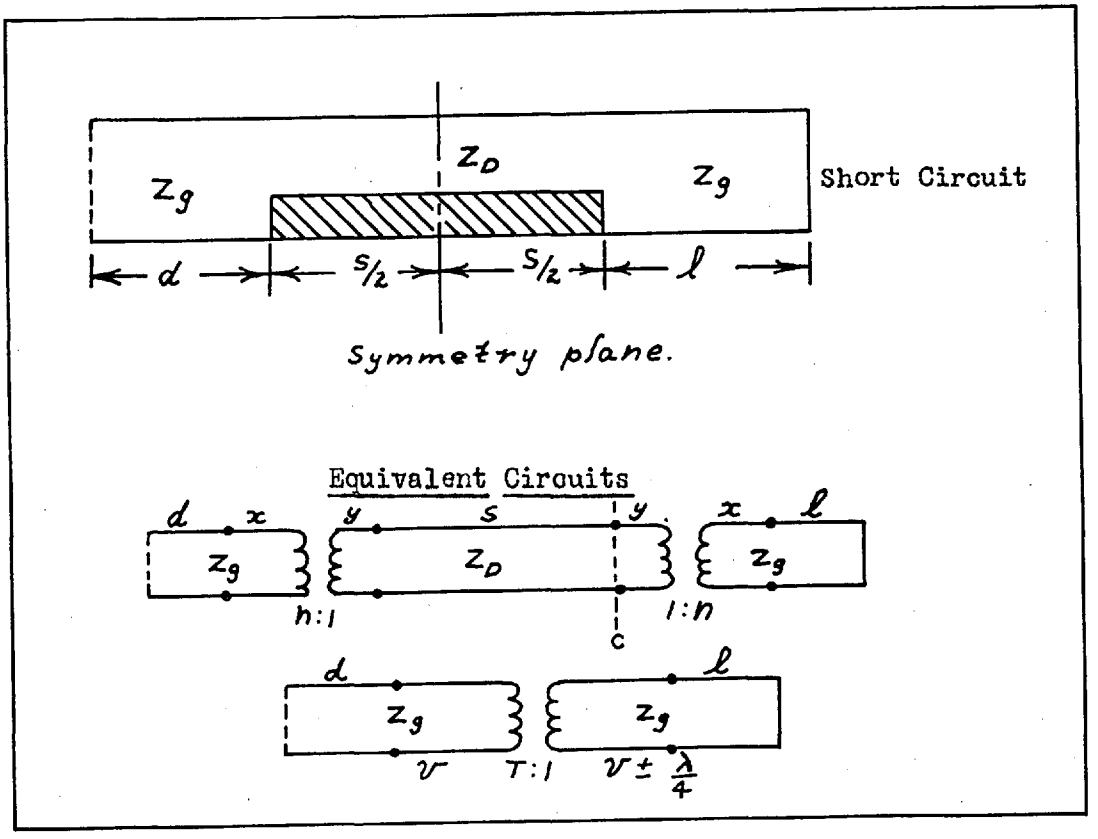


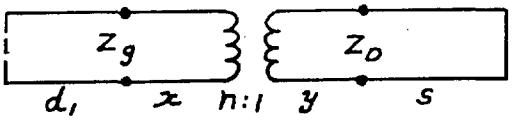
Fig. 3.3-1

For each junction there are three parameters (n, x, y) to be determined. For the overall structurd two parameters (T, v) suffice to describe completely the effect of the structure on the propagating mode.

One method of determining the equivalent circuit of one junction is to measure the position of a field minimum for a series of lengths of the structure all terminated in a short circuit. The parameters are then obtained from an analysis of the Weissfloch curve so obtained. By terminating the structure in a short circuit one junction effect is completely eliminated. However the process is tedious due to the

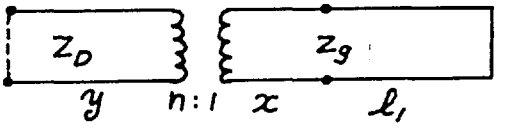
continual cutting of the sample length required.

For a symmetrical structure the following procedure can be used. With a short circuit located at the back junction let the field minimum be at d_1, measured from the front junction. This corresponds to a short at the plane C in the first equivalent circuit in figure 3.3-1. Hence the following relation holds



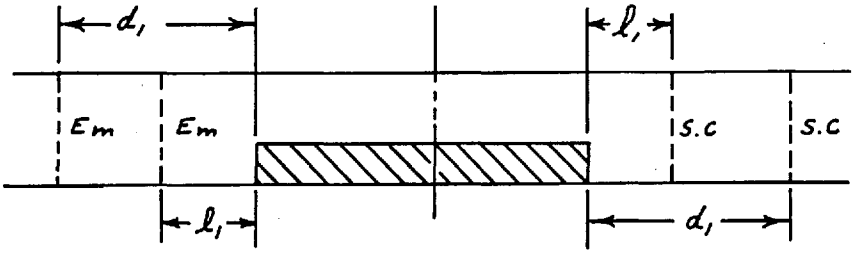
$$n^2 Z_0 \tan\beta_0(y+s) = -Z_g \tan\beta_g(x+d_1). \qquad (1)$$

Now move the short back a distance $\ell_1 + \frac{n\lambda_g}{2}$ (where n is large enough to ensure no interaction with higher order modes) so as to keep d_1 fixed. This must then correspond to a short reflected into the plane C and the following relation holds.

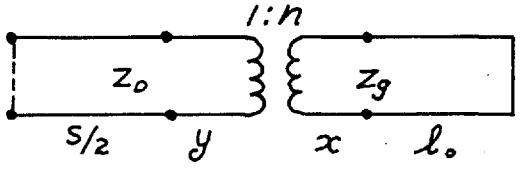


$$n^2 Z_0 \tan\beta_0 y = -Z_g \tan\beta_g(x+\ell_1). \qquad (2)$$

A check on the values of ℓ_1 and d_1 is obtained by interchanging the role of the short circuit and $E_{min.}$ position. Thus with a field minimum at the first junction the short circuit is located a distance d_1 from the back junction. In order to determine all three parameters one more relation is required and this can be obtained by a consideration of the symmetrical properties of the structure. For some setting of the short circuit an open or a short circuit is reflected into the symmetry plane. It is readily seen then that the position of a field minimum must be the same distance in front of the structure as the short circuit is behind it and hence $\ell = d = \ell_0$.



As the short circuit moves from a position at l_1 to d_1, E_m moves from d_1 to l_1 and somewhere in between l must equal d and the following relation holds



$$n^2 Z_0 \tan\beta_0(y+S/2) = -Z_g \tan\beta_g(x+l_0) \qquad (3)$$

where a short circuit has been assumed at the symmetry plane. This is permissible since the addition of $\pm \frac{\lambda_0}{2}$ to S changes a short circuit into an open circuit and is irrelevant to the problem. l_0 and d_0 are obtained from a plot of l vs d as the short circuit moves from l_1 to d_1. The values of l_0 and d_0 determine the characteristic planes for the overall structure i.e. they give the value of $\lambda_g/2 - v$ in the second equivalent circuit given in figure 3.3-1.

The three parameters can now be determined by a simultaneous solution of

$$n^2 Z_0 \tan\beta_0 y = -Z_g \tan\beta_g(x+l_1)$$
$$n^2 Z_0 \tan\beta_0(y+S/2) = -Z_g \tan\beta_g(x+l_0)$$
$$n^2 Z_0 \tan\beta_0(y+s) = -Z_g \tan\beta_g(x+d_1)$$

This method assumes a previous knowledge of β_g and β_D. If S happened to be $n\frac{\lambda_D}{2}$ long then the above equations are not independent. In this case the reflections from the front and back ends cancel and there is in effect no discontinuity in the waveguide. These equations are somewhat difficult to solve analytically but by a graphical method a solution is quite readily obtained. Thus dividing pairs of equations by each other gives

$$\frac{\tan\beta_D y}{\tan\beta_D(y+\frac{S}{2})} = \frac{\tan\beta_g(x+l_1)}{\tan\beta_g(x+l_0)}, \qquad \frac{\tan\beta_D y}{\tan\beta_D(y+S)} = \frac{\tan\beta_g(x+l_1)}{\tan\beta_g(x+d_1)}.$$

Now plot the right hand functions against x for a range of x of half a wavelength. Also plot the left hand sides versus y on another graph. By superimposing the two graphs so obtained and displacing the one longitudinally with respect to the other one the values of x and y for which both equations are satisfied is readily obtained. From any one equation n^2 is then found at once.

CHAPTER 4.

H-Plane Dielectric Step Discontinuities

4.1. The Asymmetrical Step.

The asymmetrical dielectric strip in a rectangular wave guide exhibits a considerable inductive effect at the discontinuity and was considered as an ideal specimen to use for a check on the theory developed in chapter two. Its use as a matching section is undesirable since it excites the second mode which can propagate in the dielectric filled guide. The symmetrical dielectric strip does not excite the H_{02} mode due to its symmetrical position in the guide.

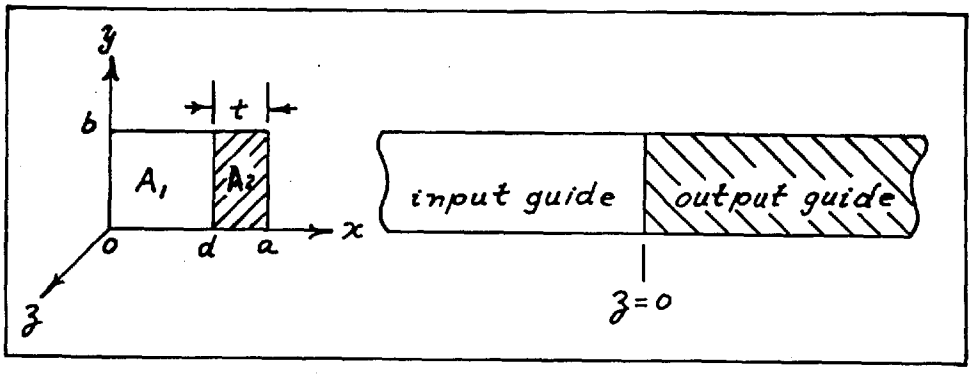


Fig. 4.1.-1

In the region A_1 the electric field is given by

$$E_y = \sum_1^\infty A_n \sin k_n x \; e^{-\gamma_n z}$$

where $\gamma_n^2 = k_n^2 - k_0^2$ and is negative for propagation to exist. The longitudinal magnetic field is given by

$$j\omega\mu H_z = - \sum_1^\infty A_n k_n \cos k_n x \; e^{-\gamma_n z}.$$

In the region A_2 filled with a lossless dielectric of relative dielectric constant $\epsilon/\epsilon_0 = K$ the electric field is taken as

$$E_y = \sum_1^\infty B_n \sin l_n(a-x)\, e^{-\gamma_n z}$$

with a longitudinal magnetic field,

$$j\omega\mu H_z = \sum_1^\infty B_n l_n \cos l_n(a-x)\, e^{-\gamma_n z}.$$

In order to satisfy the boundary conditions for all z the propagation constant γ_n must be the same in both A_1 and A_2, thus $l_n^2 - K k_0^2 = k_n^2 - k_0^2$. For some thickness of dielectric k_1 becomes zero, since the wavelength in the guide must be continuous from a value less than free space wavelength in air to a value greater than free space wavelength in air. The transition region is where k_1 changes from an imaginary quantity to a real quantity. At this critical thickness the field distribution is changed slightly from that given above although it does not increase the junction reactance. These special cases are discussed in appendix 4.

To find the conditions imposed on l_n and k_n the tangential fields are matched at the dielectric-air interface $x = d$, thus

$$A_n \sin k_n d = B_n \sin l_n t$$
$$A_n k_n \cos k_n d = -B_n l_n \cos l_n t.$$

Eliminating the constants A_n and B_n by dividing the first equation by the second gives

$$\frac{\tan k_n d}{k_n} = -\frac{\tan l_n t}{l_n}.$$

This transcendental equation together with the relation $l_n^2 - K k_0^2 = k_n^2 - k_0^2$ determines the eigenvalues l_n and k_n.

The constant B_n is given by $B_n = -\frac{\sin k_n d}{\sin l_n t} A_n$.

For large values of n it is easily seen that l_n and k_n approach each other. Also $\frac{\tan l_n t}{l_n}$ becomes increasingly closer to $\frac{\tan k_n d}{k_n}$ and hence $k_n (d+t)$ must approach $n\pi$ or the eigenvalues k_n and l_n both approach $\frac{n\pi}{a}$. This then shows that for large values of n the field distribution approaches that for the corresponding mode in the empty guide.

The complete solution for the fields existing in the partially filled guide is

$$\left.\begin{aligned} E_y &= \sum_1^\infty A_n \sin k_n x \; e^{-\gamma_n z} \\ j\omega\mu H_x &= -\sum_1^\infty A_n \gamma_n \sin k_n x \, e^{-\gamma_n z} \\ j\omega\mu H_z &= -\sum_1^\infty A_n k_n \cos k_n x \; e^{-\gamma_n z} \end{aligned}\right\} \quad 0 \le x \le d$$

$$\left.\begin{aligned} E_y &= \sum_1^\infty A_n \frac{\sin k_n d}{\sin l_n t} \sin l_n (a-x) \; e^{-\gamma_n z} \\ j\omega\mu H_x &= -\sum_1^\infty A_n \gamma_n \frac{\sin k_n d}{\sin l_n t} \sin l_n (a-x) \; e^{-\gamma_n z} \\ j\omega\mu H_z &= \sum_1^\infty A_n l_n \frac{\sin k_n d}{\sin l_n t} \cos l_n (a-x) \; e^{-\gamma_n z} \end{aligned}\right\} \quad d \le x \le a$$

Since only the transverse field components are involved in calculating the junction impedance it will now be shown by direct integration

that the transverse components of two distinct modes are orthogonal over the range $0 \leq x \leq a$. Thus

$$\int_0^d \sin k_n x \sin k_m x \, dx + \frac{\sin k_n d \sin k_m d}{\sin l_n t \sin l_m t} \int_d^a \{\sin l_n (a-x) \sin l_m (a-x)\} dx = \left\{ \frac{\sin (k_n - k_m) d}{2(k_n - k_m)} - \frac{\sin (k_n + k_m) d}{2(k_n + k_m)} \right\}$$

$$+ \frac{\sin k_n d \sin k_m d}{\sin l_n t \sin l_m t} \left\{ \frac{\sin (l_n - l_m) t}{2(l_n - l_m)} - \frac{\sin (l_n + l_m) t}{2(l_n + l_m)} \right\}.$$

The first bracket when expanded becomes

$$\frac{k_m \sin k_n d \cos k_m d - k_n \sin k_m d \cos k_n d}{2(k_n^2 - k_m^2)}.$$

The second bracket becomes

$$\frac{\sin k_n d \sin k_m d}{\sin l_n t \sin l_m t} \left\{ \frac{l_m \sin l_n t \cos l_m t - l_n \sin l_m t \cos l_n t}{2(l_n^2 - l_m^2)} \right\}$$

$$= \frac{\sin k_n d \sin k_m d}{2(l_n^2 - l_m^2)} \left\{ \frac{l_m}{\tan l_m t} - \frac{l_n}{\tan l_n t} \right\}.$$

Now by using the relations $\frac{\tan k_n d}{k_n} = -\frac{\tan l_n t}{l_n}$ and

$l_n^2 - l_m^2 = k_n^2 - k_m^2$ it follows that the second bracket finally becomes

$$\frac{k_n \sin k_m d \cos k_n d - k_m \sin k_n d \cos k_m d}{2(k_n^2 - k_m^2)}.$$

This is the negative of the first bracket and hence the integral vanishes and the orthogonality of the transverse field components is established. This result could have been taken directly from chapter 2 section 1.

The functions $F_m(x)$ will now be defined to be

$$F_m(x) = \begin{cases} \frac{1}{\sqrt{P_m}} \sin k_m x , & 0 \le x \le d , \\ \frac{1}{\sqrt{P_m}} \frac{\sin k_m d}{\sin l_m t} \sin l_m (a-x) , & d \le x \le a , \end{cases}$$

where $\sqrt{P_m}$ is a normalization constant given by

$$P_m = \int_0^d \sin^2 k_m x \, dx + \frac{\sin^2 k_m d}{\sin^2 l_m t} \int_d^a \sin^2 l_m (a-x) \, dx =$$

$$\tfrac{1}{2} d - \tfrac{1}{2} \frac{\cos k_m d \sin k_m d}{k_m} + \frac{\sin^2 k_m d}{\sin^2 l_m t} \left\{ \tfrac{1}{2} t - \tfrac{1}{2} \frac{\sin l_m t \cos l_m t}{l_m} \right\}$$

$$= \tfrac{1}{2} d - \tfrac{1}{4} \frac{\sin 2 k_m d}{k_m} + \frac{\sin^2 k_m d}{\sin^2 l_m t} \left\{ \tfrac{1}{2} t - \tfrac{1}{4} \frac{\sin 2 l_m t}{l_m} \right\}$$

$$= \tfrac{1}{2} \left\{ d + \frac{\sin^2 k_m d}{\sin^2 l_m t} t \right\} - \tfrac{1}{4} \frac{(K-1) k_0^2}{k_m l_m^2} \sin 2 k_m d .$$

The functions F_m so defined satisfy the following conditions

$$\int_0^a F_m F_n \, dx = \delta_{nm}$$

where $\delta_{nm} = 0$ for $n \neq m$, and $\delta_{nm} = 1$ for $n = m$.

To the left of the discontinuity the following set of orthogonal functions is taken to represent the incident, reflected and higher order components of the electric field.

$$\sqrt{2/a}\left\{\sin\frac{\pi x}{a}\,e^{-\Gamma_1 z} + R\sin\frac{\pi x}{a}\,e^{\Gamma_1 z} + \sum_{n=2}^{\infty} D_n \sin\frac{n\pi x}{a}\,e^{\Gamma_n z}\right\}$$

where $\Gamma_n^2 = \left(\frac{n\pi}{a}\right)^2 - k_0^2$. The corresponding transverse magnetic field is

$$\frac{j}{\omega\mu}\sqrt{2/a}\left\{\Gamma_1 \sin\frac{\pi x}{a}\,e^{-\Gamma_1 z} - \Gamma_1 R\sin\frac{\pi x}{a}\,e^{\Gamma_1 z} - \sum_{n=2}^{\infty} D_n \Gamma_n \sin\frac{n\pi x}{a}\,e^{\Gamma_n z}\right\}.$$

On the right hand side the proper functions are $F_m(x)$ and hence the total electric field is given by

$$\sum_{m=1}^{\infty} A_m F_m\, e^{-\gamma_m z}$$

with the following transverse magnetic field

$$\frac{j}{\omega\mu}\sum_{m=1}^{\infty} \gamma_m A_m F_m\, e^{-\gamma_m z}$$

As outlined in chapter two the following variational expressions for the junction admittance and impedance are obtained

$$\frac{1-R}{1+R} = \frac{\sum_{n=2}^{\infty}\Gamma_n D_n D_n^* + \sum_{m=1}^{\infty}\gamma_m \sum_{n=1}^{\infty} R_{nm} D_n \sum_{n=1}^{\infty} R_{nm} D_n^*}{\Gamma_1 D_1 D_1^*},$$

$$\frac{1+R}{1-R} = \frac{\sum_{n=2}^{\infty}\frac{1}{\Gamma_n} B_n B_n^* + \sum_{m=1}^{\infty}\frac{1}{\gamma_m}\sum_{n=1}^{\infty} R_{nm} B_n \sum_{n=1}^{\infty} R_{nm} B_n^*}{\frac{1}{\Gamma_1} B_1 B_1^*},$$

where an electric field aperture distribution of $\sum_{1}^{\infty} D_n \phi_n$ and a magnetic field aperture distribution of $\sum_{1}^{\infty} B_n \phi_n$ has been assumed, with ϕ_n identical to $\sqrt{2/a}\,\sin\frac{n\pi x}{a}$.

The factors R_{nm} are given by $R_{nm} = \int_0^a \varphi_n F_m \, dx =$

$$\frac{(K-1)\sqrt{2/a}\,P_m\, k_0^2}{\left\{k_m^2-\left(\frac{n\pi}{a}\right)^2\right\}\left\{l_m^2-\left(\frac{n\pi}{a}\right)^2\right\}}\left\{\frac{n\pi}{a}\sin k_m d\cos\frac{n\pi d}{a} - k_m\cos k_m d\sin\frac{n\pi d}{a}\right\}.$$

When the output guide is terminated in a short circuit located a distance l to the right of the junction the following variational expressions are obtained

$$\tan\frac{\theta}{2} = \frac{\sum_{n=2}^{\infty}\Gamma_n D_n^2 + \sum_{m=2}^{\infty}\gamma_m\left(\sum_{n=1}^{\infty}R_{nm}D_n\right)^2 + |\gamma_1|\tan\frac{\alpha}{2}\left(\sum_{n=1}^{\infty}R_{n1}D_n\right)^2}{\beta_1 D_1^2},$$

$$\cot\frac{\theta}{2} = \frac{\sum_{n=2}^{\infty}\frac{1}{\Gamma_n}B_n^2 + \sum_{m=2}^{\infty}\frac{1}{\gamma_m}\left(\sum_{n=1}^{\infty}R_{nm}B_n\right)^2 + \frac{\cot\frac{\alpha}{2}}{|\gamma_1|}\left(\sum_{n=1}^{\infty}R_{n1}B_n\right)^2}{1/\beta_1\ B_1^2}$$

where $\tan\frac{\theta}{2} = \tan\left(\beta_1 d+\frac{\pi}{2}\right) = -\cot\beta_1 d$ and

$\tan\frac{\alpha}{2} = \tan\left(\frac{\pi}{2}-|\gamma_1|l\right) = \cot|\gamma_1|l$.

4.2. Numerical Work

The various propagation constants, the matrix elements R_{nm}, normalization constants P_m and the other data required for the solution of the input impedance of a dielectric step discontinuity in a rectangular guide are tabulated in table 4.2-1 below. All the numerical work was done on a conventional 10" slide rule. The free space wavelength is λ_0, the empty guide wavelength λ_{g0} and the guide wavelength in the partially filled guide is λ_g.

Table 4.2-1

$\lambda_o = 3.14$ cm, $\lambda_g = 3.22$ cm, $\lambda_{go} = 4$ cm, $K = 2.47$
$a = 2.54$ cm, $b = \frac{1}{2}a$, $t = .70$ cm, $d = 1.84$ cm,

$\gamma_1 = j1.95$	$R_{11} = .925$	$k_1 = .45$
$\gamma_2 = .565$	$R_{21} = -.335$	$k_2 = 2.08$
$\gamma_3 = 2.87$	$R_{31} = .140$	$k_3 = 3.49$
$\gamma_4 = 4.36$	$R_{12} = .356$	$k_4 = 4.80$
$\Gamma_1 = j1.57$	$R_{22} = .920$	$l_1 = 2.48$
$\Gamma_2 = 1.45$	$R_{32} = -.166$	$l_2 = 3.20$
$\Gamma_3 = 3.12$	$R_{13} = -.077$	$l_3 = 4.26$
$P_1 = .578$	$R_{23} = .224$	$l_4 = 5.38$
$P_2 = 1.082$	$R_{33} = 1.03$	$\frac{\pi}{a} = 1.235$
$P_3 = 1.15$	$R_{14} = .021$	$\frac{2\pi}{a} = 2.47$
$P_4 = 1.22$	$R_{24} = -.051$	$\frac{3\pi}{a} = 3.71$
	$R_{34} = -.015$	$\frac{4\pi}{a} = 4.95$
	$R_{44} = 1.0$	

In table 4.2-2 are given the calculated values of the coefficients and input impedance and admittance for a one, two and a three term approximation to the aperture fields. The input admittance and impedance marked by a star were calculated from the variational expressions obtained by multiplying by the conjugate fields.

Table 4.2-2

Coeff. D_n	$\frac{1-R}{1+R}$	Reciprocal	Coeff. B_n	$\frac{1+R}{1-R}$	Reciprocal
$D_1 = 1.00$	$1.062 - j.0575$	$.937 + j.0507$	$B_1 = 1.00$	$.69 + j.355$	$1.15 - j.59$
			Ave.	$.826 + j.224$	
$D_1 = 1$ $D_2 =$ $-.032 + j.294$	$1.10 - j.169$ $[1.10 - j.1685]^*$	$.89 + j.137$	$B_1 = 1$ $B_2 =$ $-.258 - j.079$	$.825 + j.143$ $[.825 + j.143]^*$	$1.18 - j.204$
			Ave.	$.856 + j.140$	
$D_1 = 1$ $D_2 =$ $-.038 + j.315$ $D_3 =$ $.041 - j.072$	$1.115 - j.180$ $[1.12 - j.181]^*$	$.876 + j.141$	$B_1 = 1$ $B_2 = -.24 - j.064$ $B_3 = .115 + j.081$	$.855 + j.141$ $[.855 + j.140]^*$	$1.14 - j.188$
			Ave.	$.861 + j.141$	

It is seen that the degree of approximation obtained from the variational expressions involving the conjugate fields is almost identical with that obtained from the alternate formulation. Multiplying by the conjugate of the fields has the advantage of simplifying the numerical work to quite an extent. For a single term approximation the real part of the impedance is correct to within 7% but the reactive term is only within an order of magnitude. Two terms give a considerably more accurate result while three terms give a result within 2% for both the real and imaginary parts. It is seen that the average of the two calculations is closer to the correct result than either individual calculation. In this example the real part is always too small while the imaginary part comes out algebraically too large.

In table 4.2-3 are given the calculated values of $\tan\frac{\theta}{2}$ for various values of $\tan\frac{\alpha}{2}$ obtained by using a two term approximation to the aperture fields. The values of $\beta_1 d$ and $|\gamma_1| l$ are obtained from $\tan\frac{\theta}{2}$ and $\tan\frac{\alpha}{2}$ by the previously given relations. (see end of section 4.1). Along with each value of $\tan\frac{\theta}{2}$ is given the upper and lower bounds for it, expressed on a percentage basis.

Table 4.2-3

$\tan\frac{\alpha}{2}$	D_2	B_2	$\tan\frac{\theta}{2}$	$(\cot\frac{\theta}{2})^{-1}$	Ave. $\tan\frac{\theta}{2}$	$\beta_1 d$	$\lvert\gamma_1\rvert l+\beta_1 d$
.20	-.00374	.0823	.274	.260	.267± 2.5%	1.832	.064
.50	.0785	-.1155	.591	.585	.588 ± .5%	2.103	.068
1	.206	-.190	1.08	1.065	1.072 ± .8%	2.391	.035
2	.429	-.225	1.93	1.86	1.895 ± 2%	2.656	-.022
4	.78	-.244	3.52	3.00	3.26 ± 8%	2.844	-.053
-4	-2.033	-.283	-7.74	-11.65	-9.69 ± 20%	3.242	-.145
-2	-.799	-.303	-2.78	-3.32	-3.05 ± 9.7%	3.459	-.147
-1	-.389	-.344	-1.205	-1.371	-1.288 ± 6.5%	3.801	-.127
-.50	-.216	-.426	-.543	-.609	-.576 ± 6%	4.190	-.059
-.20	-.121	-.708	-.178	-.214	-.196 ± 9.2%	4.519	+.003

For small values of $\tan\frac{\theta}{2}$ the error in $\frac{\theta}{2}$ is of the same order as the error in $\tan\frac{\theta}{2}$ but for values of $\tan\frac{\theta}{2}$ very large the error in the angle is considerably less. Thus when $\tan\frac{\theta}{2}$ is equal to $-9.69 \pm 20\%$ the value of $\frac{\theta}{2}$ is $1.67 \pm 1.5\%$

and consequently the value of $\beta_1 d + \frac{\pi}{2}$ is also within $\pm$ 1.5%.

In table 4.2-4 are given the values of $\beta_1 d$ and $\beta_1 d + |\gamma_1| l$ as determined experimentally by measuring the position of a field minimum with various lengths l of the dielectric strip all terminated by a short circuit.

Table 4.2-4

l cm.	d cm.	$\beta_1 d$	$\lvert\gamma_1\rvert l$	$\beta_1 d + \lvert\gamma_1\rvert l - 3\pi$
3.31	1.84	2.89	6.46	-.075
2.96	2.23	3.50	5.78	-.145
2.77	2.50	3.93	5.40	-.095
2.65	2.69	4.22	5.17	-.035
2.33	3.15	4.95	4.55	.075
2.11	3.41	5.35	4.12	.045
2.02	3.52	5.52	3.94	.035
1.67	3.87	6.08	3.26	-.085
1.48	4.06	6.39	2.89	-.145
1.17	4.48	7.04	2.285	-.100
1.17	4.49	7.055	2.285	-.085
1.08	4.63	7.25	2.10	-.075
.94	4.84	7.58	1.835	-.010
.845	4.97	7.81	1.65	+.035
.71	5.16	8.11	1.385	+.070

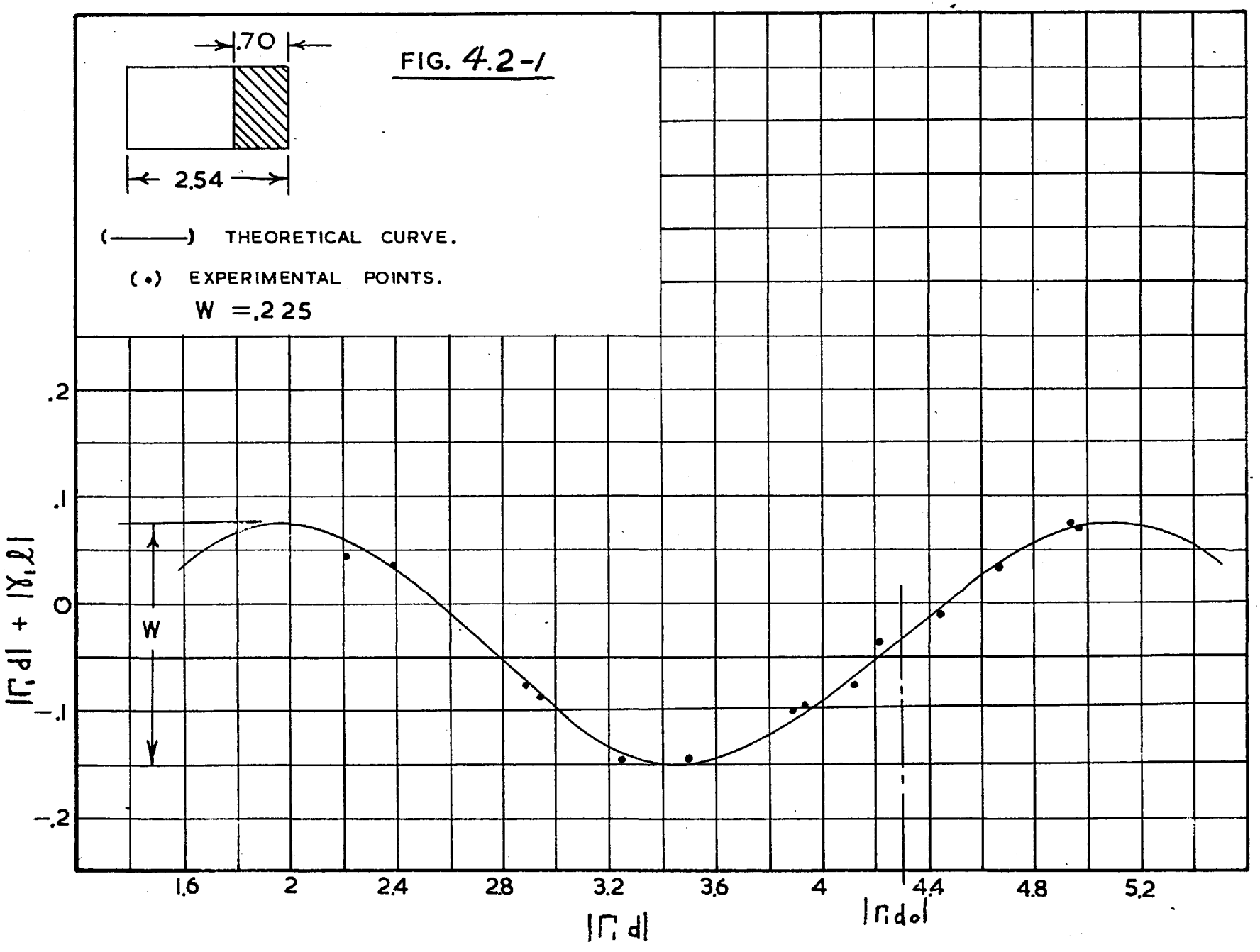
The experimental and theoretical values of $\beta_1 d + |\gamma_1| \ell$ versus $\beta_1 d$ are plotted in figure 4.2-1. There is excellent agreement between the two. The experimental points are within .015 of the theoretical values which is within the estimated experimental accuracy of the apparatus used.

From the curve a value of .797 is obtained for N^2 and a value of .125 $\lambda_{g_0}/2$ for x and .89 $\lambda_g/2$ for y . At a characteristic plane $\beta_1 d + |\gamma_1| \ell$ is equal to -.036. The calculated value of the reflection coefficient obtained from .861 $+ j$ .141 the value of $\frac{1+R}{1-R}$ taken from table 4.2-2 is .105 $\angle(\pi + .873)$. This is the reflection coefficient referred to the plane $z = 0$. The characteristic plane is located at a point where the equivalent reflection coefficient is a negative real quantity. R is taken as negative real to make $\frac{1+R}{1-R}$ less than unity so as to correspond to the characteristic planes chosen from the analysis of the curve. Therefore $.873 + \frac{4\pi}{\lambda_{g_0}} d_c = 2\pi$ or $d_c = 1.73$ cm. with a corresponding value of .135 $\lambda_{g_0}/2$ for x. The phase of the transmitted wave is obtained from the values of the three coefficients D_n taken from table 4.2-2, thus

$$A_1 = \sum_1^3 D_n R_{nm} = (R_{11} + R_{21} D_2 + R_{31} D_3)(1+R)$$

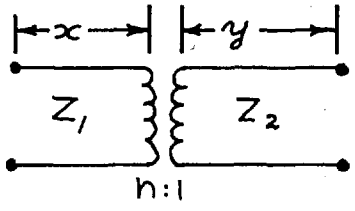
since the coefficients D_n have been solved for in terms of D_1 and D_1 is equal to $1+R$. Carrying out the numerical work gives $.89 - j.032$ for A_1 and hence $\alpha = -\tan^{-1} \frac{.032}{.89} = -.036$.

From the relation $\beta_1 d_c + |\gamma_1| \ell_c = \alpha$ given in appendix 1 a value of ℓ_c equal to .16 is obtained with a corresponding value of .90 $\lambda_g/2$ for y .


.70
2.54
FIG. 4.2-1
(———) THEORETICAL CURVE.
(•) EXPERIMENTAL POINTS.
W =.225
.2
.1
0
-.1
-.2
W
|Γ1d| + |Γ1d0|
1.6
2
2.4
2.8
3.2
3.6
4
4.4
4.8
5.2
|Γ1d|
|Γ1d0|

This value of y is within 1% of the value obtained from the curve. The value of N^2 obtained from $\frac{1-\rho}{1+\rho}$ at the characteristic plane is .81 with a value of 1.004 for n, the turns ratio of the ideal transformer. A value of .995 for n is obtained from the curve. The parameters of the equivalent circuit as obtained by the two different methods are summarized in table 4.2-5 below.

Table 4.2-5



$$\frac{Z_1}{Z_2} = \frac{\lambda_{g_0}}{\lambda_g}$$

	Output guide short circuited	Output guide matched.
x	$.125\ \frac{\lambda_{g_0}}{2}$	$.135\ \frac{\lambda_{g_0}}{2}$
y	$.89\ \frac{\lambda_g}{2}$	$.90\ \frac{\lambda_g}{2}$
n	.995	1.004

The junction impedance departs from its ideal value of λ_{g_0}/λ_g mainly by a reactive term which, although not very large, would have to be taken into consideration if asymmetrical dielectric steps were to be used for quarter-wave matching sections. The effect is inductive since only Hon modes are excited and they store more magnetic energy than electric energy.

If it had been desired to find the approximate eigenfunctions and

eigenvalues γ_m for the asymmetrical strip the functions $F_m(x)$ would have been approximated by a finite series of the functions $\sqrt{2/a}\,\sin\frac{n\pi x}{a}$. This procedure would have led to the following quadratic function

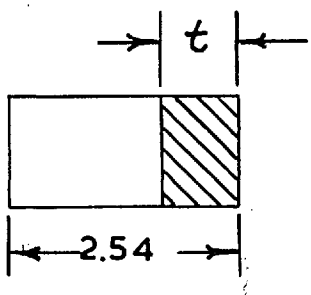
$$\sum_{n=1}^{N} \alpha_{nm}^2 \left[\gamma_m^2 + \frac{n^2\pi^2}{a^2} - \frac{8\pi}{\lambda_o^2}\left\{(K-1)\left(\frac{\pi t}{2a} - \frac{\sin 2n\pi t/a}{4n}\right) + \frac{\pi}{2}\right\}\right]$$

$$- \sum_{r,s=1}^{N} \frac{4\pi}{\lambda_o^2}\,\alpha_{rm}\,\alpha_{sm}\,(K-1)\left(\frac{\sin(r-s)\pi\frac{t}{a}}{r-s} - \frac{\sin(r+s)\pi\frac{t}{a}}{r+s}\right)(1-\delta_{rs})$$

where K is the dielectric constant and t is the thickness of the dielectric strip. This quadratic function would then be minimized by setting all $\frac{\partial}{\partial \alpha_{nm}}$ equal to zero. For the previously solved example a one term approximation of the above gave a value of $j\,1.78$ for γ_1. A two term approximation gave a value of $j\,1.83$ which is about 6% low. With the two term approximation a value of .70 was obtained for γ_2.

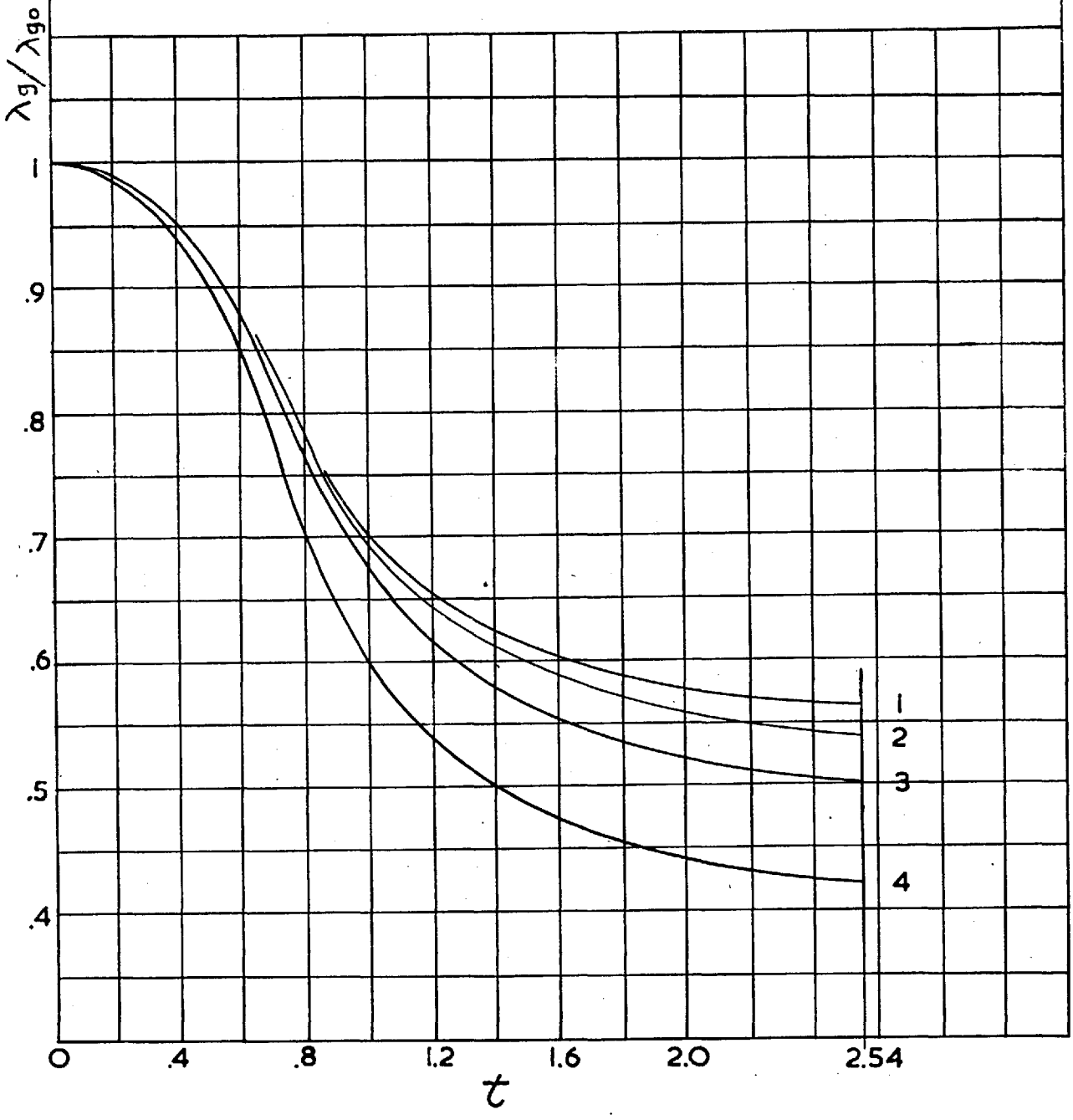
This work on the asymmetrical strip is concluded with a set of curves giving the ratio of the normalized impedance of the partially filled guide for various thicknesses of dielectric for several frequencies. From the curves in figure 4.2-2 it is seen that as the thickness increases the impedance falls off slowly at first and then more rapidly as the guide becomes about half filled. As the guide becomes almost completely filled the impedance varies more slowly again. This behaviour is caused by the concentration of the electric field lines in the centre of the guide.

FIG. 4.2-2



$\chi = 2.47$

1. $\frac{a}{\lambda_0} = .9$
2. $\frac{a}{\lambda_0} = .8$
3. $\frac{a}{\lambda_0} = .7$
4. $\frac{a}{\lambda_0} = .6$



4.3. The Symmetrical Step :

The analysis for the symmetrical dielectric strip illustrated in figure 4.3-1 is very similar to that for the asymmetrical strip so it will not be carried out in as much detail.

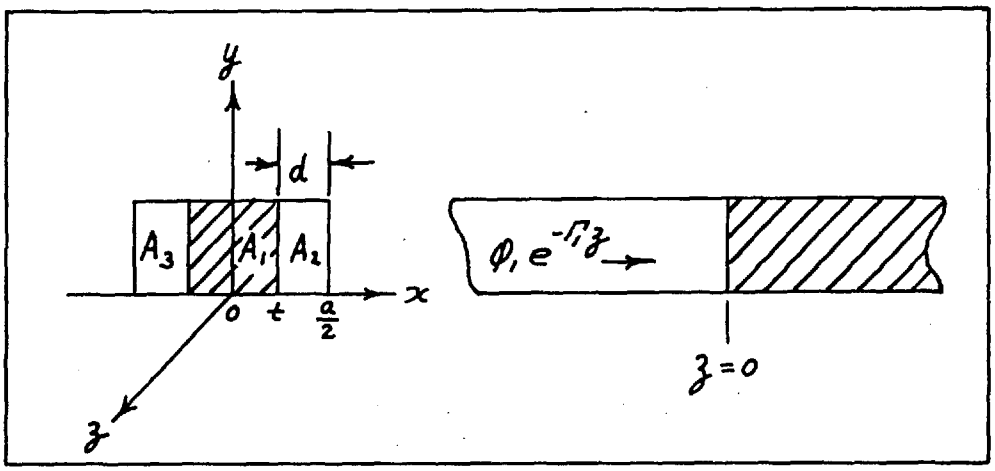


Fig. 4.3-1

In the region A_1 the fields are given by

$$E_y = \sum_1^\infty B_n \cos l_n x \; e^{-\gamma_n z},$$

$$j\omega\mu H_x = \sum_1^\infty B_n \gamma_n \cos l_n x \; e^{-\gamma_n z},$$

$$j\omega\mu H_z = \sum_1^\infty B_n l_n \sin l_n x \; e^{-\gamma_n z},$$

while in section A_2 they are given by

$$E_y = \sum_1^\infty C_n \sin k_n (c-x) \, e^{-\gamma_n z}, \quad \text{where } c = \frac{a}{2},$$

$$j\omega\mu H_x = \sum_1^\infty C_n \gamma_n \sin k_n (c-x) \, e^{-\gamma_n z},$$

$$j\omega\mu H_z = -\sum_1^\infty C_n k_n \cos k_n(c-x)\, e^{-\gamma_n z}.$$

At $x=t$ the tangential field components are continuous and hence

$$B_n \cos l_n t = -C_n \sin k_n d$$
$$B_n l_n \sin l_n t = -C_n k_n \cos k_n d$$

and therefore

$$\frac{\cot l_n t}{l_n} = \frac{\tan k_n d}{k_n} .$$

This transcendental equation together with the relation $\gamma_n^2 = k_n^2 - k_0^2 = l_n^2 - \kappa k_0^2$ determines the transverse wave numbers k_n and l_n and the propagation constants γ_n. The constants C_n are given by

$$C_n = -\frac{\cos l_n t}{\sin k_n d} B_n .$$

As before it can easily be seen that k_n and l_n both approach $(2n-1)\frac{\pi}{a}$ as n becomes large. It can be shown (see ref.1. and 2. at the end of appendix 3) that the propagation factor γ_n for the n'th mode in the partially filled guide lies between the corresponding propagation factors for the empty and completely filled guides. From this consideration it follows at once that k_n is always less than $(2n-1)\frac{\pi}{a}$ while l_n is always greater.

The solution in section A_3 is similar to that in section A_2. The complete solution for the electric field is now given by

$$E_y = \begin{cases} \sum_1^\infty B_n \cos l_n x \; e^{-\gamma_n z}, & -t \le x \le +t, \\ \sum_1^\infty B_n \dfrac{\cos l_n t}{\sin k_n d} \sin k_n (c-x) \, e^{-\gamma_n z}, & t \le x \le c, \\ \sum_1^\infty B_n \dfrac{\cos l_n t}{\sin k_n d} \sin k_n (c+x) \, e^{-\gamma_n z}, & -c \le x \le -t, \end{cases}$$

$$= \sum_1^\infty B_n F_n(x) \sqrt{P_n} \; e^{-\gamma_n z}$$ where $\sqrt{P_n}$ is a normalization constant determined so that

$$\int_{-\frac{a}{2}}^{\frac{a}{2}} F_n^2(x) \, dx = 1.$$

The transverse magnetic field is $-1/j\omega\mu \; \dfrac{\partial E_y}{\partial z}$. It can be shown by direct integration that the transverse components i.e. that the F_n are orthogonal over the range $-c \le x \le c$.

The junction is taken at the plane $z = 0$. In the input guide only the higher order H_{on} modes with n an odd integer will be excited since the dielectric strip is symmetrically located in the guide. The wave incident on the junction will be taken as

$$E_y = \cos \frac{\pi x}{a}, \quad H_x = \frac{\Gamma_1}{j\omega\mu} \cos \frac{\pi x}{a},$$

at the junction. The reflected wave plus higher order waves excited are given by

$$E_y = R \cos \frac{\pi x}{a} + \sum_2^\infty D_n \cos (2n-1) \frac{\pi x}{a}$$

$$j\omega\mu H_x = -\Gamma_1 R \cos \frac{\pi x}{a} - \sum_2^\infty \Gamma_n D_n \cos (2n-1) \frac{\pi x}{a}$$ at the junction, where $\Gamma_n^2 = (2n-1)^2 \dfrac{\pi^2}{a^2} - k_o^2$.

The functions $\phi_n(x)$ are defined to be $\sqrt{\frac{2}{a}} \cos(2n-1)\frac{\pi x}{a}$.

The matrix elements R_{nm} are by definition equal to

$$\int_{-c}^{+c} \phi_n F_m \, dx ,$$

and are given by

$$R_{nm} = \frac{\sqrt{\frac{2}{a P_m}}\, 2(K-1)k_0^2 \left\{ \frac{2n-1}{a}\pi \cos l_m t \sin \frac{2n-1}{a}\pi t - l_m \sin l_m t \cos \frac{2n-1}{a}\pi t \right\}}{\left\{ l_m^2 - \left(\frac{2n-1}{a}\pi\right)^2 \right\} \left\{ k_m^2 - \left(\frac{2n-1}{a}\pi\right)^2 \right\}}.$$

The normalization constants P_m are given by

$$P_m = \left\{ t + \frac{\cos^2 l_m t}{\sin^2 k_m d}(c-t) \right\} - \frac{(K-1)k_0^2 \sin 2 l_m t}{2 l_m k_m^2}.$$

By carrying out the analysis outlined in chapter two the following variational expressions are obtained for the input/and impedance admittance, thus

$$\frac{1+R}{1-R} = \frac{\sum_{n=2}^{\infty} \frac{1}{\Gamma_n} B_n B_n^* + \sum_{m=1}^{\infty} \frac{1}{\gamma_m} \sum_{n=1}^{\infty} R_{nm} B_n \sum_{n=1}^{\infty} R_{nm} B_n^*}{\frac{1}{\Gamma_1} B_1 B_1^*},$$

and

$$\frac{1-R}{1+R} = \frac{\sum_{n=2}^{\infty} \Gamma_n D_n D_n^* + \sum_{m=1}^{\infty} \gamma_m \sum_{n=1}^{\infty} R_{nm} D_n \sum_{n=1}^{\infty} R_{nm} D_n^*}{\Gamma_1 D_1 D_1^*}.$$

4.4. Numerical Work

In table 4.4.-1 are given the numerical values of the necessary constants for the solution of the junction impedance for a dielectric strip of .80 cm. thickness. Table 4.4.-2 gives similar data for a dielectric strip of .40 cm. thickness.

Table 4.4.-1

$\lambda_o = 3.14$ cm., $\lambda_{go} = 4$ cm, $\lambda_g = 2.49$ cm., $a = 2.54$ cm., $K = 2.47$, $2t = .80$ cm.

$\Gamma_1 = j1.57$	$\ell_1 = 1.885$	$P_1 = .915$	$R_{11} = .988$
$\Gamma_2 = 3.12$	$\ell_2 = 4.25$	$P_2 = 1.685$	$R_{12} = -.1765$
$\Gamma_3 = 5.85$	$\ell_3 = 6.51$	$P_3 = 1.295$	$R_{13} = -.0224$
$\Gamma_4 = 8.41$	$\ell_4 = 8.88$	$P_4 = 1.276$	$R_{14} = .004$
$\gamma_1 = j2.52$	$k_1 = j1.54$		
$\gamma_2 = 2.84$	$k_2 = 3.48$		
$\gamma_3 = 5.70$	$k_3 = 6.04$		
$\gamma_4 = 8.31$	$k_4 = 8.53$		

Table 4.4.-2

$\lambda_o = 3.14$ cm., $\lambda_{go} = 4$ cm., $\lambda_g = 2.937$ cm., $a = 2.54$ cm., $K = 2.47$, $2t = .40$ cm.,

$\Gamma_1 = j1.57$	$\ell_1 = 2.305$	$P_1 = .907$	$R_{11} = .984$
$\Gamma_2 = 3.12$	$\ell_2 = 4.285$	$P_2 = 1.54$	$R_{12} = -.1365$
$\Gamma_3 = 5.85$	$\ell_3 = 6.56$	$P_3 = 1.43$	$R_{13} = .0365$
$\Gamma_4 = 8.41$	$\ell_4 = 8.94$	$P_4 = 1.36$	$R_{14} = -.0135$
$\gamma_1 = j2.15$	$k_1 = j.782$		
$\gamma_2 = 2.90$	$k_2 = 3.525$		
$\gamma_3 = 5.75$	$k_3 = 6.09$		
$\gamma_4 = 8.36$	$k_4 = 8.60$		

In table 4.4.-3 are given the calculated values of the input admittance and impedance obtained by using only a one term approximation to the aperture fields.

Table 4.4.-3

$2t = .80$ cm.	$2t = .40$ cm.
$\frac{1-R}{1+R} = 1.565 - j.0636$	$\frac{1-R}{1+R} = 1.327 - j.0403$
$\frac{1+R}{1-R} = .606 + j.0158$	$\frac{1+R}{1-R} = .706 + j.0105$
Ave. $\frac{1-R}{1+R} = 1.61 \pm 3\% - j.053 \pm 20\%$	Ave. $\frac{1-R}{1+R} = 1.37 \pm 3.3\% - j.0306 \pm 30\%$
$\frac{\lambda_{g_0}}{\lambda_g} = 1.605$	$\frac{\lambda_{g_0}}{\lambda_g} = 1.362$

It is seen that a one term approximation to the aperture fields gives quite an accurate result for the resistance term. Although the reactive term is not very accurate the significant point is its very small magnitude. For a value of $1.61+j.06$ for $\frac{1-R}{1+R}$ the corresponding value of R is $-.234 \angle .075$. The value of x for the equivalent circuit is .02 cm. or 1% of $\lambda_{g_0}/2$ since $.075 + \pi d_c = 2\pi$ or $d_c = 1.98$ cm. and $x = \frac{\lambda_{g_0}}{2} - d_c = 2 - 1.98 = .02$ cm. Thus for normal values of dielectric constant the H plane symmetrical step behaves like an ideal transformer, transforming the impedance of the partially filled guide to that of the empty guide. A small junction reactance is negligible as far as the design of $\frac{1}{4}$ wave matching sections are concerned. This is due to the fact that a similar reactance at each end of a quarter-wave transformer tends to neutralize each other. This is easily seen to

be so since an inductive susceptance at one end of a quarter wave transformer is transformed into a capacitive susceptance at the other end and hence neutralizes the effect of the inductive susceptance already existing at the later end. (4.4.-1).

The above theory was not checked experimentally since it was felt that such a small junction effect could not be measured to any degree of accuracy. However a series of quarter-wave matching transformers where designed on the basis of the above theory and very good agreement was obtained between the calculated and measured bandwidth curves. This is covered in chapter six.

Approximations to the propagation constants γ_m can be obtained by minimizing the following energy integral

$$\int_{-c}^{+c} |\gamma_m|^2 \left(\sum_1^N \alpha_{nm} \phi_n\right)^2 dx + \int_{-c}^{+c} \left(\sum_1^N \alpha_{nm} \phi_n'\right)^2 dx - \int_{-c}^{+c} k_0^2 K(x) \left(\sum_1^N \alpha_{nm} \phi_n\right)^2 dx$$

where $\phi_n = \sqrt{\frac{2}{a}} \cos \frac{2n-1}{a} \pi x$ and $\phi_n' = \frac{d\phi_n}{dx}$.

Using only a one term approximation gives

$$\beta_1^2 = \frac{2}{a} k_0^2 \left\{ Kt + d + (K-1) \frac{a}{2\pi} \sin 2\pi \frac{t}{a} \right\} - \frac{\pi^2}{a^2}$$

where $2t$ is the thickness of the dielectric strip.

For $t =$ .20 cm. a value of 4.30 is obtained for β_1^2 and hence $\gamma_1 = j$ 2.08 a value about 3.2% too small. For $t =$ .40 cm., $\beta_1^2 = 5.90$ and $\gamma_1 = j$ 2.43 which is approximately 3.6% too small.

Curves for $\frac{Z_g}{Z_{go}} = \frac{\lambda_g}{\lambda_{go}}$ for various values of the parameter a/λ_o and for thicknesses ranging from zero to completely filled guide are given in figure 4.4.-1. A large scale drawing of these curves were used to obtain the design data for the dielectric step quarter-wave transformers investigated in chapter six.

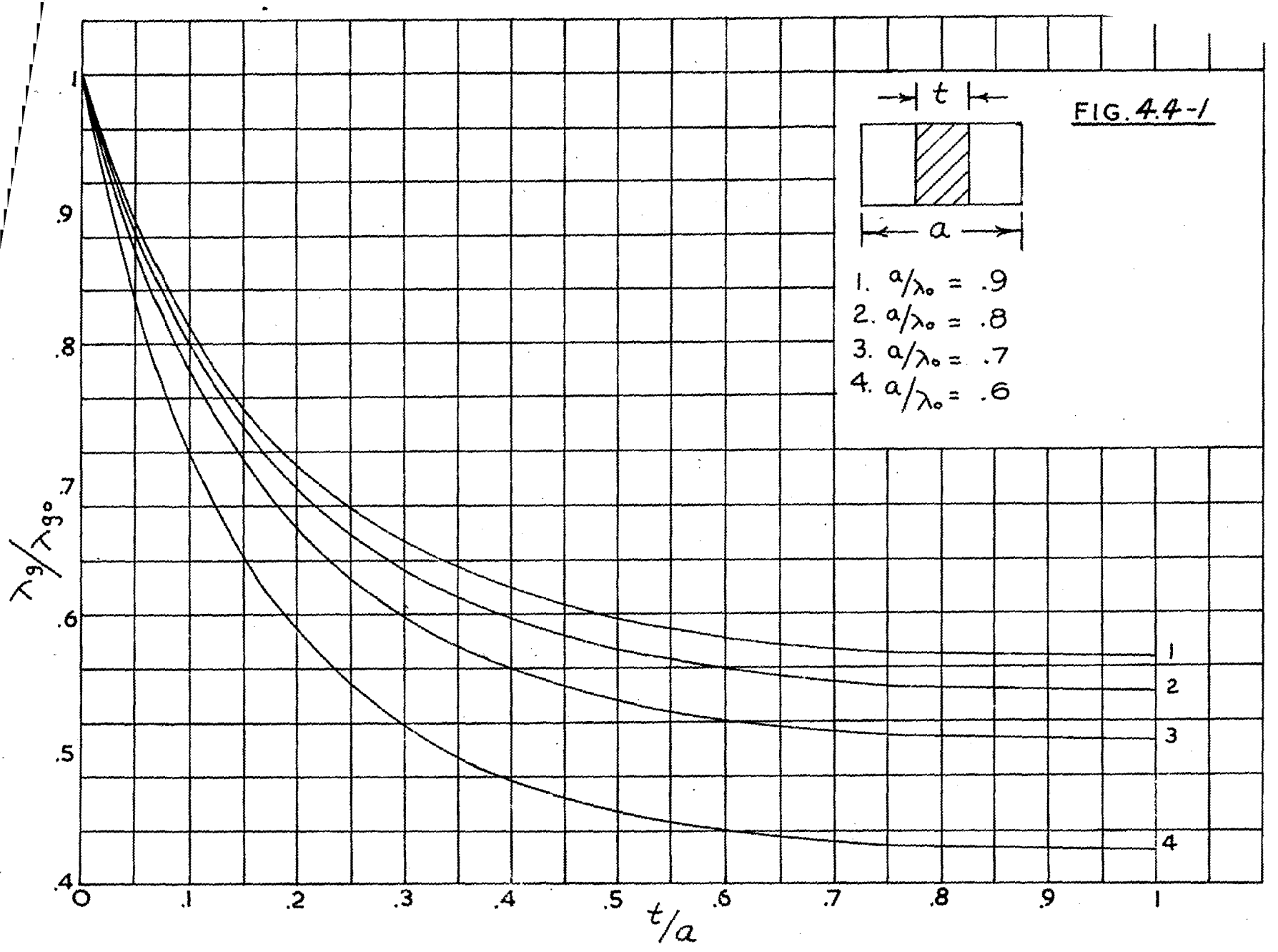

t
a
1. $a/\lambda_o = .9$
2. $a/\lambda_o = .8$
3. $a/\lambda_o = .7$
4. $a/\lambda_o = .6$
λ_g/λ_{g0}
t/a
1
.9
.8
.7
.6
.5
.4
0
.1
.2
.3
.4
.5
.6
.7
.8
.9
1
1
2
3
4

FIG. 4.4-1

Chapter 5.

E-Plane Dielectric Step in a Rectangular Wave Guide.

5.1. Theoretical Solution:

For a rectangular guide partially filled as in figure 5.1.-1, two independent types of modes can exist. The fields are not simple E or H modes but a combination of the two. For one set H_y is zero and these are called longitudinal section E waves. For the other set E_y is zero and the modes are referred to as longitudinal section H waves.(5.1.-1).

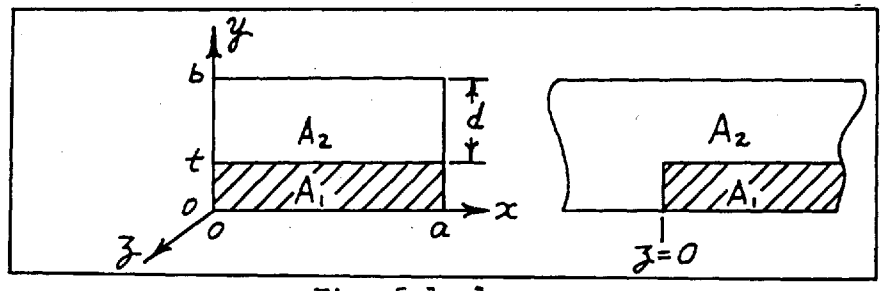


Fig. 5.1.-1.

It is easily verified that the longitudinal section E waves can be derived from an electric type Hertzian vector $\vec{\pi}_1$ directed along the y-axis by means of the following vector operations, (1.6.)

$$\vec{H} = j\omega\epsilon_0 K \nabla \times \vec{\pi}_1 ,$$

$$\vec{E} = \nabla\nabla\cdot\vec{\pi}_1 + K k_0^2 \vec{\pi}_1 ,$$

where K is the relative dielectric constant and $k_0^2 = \omega^2 \mu \epsilon_0$.

Similarly the longitudinal section H waves can be derived from a magnetic type Hertzian vector $\vec{\pi}_2$ directed along the y-axis by means of the following vector operations -

$$\vec{E} = -j\omega\mu \nabla \times \vec{\pi}_2 ,$$

$$\vec{H} = \nabla\nabla\cdot\vec{\pi}_2 + K k_0^2 \vec{\pi}_2 .$$

At the junction between the empty and partially filledguide it is found that both types of waves must be included in order to satisfy all boundary

conditions. It has been shown by Van Bladel that these normal modes form a complete set and any arbitrary field can be expanded in terms of them, (5.1-2).

The various field components are given by

$$E_x = \frac{\partial^2 \pi_1}{\partial x \partial y} + j\omega\mu \frac{\partial \pi_2}{\partial z}, \quad H_x = -j\omega\epsilon_0 K \frac{\partial \pi_1}{\partial z} + \frac{\partial^2 \pi_2}{\partial x \partial y},$$

$$E_y = \frac{\partial^2 \pi_1}{\partial y^2} + K k_0^2 \pi_1, \quad H_y = \frac{\partial^2 \pi_2}{\partial y^2} + K k_0^2 \pi_2,$$

$$E_z = \frac{\partial^2 \pi_1}{\partial z \partial y} - j\omega\mu \frac{\partial \pi_2}{\partial x}, \quad H_z = j\omega\epsilon_0 K \frac{\partial \pi_1}{\partial x} + \frac{\partial^2 \pi_2}{\partial z \partial y},$$

where both π_1 and π_2 satisfy the following wave equation

$$\nabla^2 \pi_i + K k_0^2 \pi_i = 0, \quad i = 1, 2 .$$

If the transverse field components are made continuous at the aperture plane $z = 0$, it is easily shown by taking the curl of the electric field and magnetic field in the aperture plane that the normal fluxes (i.e. $K E_z$ and H_z) are continuous respectively. Since π_1 and π_2 are not continuous across the aperture plane it is found to be more convenient to relate the fields to the y component of the total electric and magnetic field in the aperture. This procedure is justifiable since if E_y and H_y are known then π_1 and π_2 can be determined from E_y and H_y respectively. It is shown in Appendix 5 that to the first approximation the equivalent circuit of the step is independent of H_y, i.e. independent of π_2. This result is due to the fact that the longitudinal section H waves are evanescent and not very strongly excited.

If an H_{01} wave is incident on the step from the left then the input

admittance referred to the junction $z = 0$ is given by

$$\frac{1-R}{1+R}\Gamma_0 \int_0^b G_1^* \phi_0\, dy \int_0^b G_1 \phi_0\, dy = k_0^2 \left\{ \sum_1^\infty \frac{\Gamma_n}{k_0^2 - \frac{n^2\pi^2}{b^2}} \int_0^b G_1^* \phi_n\, dy \int_0^b G_1 \phi_n\, dy + \right.$$

$$\left. \sum_1^\infty \frac{\gamma_m}{k_0^2 - k_m^2} \int_0^b G_1^* F_m\, dy \int_0^b G_1 F_m\, dy \right\} - \left\{ \sum_1^\infty \frac{\Gamma_n}{k_0^2 - (\frac{n\pi}{b})^2} \int_0^b G_2^* \psi_n\, dy \int_0^b G_2 \psi_n\, dy + \sum_1^\infty \frac{\beta_m}{k_0^2 - g_m^2} \int_0^b G_2^* W_m\, dy \int_0^b G_2 W_m\, dy \right.$$

(1)

where G_1 and G_2 are complex functions of the real variable y and G_1 is equal to the y component of the electric field in the aperture and $G_2 / j\omega\mu$ is equal to the y component of the magnetic field in the aperture. G_1 and G_2 are also related through the continuity condition imposed on E_x, i.e.

$$\sum_1^\infty \frac{\Gamma_n}{k_0^2 - \frac{n^2\pi^2}{b^2}} \int_0^b G_2^* \psi_n\, dy \int_0^b G_2 \psi_n\, dy + \sum_1^\infty \frac{\beta_m}{k_0^2 - g_m^2} \int_0^b G_2^* W_m\, dy \int_0^b G_2 W_m\, dy$$

$$= \frac{\pi}{a} \left\{ \sum_1^\infty \frac{1}{k_0^2 - \frac{n^2\pi^2}{b^2}} \int_0^b G_1^* \frac{d\psi_n}{dy}\, dy \int_0^b G_2 \psi_n\, dy - \sum_1^\infty \frac{1}{k_0^2 - g_m^2} \int_0^b G_1^* \frac{dW_m}{dy}\, dy \int_0^2 G_2 W_m\, dy \right\}. \quad (2)$$

The functions ϕ_n, ψ_n, F_m, and W_m are the appropriate eigenfunctions for the Hertzian vectors π_1 and π_2 in the input and output guides and are functions of y only. The full analysis leading to the above two relations is given in appendix five. Equation (1) is clearly proportional to the difference between the electric and magnetic energy stored in the evanescent modes at the junction since it is in fact equal to $\int_a \vec{E}^* \times \vec{H} \cdot \vec{i}_z\, da$.

The longitudinal section E waves store an excess of electric energy while the longitudinal section H waves store more magnetic energy. It can be shown that $\frac{1-R}{1+R}$ is stationary with respect to arbitrary variations of G_1^* and G_2^* that satisfy equation (2). From equation (2) it can be seen that the magnetic energy stored in the H waves is small

since it is given by the difference of two quantities which are almost identical. This is due to the functions ψ_n and W_n being almost identical if the dielectric constant or t/b is not too great. Hence since $\frac{1-R}{1+R}$ is stationary a good approximation can be obtained by taking G_2 identically zero. The rest of the discussion in this chapter will be based on the assumption that G_2 is zero and so a procedure analogous to that used in chapter four will be applied here also.

The incident, reflected and higher order waves excited in the input guide will be taken as

$$E_y = \left[(1+R) k_0^2 \phi_0 + \sum_1^\infty D_n (k_x^2 - \Gamma_n^2) \phi_n \right] \sin k_x x,$$

$$H_x = j\omega\epsilon_0 \left[(1-R)\Gamma_0 \phi_0 - \sum_1^\infty \Gamma_n D_n \phi_n \right] \sin k_x x, \quad \text{at } z = 0,$$

where $\phi_0 = \sqrt{\frac{1}{b}}$, $\phi_n = \sqrt{\frac{2}{b}} \cos \frac{n\pi}{b} y$, $k_x = \frac{\pi}{a}$, $\Gamma_n^2 = \frac{n^2\pi^2}{b^2} + k_x^2 - k_0^2$, R is the reflection coefficient referred to $z = 0$, and variation with x is taken as $\sin k_x x$. The transmitted plus higher order waves excited in the output guide will be taken as

$$E_y = \sum_1^\infty A_m \frac{F_m(y)}{K(y)} (k_x^2 - \gamma_m^2) \sin k_x x,$$

$$H_x = j\omega\epsilon_0 \sum_1^\infty A_m \gamma_m F_m \sin k_x x, \quad \text{at } z = 0,$$

where the functions $F_m(y)$ are given by

$$F_m(y) = \frac{K}{\sqrt{P_m}} \begin{cases} \cos l_m y, & 0 \le y \le t, \\ \dfrac{\cos l_m t}{\cos k_m d} \cos k_m (b-y), & t \le y \le b, \end{cases}$$

with $\gamma_m^2 = l_m^2 + k_x^2 - K k_0^2 = k_m^2 + k_x^2 - k_0^2$ and $l_m \tan l_m t = -K k_m \tan k_m d$.

P_m is a normalization constant determined so that $\int_0^b \frac{F_m^2(y)}{K(y)} dy = 1$ where $K(y) = K$ for $0 \le y \le t$ and $= 1$ for $t \le y \le b$.

Equating E_y and H_x at the aperture gives

$$(1+R)k_0^2\phi_0 + \sum_1^\infty D_n(k_x^2-\Gamma_n^2)\phi_n = \sum_1^\infty A_m(k_x^2-\gamma_m^2)\frac{F_m(y)}{K(y)} = G(y),$$

$$(1-R)\Gamma_0\phi_0 - \sum_1^\infty D_n\Gamma_n\phi_n = \sum_1^\infty A_m\gamma_m F_m(y) = H(y),$$

where G and H are complex functions of the real variable y. By means of the general orthogonal principle discussed in chapter 2, section 1, the following expressions are obtained for the unknown coefficients D_n and A_m.

$$1+R = \frac{1}{k_0^2}\int_0^b G\phi_0\,dy, \quad D_n = \frac{1}{k_x^2-\Gamma_n^2}\int_0^b G\phi_n\,dy, \quad A_m = \frac{1}{k_x^2-\gamma_m^2}\int_0^b GF_m\,dy.$$

Following the same procedure as used in chapter four the following variational expression for the input admittance is obtained,

$$\frac{1-R}{1+R} = \frac{\sum_1^\infty \frac{\Gamma_n}{k_x^2-\Gamma_n^2}\int_0^b G^*\phi_n\,dy\int_0^b G\phi_n\,dy + \sum_1^\infty \frac{\gamma_m}{k_x^2-\gamma_m^2}\int_0^b G^*F_m\,dy\int_0^b GF_m\,dy}{\frac{\Gamma_0}{k_0^2}\int_0^b G^*\phi_0\,dy\int_0^b G\phi_0\,dy}.$$

Alternatively the unknown coefficients could be determined from $H(y)$ and this procedure would lead to the following variational expression for the input impedance,

$$\frac{1+R}{1-R} = \frac{\sum_1^\infty \frac{k_x^2-\Gamma_n^2}{\Gamma_n}\int_0^b H^*\phi_n\,dy\int_0^b H\phi_n\,dy + \sum_1^\infty \frac{k_x^2-\gamma_m^2}{\gamma_m}\int_0^b H^*\frac{F_m}{K(y)}dy\int_0^b \frac{HF_m}{K(y)}dy}{\frac{k_0^2}{\Gamma_0}\int_0^b H^*\phi_0\,dy\int_0^b H\phi_0\,dy}.$$

When $\frac{k_x^2 - \gamma_m^2}{\gamma_m}$ is negative an excess of electric energy is stored in the evanescent mode. In the partially filled guide there exists a thickness of dielectric for which the second mode will propagate. For thicknesses slightly less than this cutoff value $k_x^2 - \gamma_2^2$ is positive and more magnetic energy is stored in the mode.

If the output guide is terminated in a short circuit located a distance 'ℓ' from the junction then $\Gamma_0 \frac{1-R}{1+R}$ is replaced by $\beta_0 \tan\frac{\theta}{2}$ and γ_1 by $|\gamma_1| \tan\frac{\alpha}{2}$ where $\tan\frac{\alpha}{2} = \tan(\frac{\pi}{2} - |\gamma_1|\ell)$ and $\tan\frac{\theta}{2} = \tan(\beta_0 d + \frac{\pi}{2})$. The position of a field minimum in the input guide is determined by the value of 'd' measured from the junction.

If an aperture electric field distribution $\sum_0^\infty D_n \phi_n$ is assumed, then, $\frac{1-R}{1+R} = \frac{\sum_1^\infty \frac{\Gamma_n}{k_x^2 - \Gamma_n^2} D_n D_n^* + \sum_{m=1}^\infty \frac{\gamma_m}{k_x^2 - \gamma_m^2} \sum_0^\infty R_{nm} D_n \sum_0^\infty R_{nm} D_n^*}{(\Gamma_0/k_0^2)(D_0 D_0^*)}$

where R_{nm} are given by

$$R_{nm} = \int_0^b F_m \phi_n \, dy .$$

Similarly if an aperture magnetic field $\sum_0^\infty B_n \phi_n$ is assumed then

$$\frac{1+R}{1-R} = \frac{\sum_1^\infty \frac{k_x^2 - \Gamma_n^2}{\Gamma_n} B_n B_n^* + \sum_{m=1}^\infty \frac{k_x^2 - \gamma_m^2}{\gamma_m} \sum_0^\infty \chi_{nm} B_n \sum_0^\infty \chi_{nm} B_n^*}{(k_0^2/\Gamma_0)(B_0 B_0^*)}$$

where χ_{nm} are given by

$$\chi_{nm} = \int_0^b \phi_n \frac{F_m(y)}{K(y)} \, dy .$$

By suitably redefining the unknown coefficients and the matrix elements R_{nm} and χ_{nm} the factors $\frac{k_x^2 - \Gamma_n^2}{\Gamma_n}$ and $\frac{k_x^2 - \gamma_m^2}{\gamma_m}$ can be absorbed in them and this procedure would simplify the numerical work involved in solving for the unknown coefficients and evaluating the variational expression. This procedure is not adopted here since the above

formulation is somewhat more straightforward.

The normalization constants P_m and the matrix elements R_{nm} and χ_{nm} are given by the following expressions

$$P_m = \frac{K}{2}\left[\left(t + \frac{\sin 2\ell_m t}{2\ell_m}\right) + K\frac{\cos^2 \ell_m t}{\cos^2 k_m d}\left(d + \frac{\sin 2k_m d}{2k_m}\right)\right]$$

where $d = b - t$.

$$R_{om} = \sqrt{\frac{1}{b P_m}}\, K\left[\frac{\sin \ell_m t}{\ell_m} + \frac{\cos \ell_m t \sin k_m d}{k_m \cos k_m d}\right],$$

$$R_{nm} = \sqrt{\frac{2}{b P_m}}\,\frac{K}{2}\left[\left\{\frac{\sin(\ell_m + \frac{n\pi}{b})t}{\ell_m + \frac{n\pi}{b}} + \frac{\sin(\ell_m - \frac{n\pi}{b})t}{\ell_m - \frac{n\pi}{b}}\right\}\right.$$

$$\left. + \frac{\cos \ell_m t}{\cos k_m d}\left\{\frac{\sin(k_m d + \frac{n\pi t}{b})}{k_m - \frac{n\pi}{b}} + \frac{\sin(k_m d - \frac{n\pi t}{b})}{k_m + \frac{n\pi}{b}}\right\}\right],$$

for $n \geq 1$.

$$\chi_{om} = \sqrt{\frac{1}{b P_m}}\left[\frac{\sin \ell_m t}{\ell_m} + \frac{K \cos \ell_m t \sin k_m d}{k_m \cos k_m d}\right],$$

$$X_{nm} = \sqrt{\frac{2}{b P_m}} \frac{1}{2} \left[\left\{ \frac{\sin(l_m + \frac{n\pi}{b})t}{l_m + \frac{n\pi}{b}} + \frac{\sin(l_m - \frac{n\pi}{b})t}{l_m - \frac{n\pi}{b}} \right\} \right.$$

$$\left. + K \frac{\cos l_m t}{\cos k_m d} \left\{ \frac{\sin(k_m d + \frac{n\pi}{b}t)}{k_m - \frac{n\pi}{b}} + \frac{\sin(k_m d - \frac{n\pi}{b}t)}{k_m + \frac{n\pi}{b}} \right\} \right]$$

for $n \geq 1$.

5.2. Numerical Work

The equivalent circuit of a dielectric step ($t/b = .25$) will be obtained from a Weissfloch curve which will be calculated theoretically and checked experimentally. For this purpose the variational expressions appropriate to the case when the output guide is short circuited will be used. The aperture fields are real functions and each variational expression is a maximum for the correct fields since the second variation is negative. The second variation is negative because $k_x^2 - \Gamma_n^2$ and $k_x^2 - \gamma_m^2$ are negative. Upper and lower bounds are thus obtained for $\tan \frac{\theta}{2}$. If some of the modes store an excess of magnetic energy then the variational expressions are not positive definite quadratic forms and upper and lower bounds cannot be obtained. The calculated values of all the factors required for the solution of the problem are given in table 5.2.-1. The theoretical values of $\beta_0 d$ for various values of $|\gamma_1|l$ are given in table 5.2.-2. These values were calculated by using a two term approximation to the aperture fields. The values of B_1 and D_1 were found to be

$$B_1 = \frac{1.44 - \cot\frac{\alpha}{2}}{19.23 - .036\cot\frac{\alpha}{2}}, \qquad D_1 = \frac{1.053 - \tan\frac{\alpha}{2}}{.234\tan\frac{\alpha}{2} - 21.9}.$$

Table 5.2.-1.

$b = 1.27cm$, $t/b = .25$, $k_o^2 = 4$, $K = 2.56$, $k_x^2 = 1.53$, $\lambda_o = 3.14cm$, $\frac{\pi^2}{b^2} = 6.12$

$\Gamma_0 = j1.572$	$k_1 = j1.035$	$P_1 = 2.785$	$R_{11} = .268$	$\chi_{01} = .902$
$\Gamma_1 = 1.91$	$k_2 = 2.42$	$P_2 = 1.662$	$R_{12} = 1.252$	$\chi_{02} = -.19$
$\Gamma_2 = 4.70$	$k_3 = 4.68$	$P_3 = 1.058$	$R_{13} = .228$	$\chi_{03} = -.045$
$\Gamma_3 = 7.25$	$k_4 = 7.00$	$P_4 = 2.24$	$R_{14} = .081$	$\chi_{04} = -.0047$
$\gamma_1 = j1.88$	$\ell_1 = 2.275$	$R_{01} = 1.141$		$\chi_{11} = -.042$
$\gamma_2 = 1.84$	$\ell_2 = 3.48$	$R_{02} = .0853$		$\chi_{12} = .895$
$\gamma_3 = 4.41$	$\ell_3 = 5.30$	$R_{03} = .207$		$\chi_{13} = -.11$
$\gamma_4 = 6.825$	$\ell_4 = 7.44$	$R_{04} = .0825$		$\chi_{14} = -.051$

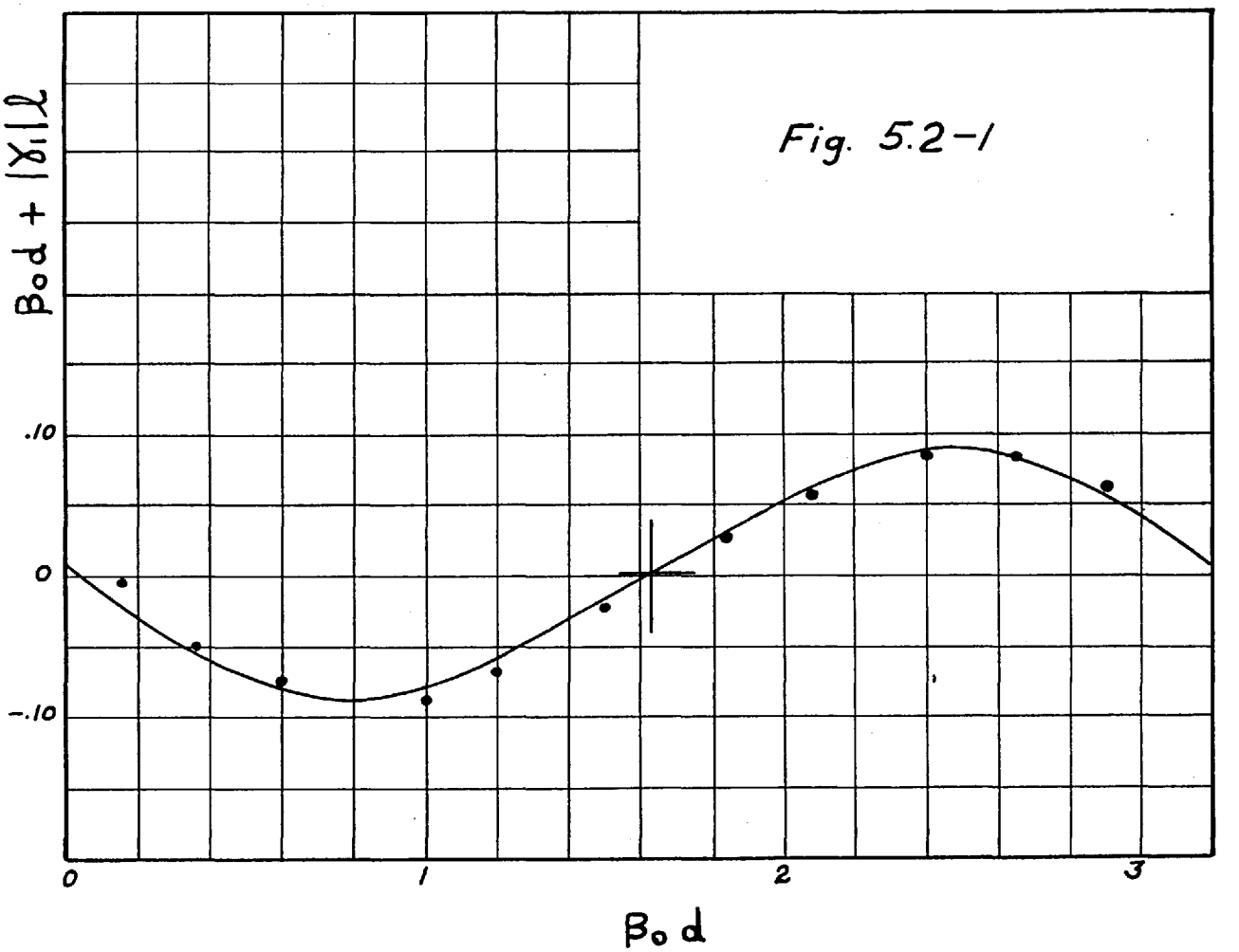
The calculated theoretical Weissfloch curve and the experimental points are plotted in figure 5.2.-1. The experimental procedure used was that given in chapter 3 - section 2.

The equivalent circuit for the above example is given in figure 5.2.-2. The equivalent circuit for a guide half filled is also given in figure 5.2.-2. This equivalent circuit was determined experimentally. It is seen that the step acts very nearly like an ideal transformer with a turns ratio of $\sqrt{\Gamma_0/\gamma_1}$. For the case when $t/b = .5$, $k_x^2 - \gamma_2^2$ is positive and the second mode in the partially filled guide stores an excess of magnetic energy which tends to neutralize the electric energy stored in the other modes. The difference between the electric and

magnetic energy stored is consequently very small and a very small phase shift is produced in the reflected and transmitted waves. From the equivalent circuit for the case when $t/b = .5$ it can easily be shown that there is an excess of magnetic energy stored at the junction. Thus for some thickness between $.25b$ and $.5b$ a condition of resonance exists and no phase shift is produced in the reflected and transmitted waves. The behaviour is analogous to that of the tuned window in a rectangular waveguide.

Table 5.2-2

$\tan\frac{\alpha}{2}$	D_1	B_1	$\tan\frac{\theta}{2}$	$(\cot\frac{\theta}{2})^{-1}$	Ave. $\tan\frac{\theta}{2}$	$\beta_0 d$	$\beta_0 d + 1/1.1 l$
.25	-.0367	-.134	.27	.29	.28 ± 3.6%	1.844	.028
.50	-.0254	-.0292	.575	.589	.58 ± 1.2%	2.098	.063
1	-.0024	.023	1.18	1.186	1.183 ± .3%	2.44	.083
2	+.044	.049	2.43	2.41	2.42 ± .4%	2.75	.072
-2	-.136	.10	-2.38	-2.26	-2.32 ± 2.6%	.407+π	-.057
-1	-.093	.127	-1.215	-1.16	-1.19 ± 2.4%	.70+π	-.089
-.50	-.0705	.178	-.63	-.584	-.607 ± 3.8%	1.025+π	-.082
-.25	-.0595	.28	-.33	-.29	-.31 ± 6.4%	1.27+π	-.066


Fig. 5.2-1
$\beta_0 d + |\gamma_1| l$
.10
0
-.10
0
1
2
3
$\beta_0 d$

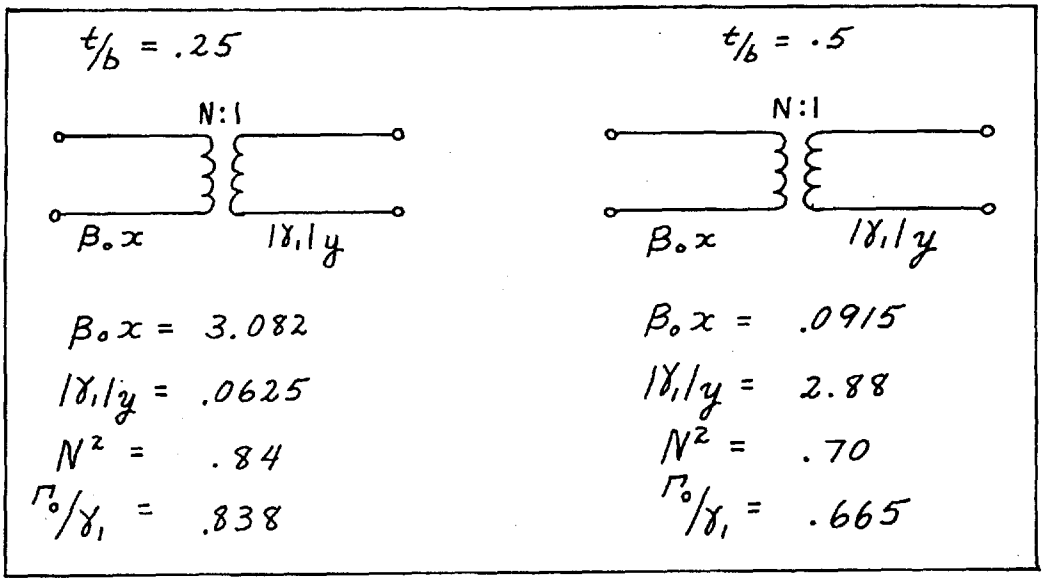


Fig. 5.2-2.

By image theory the above equivalent circuits are valid for the configurations shown in figure 5.2-3 also.

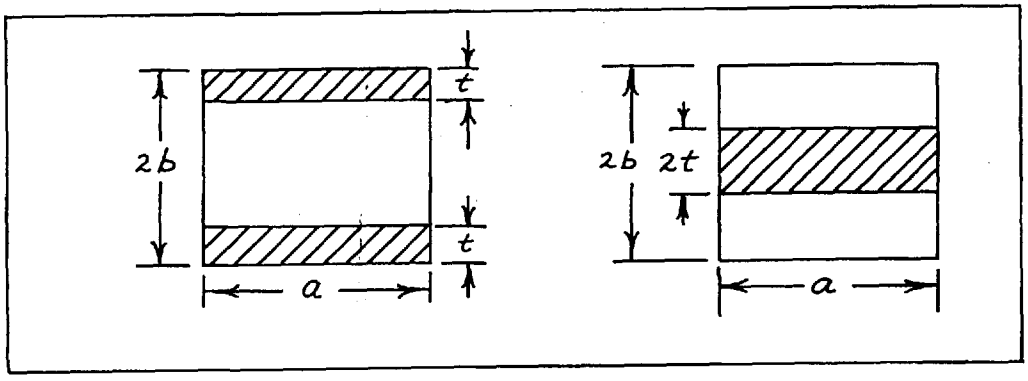
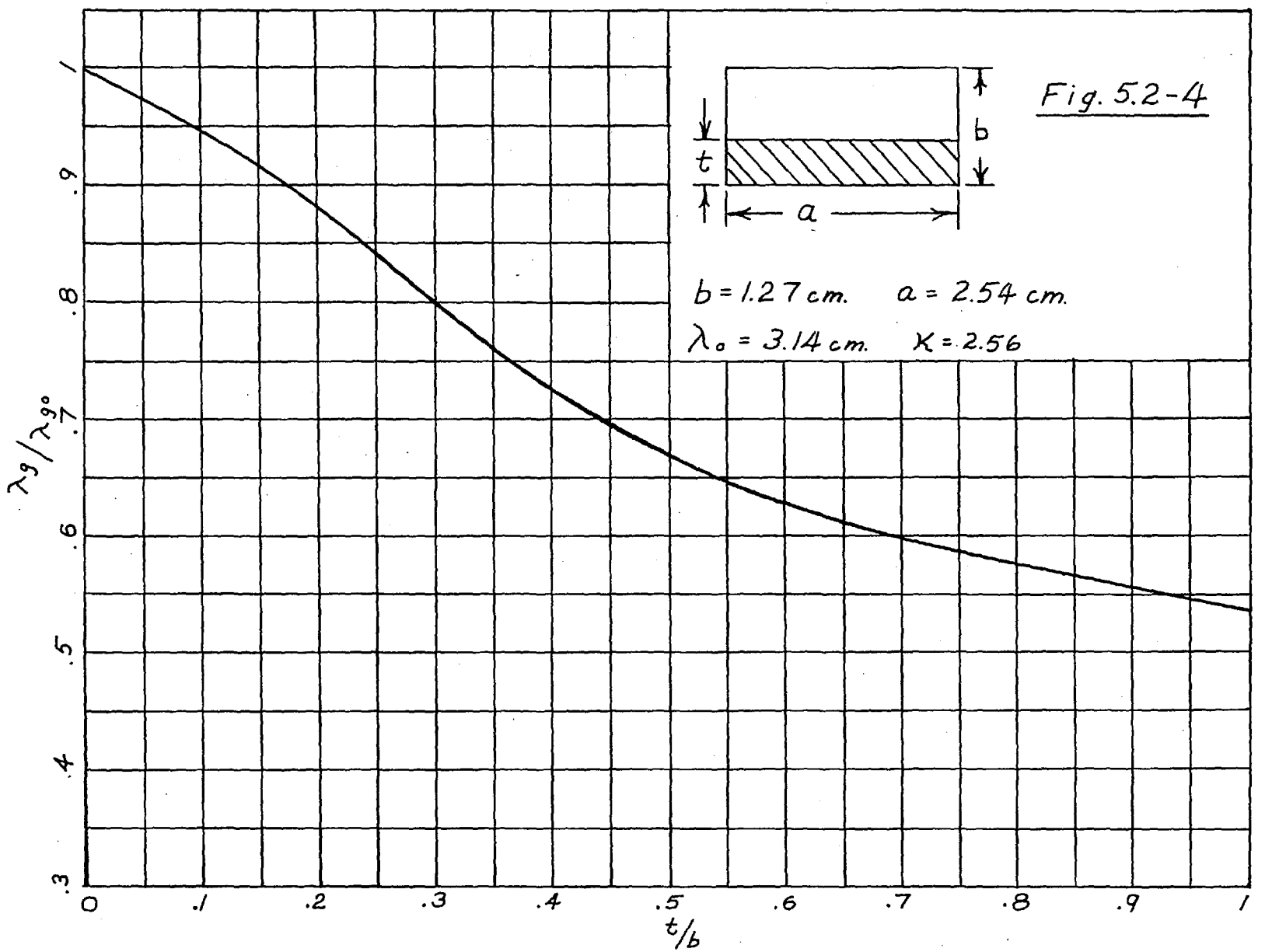


Fig. 5.2-3.

Figure 5.2-4 shows the typical curve for variation of the partially filled guide wavelength with thickness of dielectric filling for a free space wavelength of 3.14 cm. The guide wavelength varies roughly as the thickness of dielectric filling.


Fig. 5.2-4
b
t
a
b = 1.27 cm.
a = 2.54 cm.
λ₀ = 3.14 cm.
K = 2.56
λg/λg°
t/b
1
.9
.8
.7
.6
.5
.4
.3
0
.1
.2
.3
.4
.5
.6
.7
.8
.9
1

CHAPTER 6.

Properties of Quarter-Wave Transformers

6.1. Ideal Transformers :

The fundamental properties of ideal quarter-wave transformers are well known and are fully treated in many standard texts (6.1-1, 6.1-2). The ideal transformer is considered as having a characteristic impedance and a phase velocity which does not vary with frequency and all end effects are considered as absent. In practice these assumptions are violated but nevertheless the approximation is a good one in most cases and the properties of the ideal model forms the basis on which any actual transformer is designed. A single section transformer has a narrow bandwidth (6.1-3) and consequently for wider bandwidth applications multisection transformers must be used. To date the general opinion seems to be that for a maximum bandwidth the multisection transformer should be designed so that the characteristic impedance of the various sections are proportional to the coefficients of the binomial expansion. Such a transformer is called a binomial transformer (6.1.-1). It was suggested by J. Brown that perhaps a more suitable choice of the parameters of each quarter-wave section could result in a greater overall usable bandwidth. This was shown to be the case for the two section transformer independently by J. Brown and the author (6.1-4). Since each quarter-wave section introduces two new parameters i.e. a length and a characteristic impedance, it is possible to obtain a perfect match at as many different frequencies as there are sections. This follows at once since at any one frequency the phase and modulus of the input impedance

to the transformer section can be adjusted to a value equal to the characteristic impedance of the input transmission line by varying two parameters only. Thus the reflection from the transformer is made to vanish at 'n' different frequencies. The resulting bandwidth curve is similar to that for overcoupled circuits in circuit theory. As all these zeros are made to coalesce at one frequency the resulting transformer becomes identical with the binomial transformer. The bandwidth curve now corresponds to the case of a maximally flat filter. In the following sections the two and three section quarter-wave transformers are analysed in some detail.

6.2. Single Section Quarter-Wave Transformer :

The characteristic impedance of the quarter-wave section is Z_1 and the load impedance R is taken as resistive. All impedances are normalized with respect to the characteristic impedance of the input line and are taken as independent of frequency.

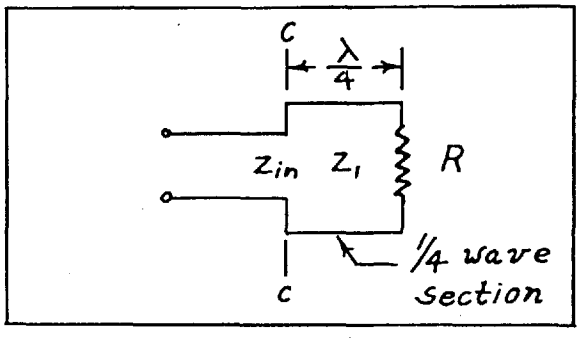


Fig. 6.2-1

The input impedance at the plane $C-C$ in figure 6.2-1 is by conventional transmission line theory given by

$$Z_{in} = \frac{Z_1 (R + j Z_1 t)}{Z_1 + j R t},$$

where $t = \tan \frac{\pi}{2} \frac{f}{f_o}$. The matching frequency is f_o and Z_1 is chosen so that $Z_1 = R^{1/2}$, thus Z_{in} equals unity when $f = f_o$. The reflection coefficient r is given by

$$r = \frac{1 - Z_{in}}{1 + Z_{in}} = \frac{Z_1(1-R)}{Z_1(1+R)+2jRt} ,$$ where the relation $Z_1^2 = R$

has been used. By using the relation $1+t^2 = \sec^2 \frac{\pi}{2} \frac{f}{f_o}$ it is easily shown that the modulus of the reflection coefficient is given by

$$\rho^2 = |r|^2 = \frac{1}{1 + \left(\frac{2\sqrt{R}}{R-1}\right)^2 \sec^2 \frac{\pi}{2} \frac{f}{f_o}} .$$ For large

values of $\sec \frac{\pi}{2} \frac{f}{f_o}$, ρ is given by

$$\rho = \frac{R-1}{2\sqrt{R}} \left| \cos \frac{\pi}{2} \frac{f}{f_o} \right|$$ and it is seen at once

that the bandwidth will be small since ρ rises rapidly on either side of f_o .

6.3. Two Section Quarter-Wave Transformers :

The circuit to be analysed is illustrated in figure 6.3-1.

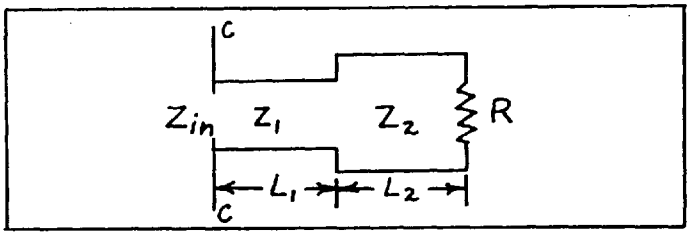


Fig. 6.3-1

All the impedances are normalized with respect to the characteristic impedance of the input line which for convenience sake is taken as unity. The matching section consists of the two sections 1 and 2,

whose lengths are L_1 and L_2 respectively. The characteristic impedance of the lines are Z_1 and Z_2 respectively. The four parameters L_1, L_2, Z_1 and Z_2 will be determined so that the complete termination is as well matched as possible over the widest possible frequency range. It is found to be extremely difficult to tackle the problem in its complete generality so one restriction will be imposed, namely that the quarter-wave sections are both a quarter of a wavelength long at at the centre frequency f_o. Further it is assumed that the phase velocities and impedances are all independent of frequency.

In view of the above assumptions the input impedance of the structure to the right of the plane $C-C$ in figure 6.3-1 is found by usual transmission line theory to be

$$Z_{in} = \frac{Z_1 R(Z_2 - Z_1 t^2) + j Z_1 Z_2 (Z_1 + Z_2) t}{Z_2 (Z_1 - Z_2 t^2) + j R (Z_1 + Z_2) t} \qquad (1)$$

where $t = \tan \frac{\pi}{2} \frac{f}{f_o}$.

Now Z_{in} will be made equal to unity at a frequency f_s less than f_o. From the symmetry of the expression for Z_{in} it follows that Z_{in} will equal unity again at a frequency $f = 2f_o - f_s$. The corresponding value of $\tan \frac{\pi}{2} \frac{f_s}{f_o}$ will be donated by t_s. For Z_{in} to reduce to unity, the real and imaginary parts of the numerator and denominator in equation (1) must be equal when $t = t_s$. This condition gives the two following relations,

$$Z_1 Z_2 (Z_1 + Z_2) t_s = R(Z_1 + Z_2) t_s \quad \text{or}$$
$$Z_1 Z_2 = R, \qquad (2)$$

and

$$Z_1 R(Z_2 - Z_1 t_s^2) = Z_2(Z_1 - Z_2 t_s^2). \qquad (3)$$

Substituting from (2) into (3) and solving for t_s^2 gives

$$t_s^2 = \frac{Z_1 Z_2 (R-1)}{Z_1^2 R - Z_2^2} = \frac{R(R-1)}{Z_1^2 R - \frac{R^2}{Z_1^2}} = \frac{Z_1^2 (R-1)}{Z_1^4 - R}. \qquad (4)$$

Alternatively solving equation (4) for Z_1 gives

$$Z_1 = \left[\sqrt{\frac{(1-R)^2}{4 t_s^4} + R} - \frac{1-R}{2 t_s^2} \right]^{1/2} \qquad (5)$$

$$\approx \left[1 + \frac{R-1}{2\sqrt{R}\, t_s^2} \right]^{1/2} R^{1/4} \qquad \text{since } t_s^2 \text{ is large}$$

if the mistmatch at the centre frequency is to be small. It is seen that Z_1 is slightly larger than $R^{1/4}$ which is the appropriate value for the binomial transformer. The input impedance at the midband frequency f_o is

$$Z_{in} = \frac{Z_1^2 R}{Z_2^2} = \frac{Z_1^4}{R}, \qquad (6)$$

and is purely resistive. At the midband frequency f_o the maximum tolerable reflection coefficient r will be taken as ρ_o. Since $r = \frac{1 - Z_{in}}{1 + Z_{in}}$ it follows that

$$\rho_o = \frac{Z_1^4 - R}{Z_1^4 + R}, \qquad (7)$$

where R has been assumed to be greater than unity. This restriction will be applied in the remainder of this analysis. At the end of the

analysis the slight modifications required when R is less than unity will be given.

Solving equation (7) for Z_1^4 gives

$$Z_1^4 = \frac{1+\rho_o}{1-\rho_o} R = R S_o \qquad (8)$$

where S_o is the maximum tolerable value of the corresponding voltage standing wave ratio (taken greater than unity). For any value of t the corresponding value of ρ^2 is given by

$$\rho^2 = \left|\frac{1-Z_{in}}{1+Z_{in}}\right| = \frac{(Z_1^2 - Rt^2 - RZ_1^2 - Z_1^4 t^2)^2}{(Z_1^2 - Rt^2 + RZ_1^2 - Z_1^4 t^2)^2 + 4t^2(Z_1^3 + Z_1 R)^2} .$$

Expanding this expression and substituting for ρ_o from equation (7) gives

$$\rho^2 = \frac{\left(\frac{Z_1^2(R-1)}{Z_1^4+R} - \rho_o t^2\right)^2}{\frac{Z_1^4(R+1)^2}{(Z_1^4+R)^2} + t^4 + 2t^2 Z_1^2 \left(\rho_o \frac{R-1}{R+Z_1^4} + \frac{4Z_1^2 R}{(R+Z_1^4)^2}\right)} .$$

From equation (4) $Z_1^2(R-1) = (Z_1^4 - R)t_s^2$ and consequently

$$\rho^2 = \frac{\rho_o^2 (t_s^2 - t^2)^2}{t^4 - 2\rho_o^2 t_s^2 t^2 + Z_1^4 \frac{(8Rt^2 + 1 + 2R + R^2)}{(R+Z_1^4)^2}} .$$

Replace $1+2R+R^2$ by $(R-1)^2 + 4R$ and use the relations $1-\rho_o = \frac{2R}{R+Z_1^4}$ and $1+\rho_o = \frac{2Z_1^4}{R+Z_1^4}$

and the following expression for ρ^2 is obtained

$$\rho^2 = \frac{\rho_o^2 (t_s^2 - t^2)^2}{t^4 - 2\rho_o^2 t_s^2 t^2 + \rho_o^2 t_s^4 + (1-\rho_o^2)(2t^2+1)} .$$

Now replace t^4 and t_s^4 by $\sec^4 \frac{\pi}{2}\frac{f}{f_o} - 2t^2 - 1$ and $\sec^4 \frac{\pi}{2}\frac{f_s}{f_o} - 2t_s^2 - 1$ respectively and after simplifying the following final result is obtained,

$$\rho^2 = \frac{1}{1 + \frac{1-\rho_0^2}{\rho_0^2} \frac{\sec^4\theta}{(\sec^2\theta_s - \sec^2\theta)^2}} \qquad (9)$$

where $\theta = \frac{\pi f}{2 f_0}$ and $\theta_s = \frac{\pi f_s}{2 f_0}$. The bandwidth limits are determined by the condition that ρ is again equal to ρ_0. From equation (9) it follows at once that $\sec\theta_L = \frac{\sec\theta_s}{\sqrt{2}}$ at the bandwidth limit, where $\theta_L = \frac{\pi}{2}\frac{f_L}{f_0}$ and f_L is by definition the frequency at which $\rho = \rho_0$. There is a very simple relation between t_s and t_L the values of t at which ρ equals zero and ρ_0 respectively. From the secant relation given above it is found to be

$$t_L^2 = \frac{1}{2}(t_s^2 - 1), \qquad (10)$$

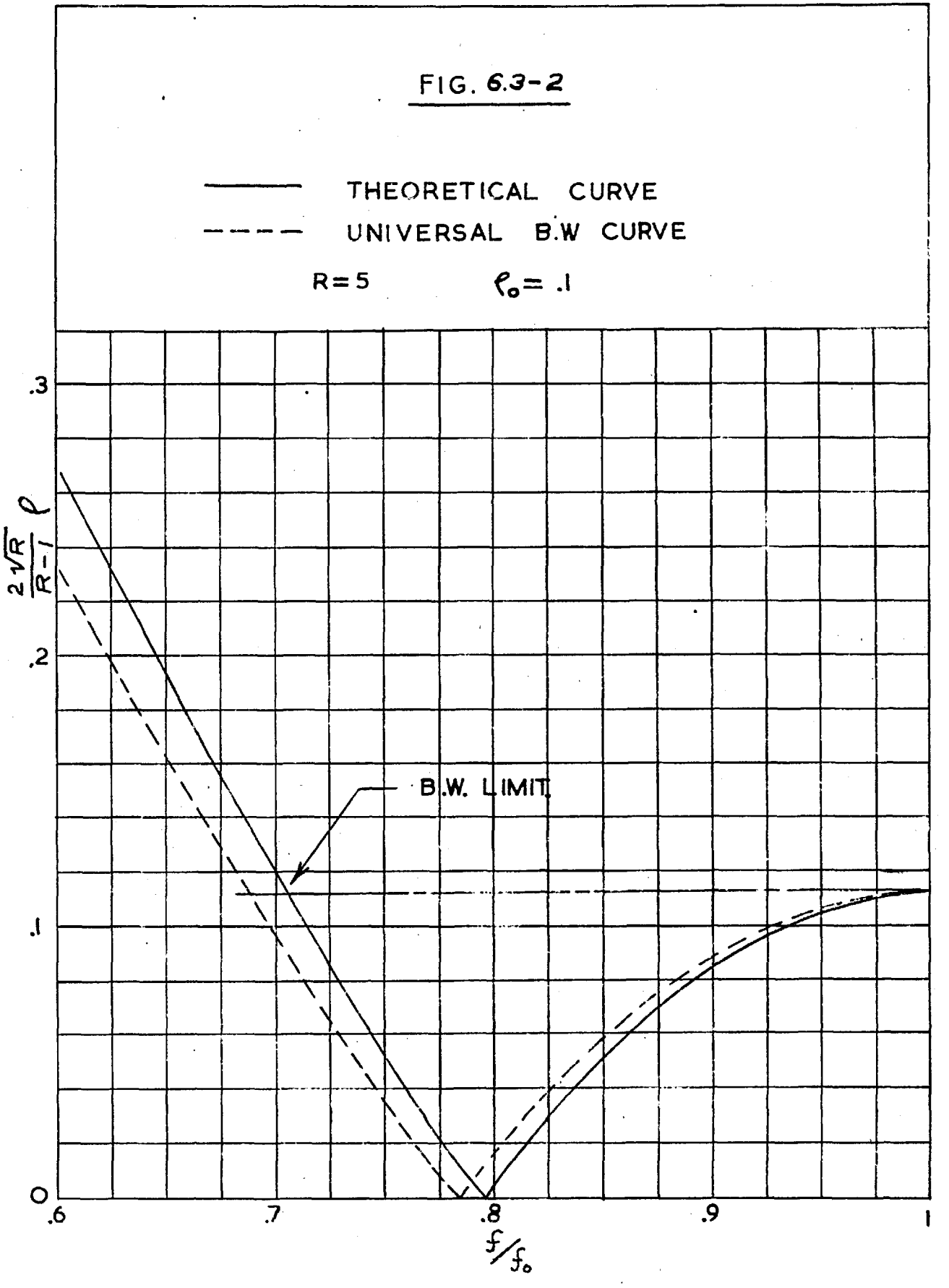
A typical bandwidth curve is shown in figure 6.3-2.

The properties of a two section binomial transformer are most easily obtained as a special case of the previous analysis. Suppose the two frequencies at which the reflection is zero are made to become closer together, eventually coinciding at the design frequency f_0. It follows at once from equations (5) and (2) that

$$Z_1 = R^{1/4}, \quad Z_2 = R^{3/4}. \qquad (11)$$

The reflection coefficient has a double zero at the design frequency and so its first derivative with respect to frequency will also be zero. The binomial transformer so obtained has therefore a similar behaviour to a maximally flat band-pass filter. The bandwidth of this arrangement is obtained, as before, by finding the frequency for which the modulus of the reflection coefficient equals ρ_0.

FIG. 6.3-2


THEORETICAL CURVE
UNIVERSAL B.W CURVE
R=5
$\rho_0 = .1$
.3
.2
.1
0
$\frac{2\sqrt{R}}{R-1}\rho$
B.W. LIMIT
.6
.7
.8
.9
1
f/f_0

For the binomial transformer $Z_1 = R^{1/4}$ and $Z_2 = R^{3/4}$, therefore

$$Z_{in} = \frac{R(R - \sqrt{R}\,t^2) + jR(R^{1/4} + R^{3/4})t}{R - R^{3/2}t^2 + jR(R^{1/4} + R^{3/4})t},$$

and

$$\rho^2 = \frac{R^2(R-1)^2}{(R^2 + R - 2R^{3/2}t^2)^2 + 4R^2\sqrt{R}(1+\sqrt{R})^2 t^2}$$

$$= \frac{(R-1)^2}{(1 + R - 2\sqrt{R}\,t^2)^2 + 4\sqrt{R}\,t^2(1+\sqrt{R})^2}.$$

Expanding this and using the relation $1 + t^2 = \sec^2\theta$ this expression reduces to

$$\rho^2 = \frac{1}{1 + \left(\frac{2\sqrt{R}}{R-1}\right)^2 \sec^4 \frac{\pi}{2}\frac{f}{f_0}}, \qquad (12)$$

which differs from that for a single section transformer in that it involves $\sec\theta$ to the fourth power instead of the second power. For values of f close to f_0, ρ is given by

$$\rho = \frac{R-1}{2\sqrt{R}} \cos^2 \frac{\pi}{2}\frac{f}{f_0},$$

and it is obvious that $\frac{d\rho}{d\theta}$ equals zero when $\theta = \frac{\pi}{2}$.

When $\rho = \rho_0$ let $t = t_B$, where t_B defines the bandwidth limits of the binomial transformer, and it follows that

$$1 + t_B^2 = \sec^2\theta_B = \frac{(1-\rho_0^2)^{1/2}(R-1)}{2\rho_0\sqrt{R}}.$$

Now from equation (4) $(Z_1^4 - R)t_s^2 = Z_1^2(R-1)$,

and hence $t_s^2 = \frac{Z_1^2(R-1)(1-\rho_0)^{1/2}(1+\rho_0)^{1/2}(R+Z_1^4)}{(Z_1^4 - R)(2R)^{1/2}(2Z_1^4)^{1/2}} = \frac{(1-\rho_0^2)^{1/2}(R-1)}{\rho_0\, 2\sqrt{R}}$

and therefore $t_B^2 = t_s^2 - 1$. It is seen that there is a unique relation between the bandwidth of the binomial transformer and that based on the alternative design given above. With reference to equation (10) this relation is

$$t_L = \frac{t_B}{\sqrt{2}} \quad . \tag{13}$$

The improvement resulting from the use of this optimum design is illustrated in figure 6.3.-3 in which the ratio of optimum bandwidth to that of the binomial bandwidth is plotted against binomial bandwidth. It is seen that a maximum improvement of about 45% is possible. In practice an increase of 30% or more is usually obtained. The bandwidth is expressed as a fraction of the centre frequency f_0 so that for the above transformer the bandwidth is taken as $2\frac{f_0 - f_L}{f_0}$.

Although the lengths of the quarter wave sections were chosen as a quarter wave long at the centre frequency f_0 it does not seem logical to expect any significant improvement in bandwidth by staggering the lengths. It is possible to make ρ go to zero at two frequencies only since each zero requires an adjustment of two out of the total of four parameters to make the modulus of Z_{in} unity and the phase of Z_{in} zero.

6.4. Design Procedure and Universal Band Width Curves :

Case 1 - When S_0, the maximum tolerable voltage standing wave ratio is given, then Z_1 is determined by equation (8) as

$$Z_1 = (R S_0)^{1/4}$$

The corresponding value of Z_2 is $R^{3/4} / S_0^{1/4}$.

FIG. 6.3-3

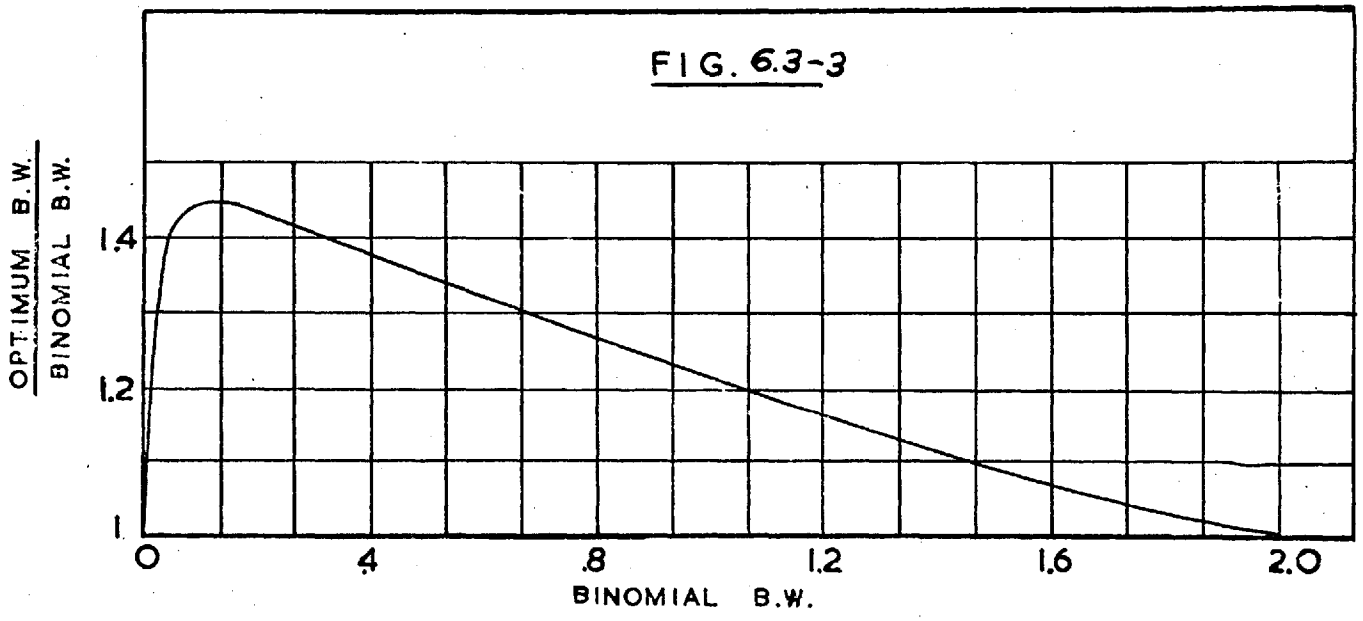
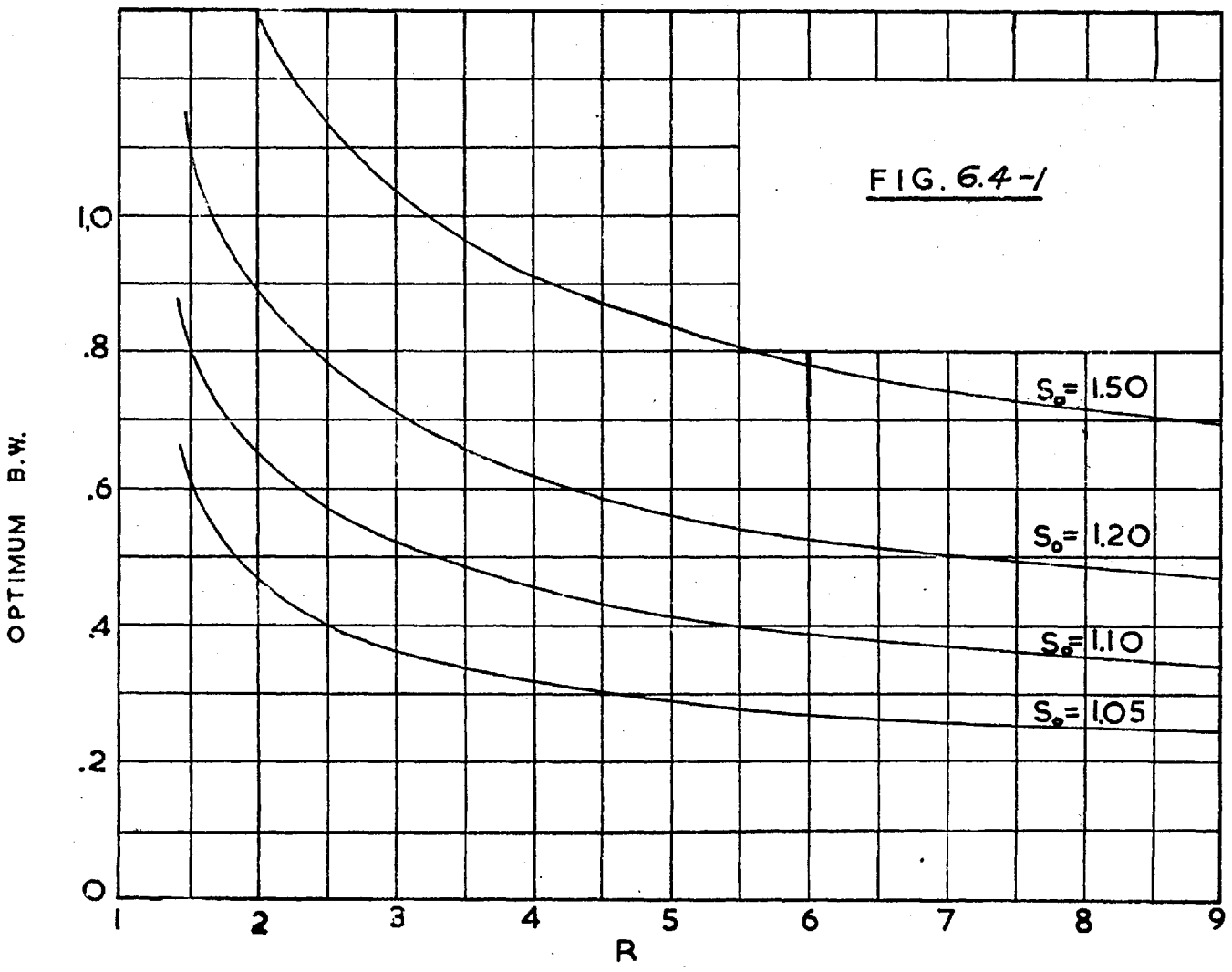


FIG. 6.4-1



The bandwidth is determined from equations (4) and (10) which when combined give

$$t_L^2 = \frac{1}{2}\left(\frac{R-1}{\sqrt{R}}\,\frac{\sqrt{S_0}}{S_0-1} - 1\right)$$

thus

$$\text{Fractional Bandwidth} = 2\,\frac{f_0 - f_L}{f_0} \quad \text{where} \quad f_L = \frac{2f_0}{\pi}\tan^{-1} t_L .$$

Case 2 - If the required bandwidth is specified then f_L is fixed and this in turn fixes t_L and t_S.

Thus $t_L = \tan\frac{\pi}{2}\frac{f_L}{f_0}$ and $t_S^2 = 2t_L^2 + 1$.

From this value of t_S^2 the value of S_0 is determined from

$$\frac{S_0}{(S_0-1)^2} = \frac{R}{(R-1)^2}\,t_S^4 = a$$

and hence

$$S_0 = \left(1 + \frac{1}{2a}\right) + \sqrt{\frac{(2a+1)^2}{4a^2} - 1} \; .$$

Since S_0 must be positive only the positive root is applicable.

Alternatively Z_1 may be obtained from the relation

$$Z_1 = \left[\sqrt{\frac{(R-1)^2}{4t_S^4} + R} - \frac{R-1}{2t_S^2}\right]^{1/2} .$$

The corresponding value of Z_2 is R/Z_1.

When R is less than unity the only alternation required in the above design formulas is replacing R by $\frac{1}{R}$, Z_1 by $\frac{1}{Z_1}$, and Z_2 by $\frac{1}{Z_2}$.

In figure 6.4.-1 is plotted a family of curves giving the optimum fractional bandwidth as a function of R for four values of S_0. The performance for any particular case can be obtained from these curves.

In practice it is usually desirable to have an overall match that does not produce a voltage standing wave ratio greater than 1.20. The corresponding maximum value of ρ_0 is .10. For values of ρ_0 not exceeding this maximum value a set of universal bandwidth curves can be

constructed that are independent of the value of R the load impedance. From these curves the modulus of the reflection coefficient and the bandwidth can readily be determined to within a few per cent which is adequate for any engineering application. The value of ρ^2 for the binomial transformer is

$$\rho^2 = \frac{1}{1 + \frac{4R}{(R-1)^2}\sec^4\theta}.$$

When ρ^2 does not exceed .01 the factor 1 in the denominator can be neglected in comparison with $\frac{4R}{(R-1)^2}\sec^4\theta$. Thus to a good degree of approximation ρ is given by $\rho = \frac{R-1}{2\sqrt{R}}\cos^2\theta$.

A plot of $\frac{2\sqrt{R}}{R-1}\rho$ against $\cos^2\theta$ then results in a universal bandwidth curve for the binomial transformer.

For the optimum bandwidth transformer ρ^2 is given by

$$\rho^2 = \frac{1}{1 + \frac{1-\rho_0^2}{\rho_0^2}\frac{\sec^4\theta}{(\sec^2\theta_s - \sec^2\theta)^2}}.$$

It is seen again that for $\rho^2 \leq .01$ that the factor unity in the denominator can be neglected, thus take

$$\rho = \frac{\rho_0 \left|\sec^2\theta_s - \sec^2\theta\right|}{(1-\rho_0^2)^{1/2}\sec^2\theta}$$

$$= \frac{\rho_0 \sec^2\theta_s}{(1-\rho_0^2)^{1/2}} \left|\cos^2\theta_s - \cos^2\theta\right|.$$

Now $t_s^2 = \frac{(1-\rho_0^2)^{1/2}}{\rho_0}\frac{R-1}{2\sqrt{R}}$ and for values of t_s^2

large compared with unity $t_s^2 \approx \sec^2\theta_s$, therefore

$$\rho \approx \frac{R-1}{2\sqrt{R}} \left| \cos^2\theta_s - \cos^2\theta \right| .$$

This value of ρ is slightly too small since $\sec^2\theta_s$ has been approximated by a smaller quantity t_s^2. However the neglect of the factor unity in the correct expression for ρ tends to offset this error. Now θ_s is not independent of R but from the relation

$$t_B^2 = t_s^2 - 1$$

it is seen that θ_s can be approximated by θ_B the value of θ at the bandwidth limit of the binomial transformer. Since θ_B is less than θ_c, $\cos\theta_B$ is greater than $\cos\theta_s$ and this almost completely neutralizes the error in the approximate expression for ρ. There will of course be an error in the matching frequency and the bandwidth but these will be small for the range of ρ under consideration. A plot of $\frac{2\sqrt{R}}{R-1}\rho$ against $\left|\cos^2\theta_B - \cos^2\theta\right|$ results in a universal bandwidth curve for the optimum bandwidth transformer. From these curves, illustrated in figure 6.4.-2 the overall performance of any transformer is readily obtained.

6.5. The Three Section Transformer :

The same type of analysis as applied to the two section transformer will now be applied to the three section transformer illustrated in figure 6.5.-1.

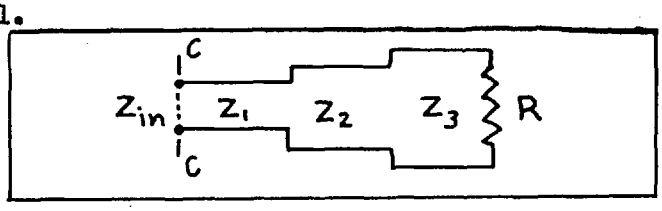
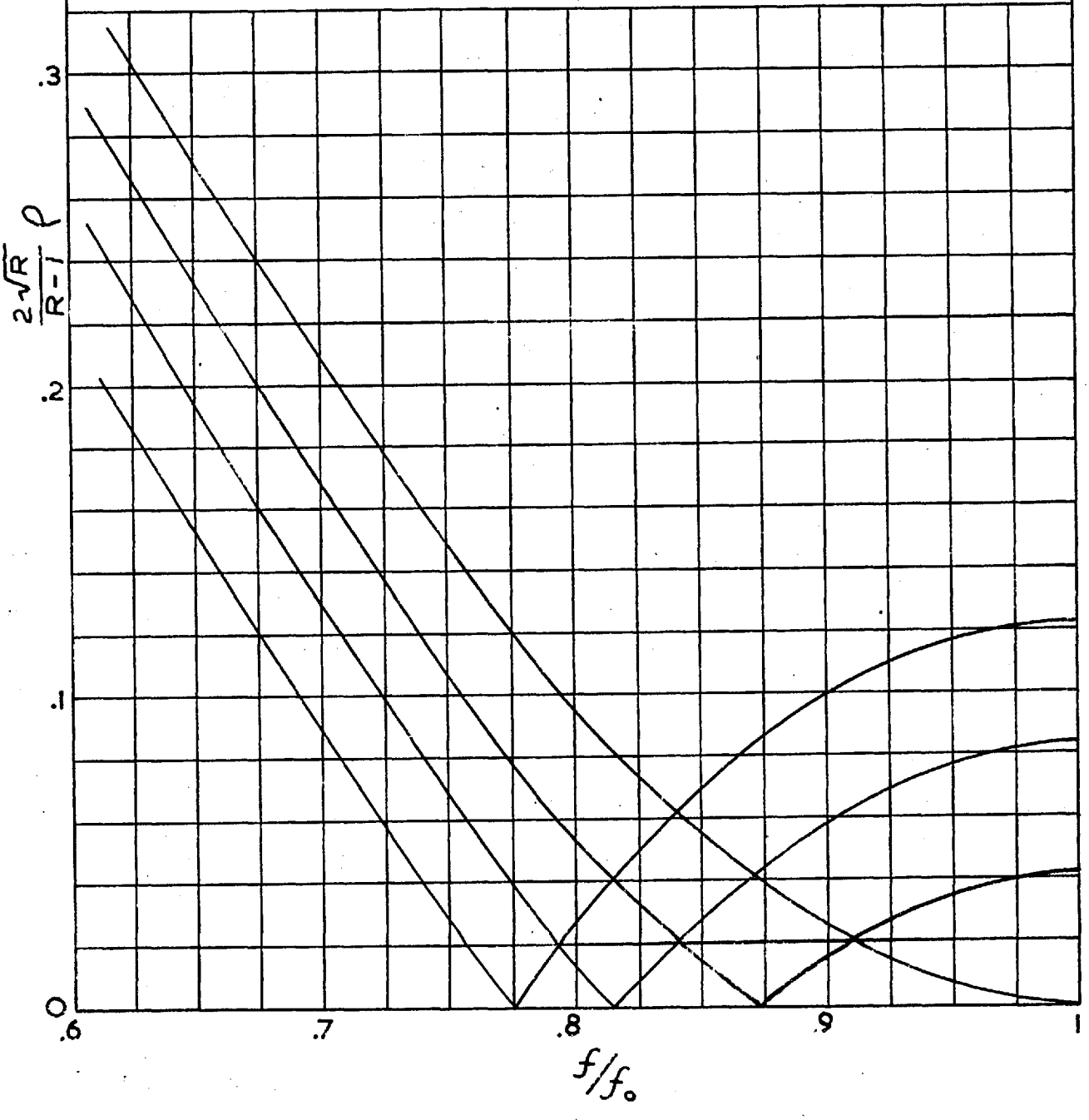


Fig. 6.5.-1

FIG. 6.4-2

UNIVERSAL B.W. CURVES.



The same restrictions as applied to the two section transformer is applied here also, i.e. the impedance and phase velocities are taken independent of frequency and each section is a quarter-wave long at the centre frequency f_o. It does not seem to be possible to derive any simple formulas for the bandwidth or reflection coefficient for the three section transformer. However the analysis is complete enough to indicate the type of performance to be expected and to enable one to quite readily produce a suitable design.

Using conventional transmission line theory the input impedance at the plane $C-C$ in figure 6.5.-1. is found to be

$$Z_{in} = \frac{a + jb}{c + jd} \qquad (1)$$

where

$$\begin{aligned} a &= Z_1 Z_2 Z_3 R - Z_1 Z_2^2 R t^2 - Z_1^2 Z_2 R t^2 - Z_1^2 Z_3 R t^2, \\ b &= Z_1 Z_2 Z_3^2 t + Z_1 Z_2^2 Z_3 t + Z_1^2 Z_2 Z_3 t - Z_1^2 Z_3^2 t^2, \\ c &= Z_1 Z_2 Z_3 - Z_1 Z_3^2 t^2 - Z_2 Z_3^2 t^2 - Z_3 Z_2^2 t^2, \\ d &= Z_1 Z_2 R t + Z_1 Z_3 R t + Z_2 Z_3 R t - Z_2^2 R t^3, \end{aligned}$$

and $t = \tan\theta = \tan \frac{\pi}{2} \frac{f}{f_o}$.

Since there are three frequencies at which the reflection can be made to vanish one of these zeros will be chosen at the centre frequency f_o. The other two will be symmetrically located on either side at a frequency f_s. Thus for a match at $f = f_o$ where $\tan\theta$ becomes infinite it is seen at once from the expression for Z_{in} that Z_{in} reduces to unity if

$$Z_1^2 Z_3^2 = Z_2^2 R. \qquad (2)$$

For Z_{in} to be unity at a frequency f_s the real and imaginary parts of the numerator and denominator must be equal when $t = t_s$ and hence $Z_1 Z_2 Z_3^2 + Z_1 Z_2^2 Z_3 + Z_1^2 Z_2 Z_3 - Z_1^2 Z_3^2 t_s^2 =$

$$Z_1 Z_2 R + Z_1 Z_3 R + Z_2 Z_3 R - Z_2^2 R t_s^2 ,$$

which by virtue of equation (2) becomes

$$(Z_1 + Z_2 + Z_3) Z_1 Z_2 Z_3 = R(Z_1 Z_2 + Z_1 Z_3 + Z_2 Z_3), \quad (3)$$

and

$$Z_1 Z_2 Z_3 R - (Z_1 Z_2^2 + Z_1^2 Z_2 + Z_1^2 Z_3) R t_s^2 =$$

$$Z_1 Z_2 Z_3 - (Z_1 Z_3^2 + Z_2 Z_3^2 + Z_2^2 Z_3) t_s^2, \quad (4)$$

Now

$$Z_1 Z_3 = R = Z_2^2 \quad (5)$$

is a solution of equation (3) and this relation is appropriate for the three section binomial transformer also. Divide equation (4) by $Z_1 Z_2 Z_3$ thus

$$1 - t_s^2 \left(\frac{Z_3}{Z_2} + \frac{Z_3}{Z_1} + \frac{Z_2}{Z_1} \right) = R \left[1 - t_s^2 \left(\frac{Z_2}{Z_3} + \frac{Z_1}{Z_3} + \frac{Z_1}{Z_2} \right) \right]$$

which by using equation (5) reduces to

$$1 - t_s^2 \left(\frac{2\sqrt{R}}{Z_1} + \frac{R}{Z_1^2} \right) = R - R t_s^2 \left(2 Z_1 R^{1/2} + Z_1^2 \right). \quad (6)$$

Solving this equation for t_s^2 gives

$$\frac{R-1}{t_s^2} = Z_1^2 + 2\sqrt{R}\, Z_1 - \frac{R}{Z_1^2} - 2\frac{\sqrt{R}}{Z_1} ,$$

which is a fourth degree equation in the variable Z_1. Although this equation has no simple solution it is interesting to note that t_s^2 and hence f_s/f_o is almost independent of R for a large range of R provided $Z_1 = R^x$ and the parameter x is held constant. Substituting R^x for Z_1 in the above equation gives

$$\frac{R-1}{t_s^2} = R^{2x} + 2R^{\frac{1}{2}+x} - (R^{1-2x} + 2R^{\frac{1}{2}-x}) \quad (7)$$

The parameter x will usually lie in the range $1/8 \leq x \leq 1/5$.

From the curves given in figure 6.5.-2 it is seen that f_s/f_o increases by less than 5% as R varies from 1 to 12. Thus the matching frequency f_s is determined by the parameter x. As x approaches $1/8$ all the zeros coalesce at the centre frequency f_o. When all three zeros coincide at f_o the transformer is maximally flat. For small values of R say $R = 1+\epsilon$ with $\epsilon \ll 1$,

$$\frac{R-1}{t_s^2} = \frac{\epsilon}{t_s^2} = (1+\epsilon)^{2x} + 2(1+\epsilon)^{\frac{1}{2}+x} - (1+\epsilon)^{1-2x} - 2(1+\epsilon)^{\frac{1}{2}-x}$$

$$= (8x-1)\epsilon \quad \text{if higher powers of } \epsilon \text{ are}$$

neglected. It is seen that t_s becomes infinite when $8x = 1$ or $x = 1/8$ and consequently all three zeros come together at f_o when $x = 1/8$ for values of R close to unity. When $Z_1 = R^{1/8}$ the binomial transformer is obtained. For large values of R all three zeros coalesce for a value of x slightly less than $\frac{1}{8}$. Consequently the binomial transformer is maximally flat only for small values of R. The departure from maximum flatness at large values of R is however

FIG. 6.5-2

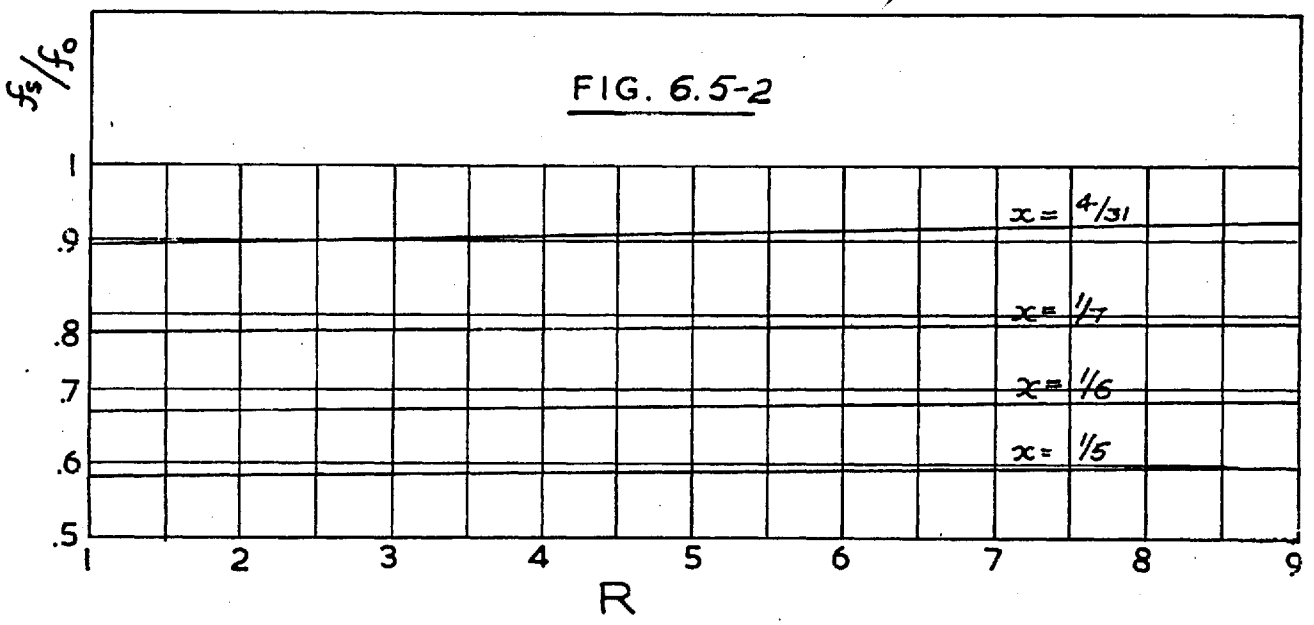
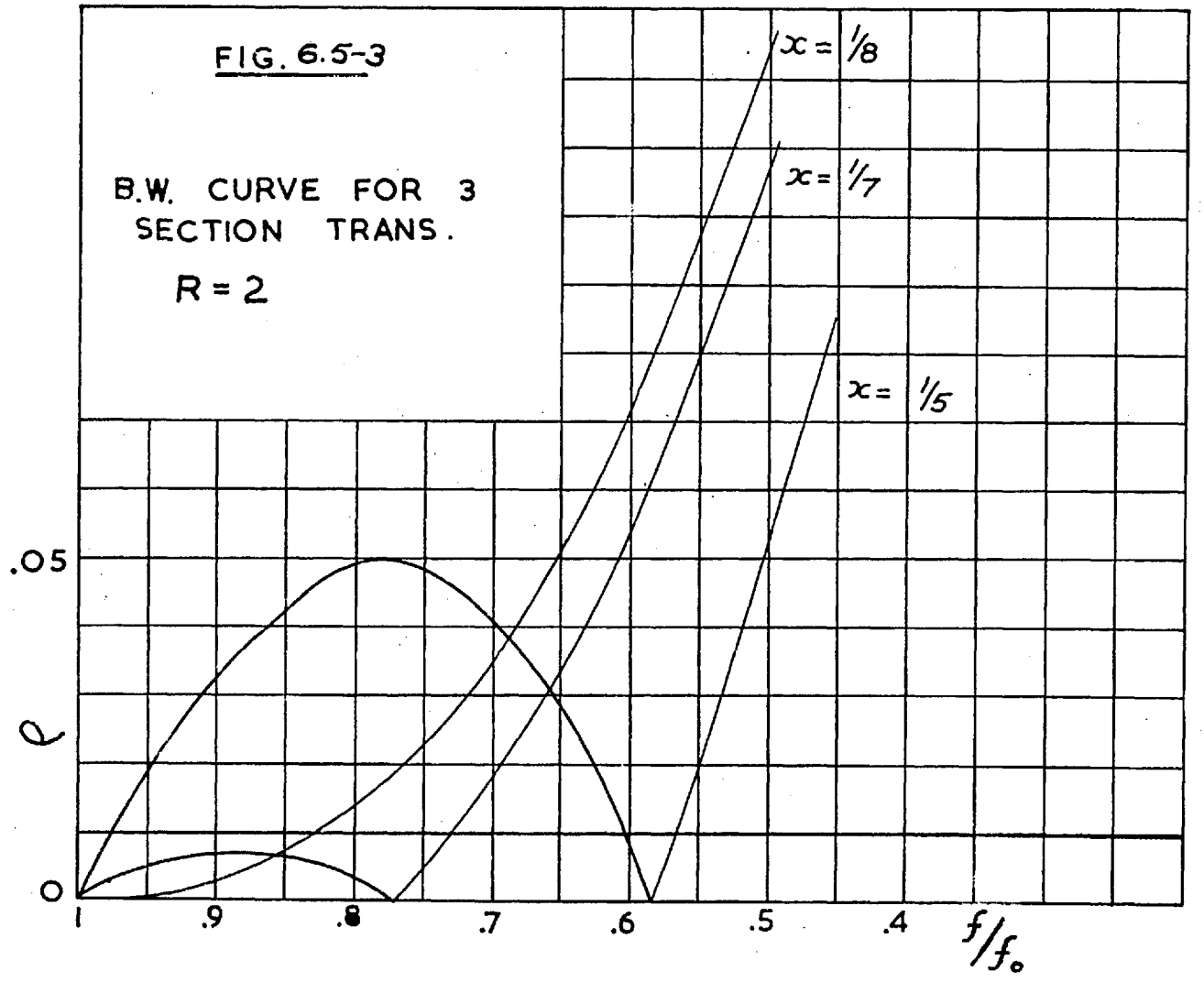


FIG. 6.5-3

B.W. CURVE FOR 3 SECTION TRANS.

R = 2



small. It is obvious that a three section binomial transformer will have a greater bandwidth than the two section binomial transformer since it has one more zero at the centre frequency f_o.

Dividing a, b, c, and d in the expression for Z_{in} in equation (1) by $Z_1 Z_2 Z_3$ and using equations (3) and (5) it can be shown that

$$b = d = t(Z_s - \sqrt{R}\,t^2) \quad \text{where} \quad Z_s = Z_1 + Z_2 + Z_3,$$

$$a = R\left[1 - (2Z_1\sqrt{R} + Z_1^2)t^2\right],$$

$$c = 1 - \left(\frac{2\sqrt{R}}{Z_1} + \frac{R}{Z_1^2}\right).$$

Thus since $Z_{in} = \frac{a+jb}{c+jd}$ it follows that the reflection coefficient Γ is given by

$$\Gamma = \frac{1-Z_{in}}{1+Z_{in}} = \frac{c+jb-a-jb}{c+jb+a+jb} = \frac{c-a}{c+a+2jb}.$$

Substituting for a, b, and c in this relation gives

$$|\Gamma|^2 = \rho^2 = \frac{(R-1)^2\left(1-\frac{t^2}{t_s^2}\right)}{(R+1-Wt^2)^2 + 4t^2(Z_s - \sqrt{R}\,t^2)^2} \quad (8)$$

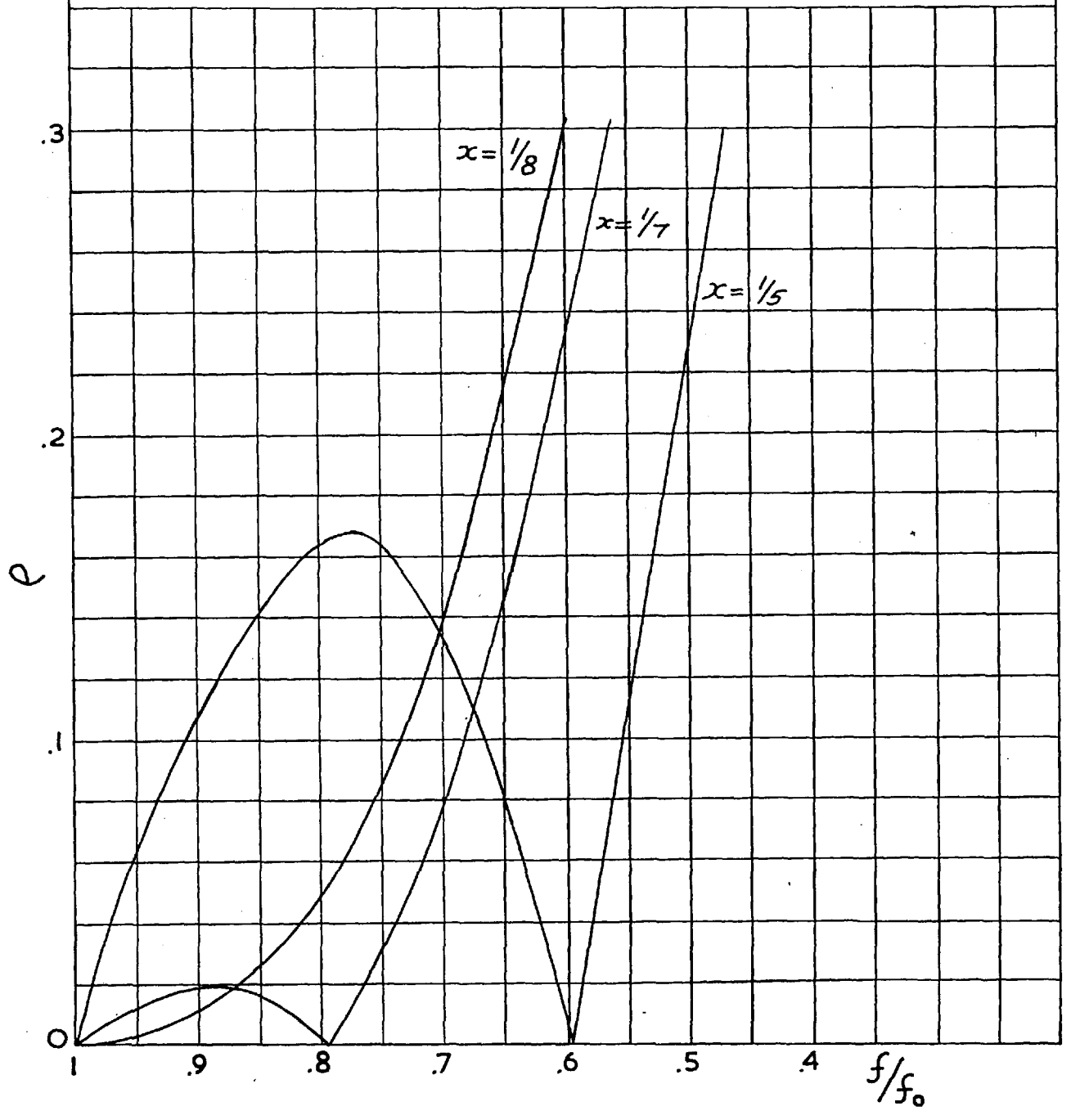
where $W = (Z_1 + \sqrt{R})^2(1+Z_1^{-2}) - (R+1)$ and t_s^2

has been introduced in the numerator by means of equation (6). For any particular case the bandwidth curve can be obtained from this expression. For a given value of R it can be shown that W and Z_s are for all practical purposes constant for a range of x from 1/8 to 1/5, the actual variation being of the order of 1 or 2 per cent. Thus if a bandwidth curve for a given R and for $x = 1/6$ say, is plotted,

FIG. 6.5-4

B.W. CURVE FOR THREE SECTION TRANS.

R = 8



then the corresponding curve for any other value of α can be scaled from the first curve by multiplying by a suitable factor

i.e. $$\frac{\rho_1}{\rho_2} = \frac{1 - t^2/t_{s1}^2}{1 - t^2/t_{s2}^2} .$$

Typical bandwidth curves which are obtainable are illustrated in figures 6.5.-3 and 6.5.-4. It is seen that bandwidth increases of 50% or more are obtainable.

6.6. H-Plane Dielectric Step Transformers in a Rectangular Waveguide.

The asymmetrical dielectric step is not very suitable as a matching transformer since it excites the second order H_{02} mode which can propagate in the dielectric filled guide. Furthermore there exists a considerable junction reactance which complicates the design of a quarter-wave transformer. It was shown in chapter 4 that the junction reactance for a symmetrical step is very small and since it excites only the odd order H_{0n} modes it is much more suitable for use as a matching section.

The behaviour of such quarter-wave transformers departs from the ideal case since the impedance and phase velocity of each section varies with the frequency. However the ratio of the impedance and phase velocity of any one section to that of any other section remains essentially constant and the overall behaviour is very similar to that of an ideal transformer. The ideal transformer will be taken as a transformer for which the normalized impedance of all sections remains constant at their values for the design wavelength λ_o and for which the phase shift across any section 'n' is given by $\tan \frac{\pi}{2} \frac{\lambda_{go}}{\lambda_g}$ at

the wavelength λ. The following notation is used :

λ_o = free space wavelength at the design frequency f_o,

λ = free space wavelength at any frequency f,

λ_{go} = empty guide wavelength at the frequency f_o,

λ_g = empty guide wavelength at any frequency f,

λ_{no} = wavelength in section 'n' at the frequency f_o,

λ_n = wavelength in section 'n' at any frequency f.

The impedance of any section is taken proportional to the wavelength in that section. Thus for the ideal transformer the normalized impedances are assumed to remain constant at the value $\frac{\lambda_{no}}{\lambda_{go}}$. The thickness of any section is determined by a solution of the eigenvalue equations given in chapter four, section 3, once the required impedance and hence the wavelength has been decided on. Thus

$$k_1 \cot l_1 t = l_1 \tan k_1 d \quad \text{and} \quad \left(\frac{2\pi}{\lambda_{no}}\right)^2 = k_o^2 - k_1^2 = K k_o^2 - l_1^2$$

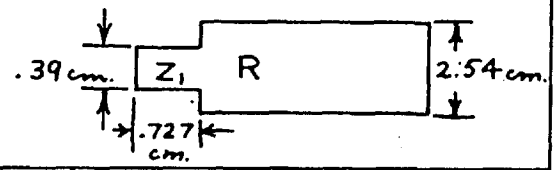
where t is half the thickness of the section and $2d = a - 2t$ and λ_{no} is the required wavelength.

A series of quarter wave transformers designed according to the above principles where made to match an empty guide to a completely filled guide filled with a lossless dielectric of dielectric constant 2.47. It was found that the calculated values of reflection coefficients and the measured values agreed closely. The theoretical value of the reflection coefficient was calculated using conventional transmission line theory and the appropriate values of Z_n and λ_n.

In table 6.6.-1 are given the calculated values of the various parameters and the theoretical value of the modulus of the reflection coefficient for a single step quarter-wave transformer. Table 6.6.-2 gives the measured values of the reflection coefficient.

Table 6.6.-1

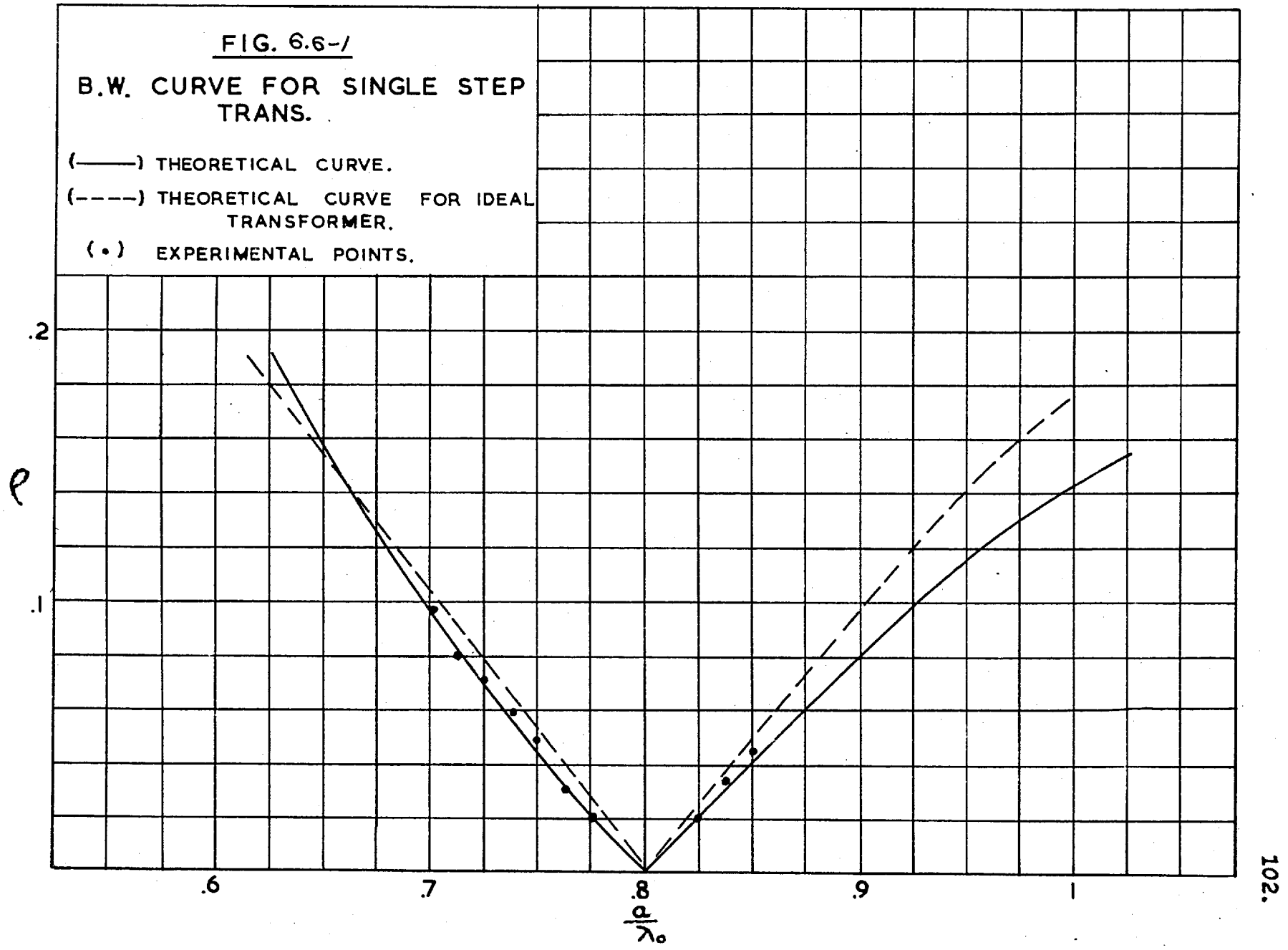
$a/\lambda_0 = .8$, $K = 2.47$,
length of step = $\lambda_{10}/4$



a/λ	λ_g cm.	λ_1 cm.	R	Z_1	ρ	ρ (ideal trans.)
.6	7.59	4.81	.422	.635	.23	.204
.65	6.11	4.15	.466	.679	.15	.154
.7	5.18	3.68	.502	.710	.095	.103
.75	4.55	3.29	.524	.724	.042	.051
.8	4.08	2.99	.539	.734	0	0
.85	3.69	2.73	.555	.740	.042	.05
.9	3.40	2.54	.565	.746	.080	.097
.95	3.15	2.36	.575	.750	.112	.14
1	2.93	2.20	.582	.753	.142	.177

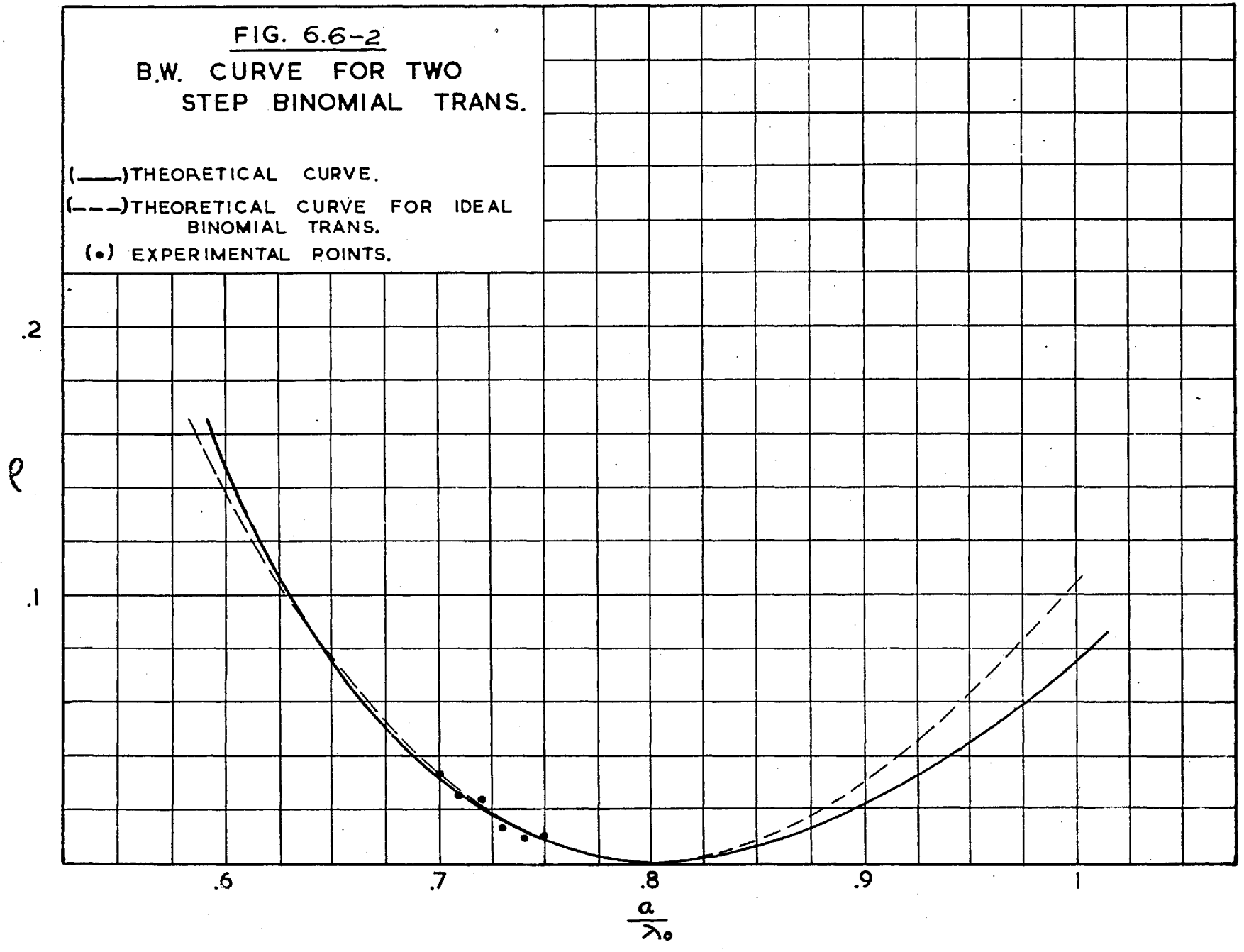
Table 6.6.-2

a/λ	.7	.725	.75	.775	.825	.85	.7125	.7375	.7625	.8375
Ex. ρ	.096	.07	.048	.02	.02	.045	.08	.058	.03	.034


FIG. 6.6-1
B.W. CURVE FOR SINGLE STEP TRANS.
(——) THEORETICAL CURVE.
(----) THEORETICAL CURVE FOR IDEAL TRANSFORMER.
(•) EXPERIMENTAL POINTS.
.2
.1
ρ
.6
.7
.8
.9
1
d/λ0

In figure 6.6.-1 are plotted the two theoretical bandwidth curves and the experimental points. It is seen that the behaviour is very close to that of an ideal transformer. For all practical purposes a design based on the ideal model is adequate, in fact it gives a rather conservative design. The reason why an ideal transformer has a slightly larger reflection coefficient is that the wavelength in the matching section tends to remain closer to a quarter-wave length than that given by $Z_1 \frac{\lambda_g}{4}$ with Z_1 fixed. This is caused by the wavelength in the empty guide being more susceptible to a change of frequency than the wavelength in a partially filled guide is. The bandwidth curve is not symmetrical since for values of λ approaching $2a$ cut-off is approached in the empty guide and the reflection coefficient rises rapidly. For small values of λ the reflection coefficient approaches the value due to reflection from the dielectric interface only. For small values of λ the guide wavelength approaches free space wavelength and consequently the reflection coefficient is asymptotic to $\frac{\eta - 1}{\eta + 1}$ where η is the index of refraction defined as $\sqrt{K}$. For $K = 2.47$ this asymptotic value is .223. The same type of behaviour is characteristic of the multi-section transformers. The effect of higher order modes that may propagate has been neglected. The first of these modes to propagate is the H_{03} mode in the completely filled guide. Thus when $\left(\frac{3\pi}{a}\right)^2 < \left(\frac{2\pi}{\lambda}\right)^2 K$ or $\frac{a}{\lambda} > \frac{1.5}{\sqrt{K}} = .955$ the H_{03} mode will propagate.

Table 6.6.-3 gives the calculated values of the parameters for a two section binomial transformer, while table 6.6.-4 gives the measured values of the modulus of the reflection coefficient. The impedances of


FIG. 6.6-2
B.W. CURVE FOR TWO STEP BINOMIAL TRANS.
(——)THEORETICAL CURVE.
(– – –)THEORETICAL CURVE FOR IDEAL BINOMIAL TRANS.
(•) EXPERIMENTAL POINTS.
.2
.1
ρ
.6
.7
.8
.9
1
a/λ₀

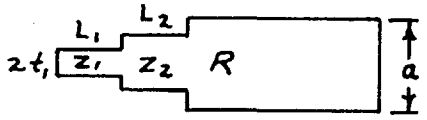
the binomial transformer at the design frequency f_o were chosen to obey the following relations

$$Z_1 = R^{1/4}, \quad Z_2 = R^{3/4}.$$

The theoretical bandwidth curves and experimental points are plotted in figure 6.6.-2

Table 6.6 -3

$\frac{a}{\lambda_o} = .8$, $a = 2.54$ cm, $K = 2.47$
$L_1 = .875$ cm. $L_2 = .642$ cm.
$2t_1 = .162$ cm. $2t_2 = .76$ cm.



a/λ	λ_g cm.	R	Z_1	Z_2	ρ	ρ(ideal trans.)
.6	7.59	.422	.796	.515	.148	.138
.65	6.11	.466	.826	.562	.076	.078
.7	5.18	.502	.843	.597	.032	.034
.75	4.55	.524	.850	.615	.008	.0083
.8	4.08	.539	.858	.630	0	0
.85	3.69	.555	.862	.643	.007	.008
.9	3.40	.565	.866	.652	.023	.030
.95	3.15	.575	.870	.659	.045	.062
1	2.93	.582	.873	.665	.074	.103

Table 6.6.-4

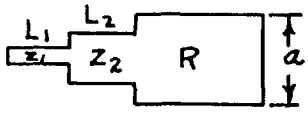
a/λ	.7	.71	.72	.73	.74	.75
Ex. ρ	.034	.026	.024	.014	.010	.010

Tables 6.6.-5 and 6.6.-6 give the corresponding data for a two section linear transformer. The impedances of an 'n' section linear transformer are chosen to obey the linear relation $Z_n = 1 - \alpha n$ where α is a constant chosen so that a perfect match is obtained at $f = f_o$. The input impedance W_n at any section is then $W_n = \frac{(1-\alpha n)^2}{W_{n+1}}$.

The theoretical bandwidth curve and experimental points are given in figure 6.6.-3.

Table 6.6.-5

$a/\lambda_o = .8$, $a = 2.54$ cm. $K = 2.47$, $L_1 = .805$ cm. $L_2 = .591$ cm.



$2t_1 = .27$ cm. $2t_2 = 1.16$ cm. $Z_n = 1 - \alpha n$, $\alpha = .21$,

a/λ	Z_1	Z_2	R	ρ
.6	.706	.46	.422	.191
.65	.746	.507	.466	.115
.7	.77	.544	.502	.063
.75	.78	.563	.524	.028
.8	.79	.58	.534	0
.85	.795	.59	.555	.0278
.9	.80	.601	.565	.053
.95	.803	.609	.575	.08
1	.806	.617	.582	.103

Table 6.6.-6

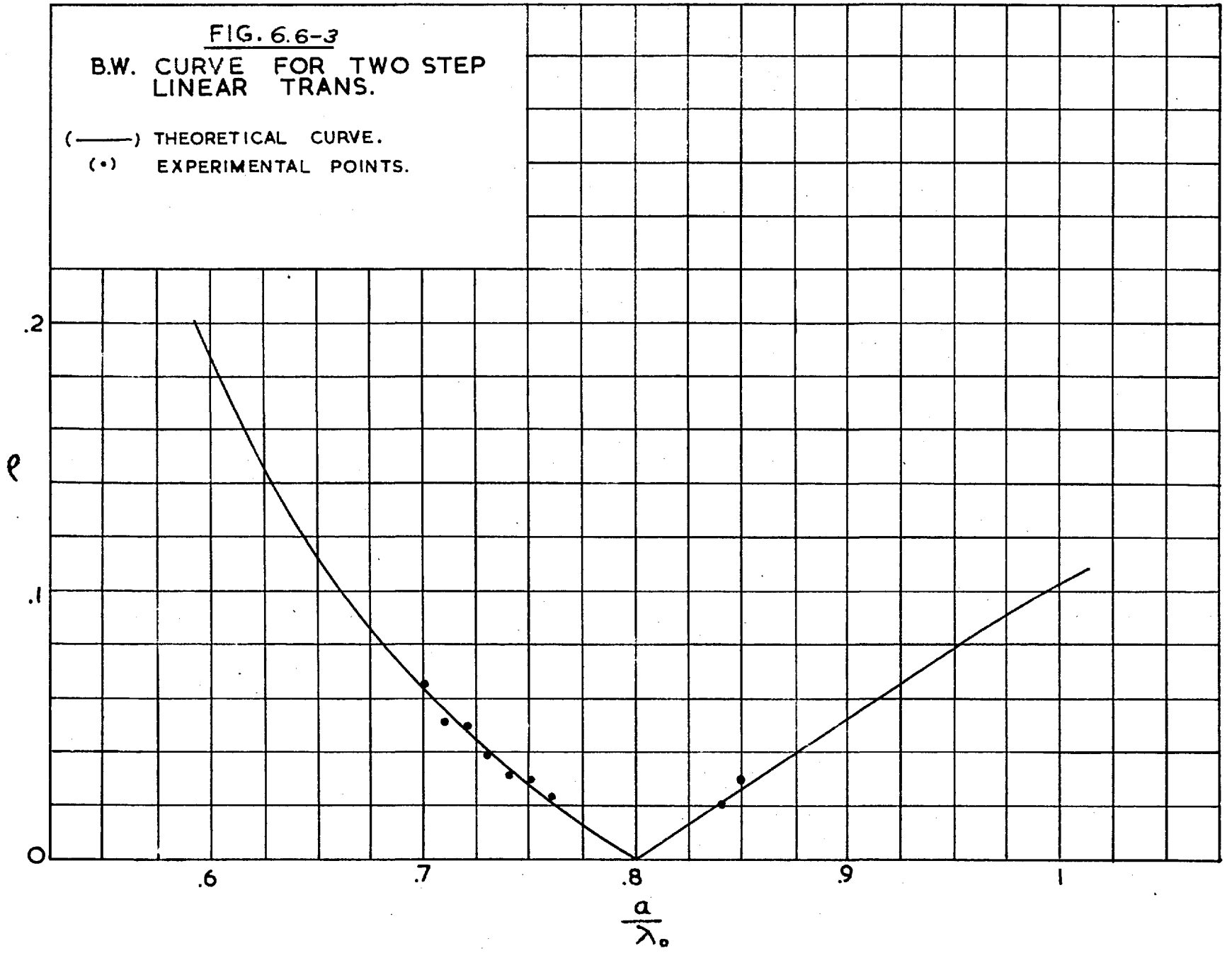
a/λ	.70	.71	.72	.73	.74	.75	.76	.84	.85
Ex. ρ	.066	.052	.05	.04	.032	.03	.024	.022	.03

FIG. 6.6-3

B.W. CURVE FOR TWO STEP LINEAR TRANS.

(——) THEORETICAL CURVE.

(•) EXPERIMENTAL POINTS.

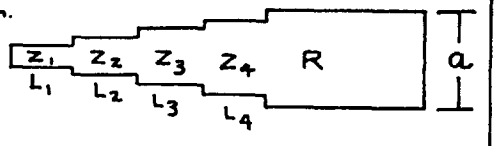


In figure 6.6.-4 are plotted the bandwidth curves for the above three transformers. The two step linear transformer is seen to offer very little improvement over the single step transformer. The binomial transformer has a considerably wider bandwidth and is also maximally flat. Furthermore since the binomial transformer departs very little from the ideal transformer it follows that the optimum bandwidth design given in section 6.4. can be applied directly to the design of a two section matching transformer to match an empty guide to a completely filled guide.

The final two tables 6.6.-7 and 6.6.-8 give the calculated theoretical reflection coefficients for a four section binomial transformer and a four section linear transformer. The impedance of the binomial transformer were chosen as $Z_1 = (1-\alpha)^1$, $Z_2 = (1-\alpha)^{1+4}$, $Z_3 = (1-\alpha)^{1+4+6}$, $Z_4 = (1-\alpha)^{1+4+6+4}$, $R = (1-\alpha)^{1+4+6+4+1}$.

Table 6.6.-7

$L_1 = .981$cm. $2t_1 = .037$cm. $a = 2.54$cm.
$L_2 = .84$cm. $2t_2 = .213$cm. $K = 2.47$
$L_3 = .665$cm. $2t_3 = .65$cm. $\frac{a}{\lambda_0} = .8$
$L_4 = .571$cm. $2t_4 = 1.51$cm.



a/λ	Z_1	Z_2	Z_3	Z_4	R	ρ
.6	.945	.75	.542	.442	.421	.044
.65	.949	.783	.590	.488	.466	.022
.7	.953	.806	.620	.523	.502	.01
.75	.958	.814	.638	.543	.524	.003
.8	.962	.824	.654	.560	.539	0
.85	.964	.829	.665	.572	.555	.001
.9	.966	.834	.673	.582	.565	.004
.95	.967	.837	.680	.591	.575	.012
1	.968	.840	.685	.598	.582	.025

FIG. 6.6-4

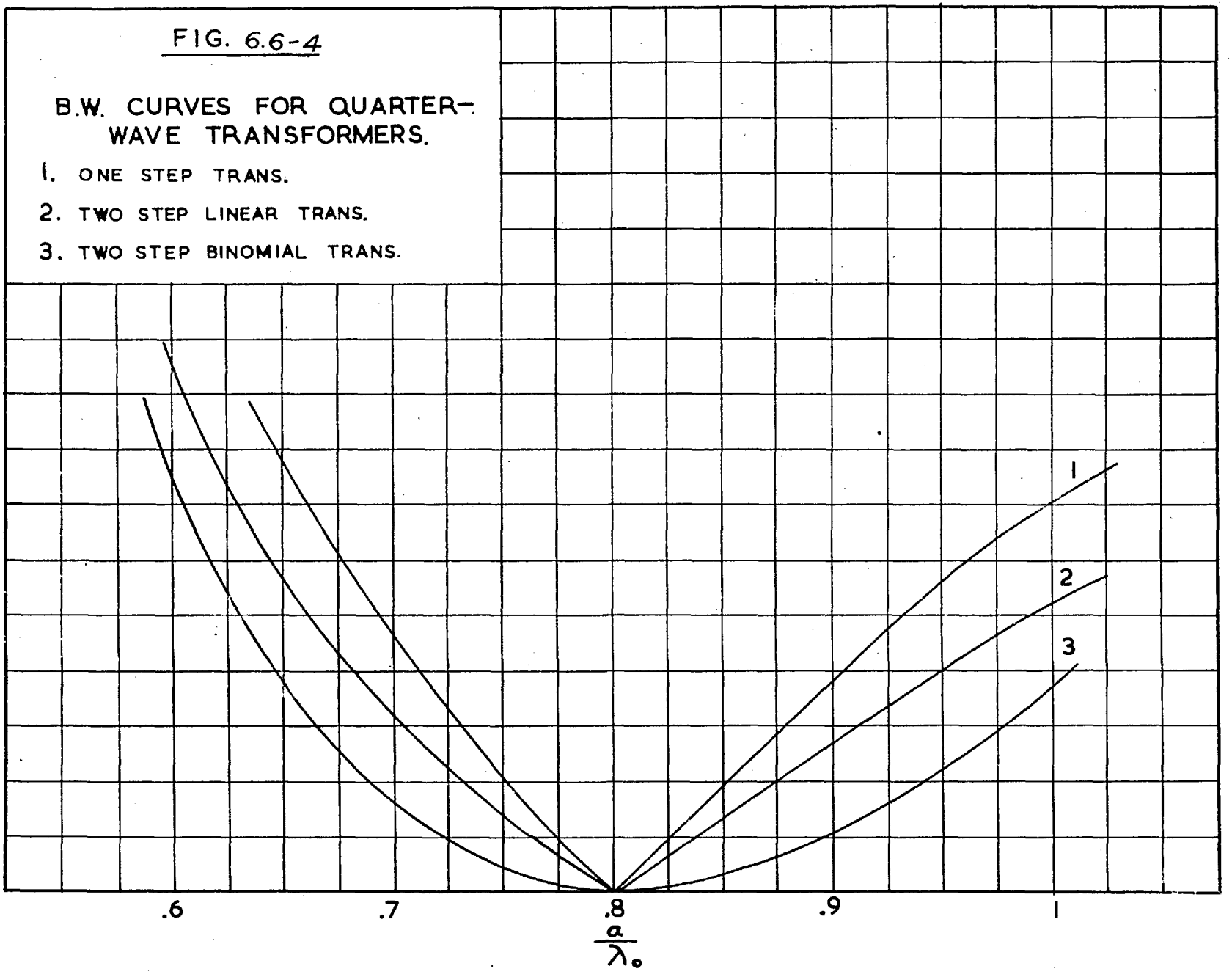
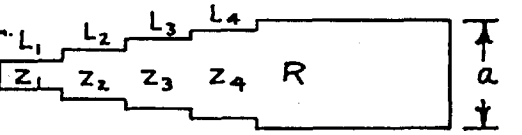

B.W. CURVES FOR QUARTER-WAVE TRANSFORMERS.
1. ONE STEP TRANS.
2. TWO STEP LINEAR TRANS.
3. TWO STEP BINOMIAL TRANS.
.2
.1
ρ
.6
.7
.8
.9
1
a/λ₀
1
2
3

Table 6.6.-8

$L_1 = .918$ cm. $2t_1 = .11$ cm. $a = 2.54$ cm.
$L_2 = .816$ cm. $2t_2 = .25$ cm. $\frac{a}{\lambda_0} = .8$
$L_3 = .714$ cm. $2t_3 = .48$ cm.
$L_4 = .581$ cm. $2t_4 = 1.16$ cm.



$K = 2.47$, $Z_n = 1 - \alpha n$, $\alpha = .1$,

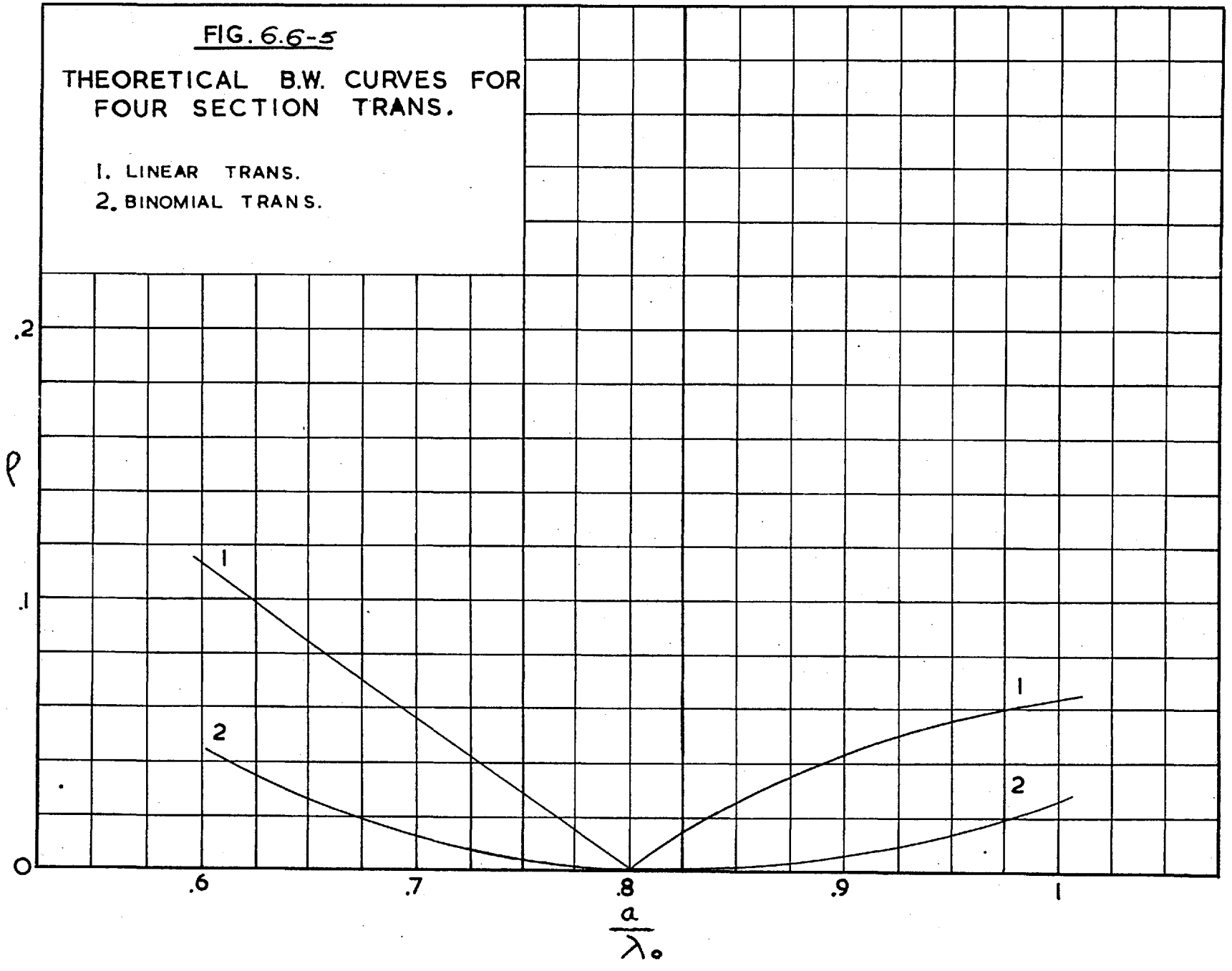
a/λ	Z_1	Z_2	Z_3	Z_4	R	ρ
.6	.852	.720	.594	.460	.422	.115
.65	.870	.758	.642	.508	.466	.0825
.7	.885	.780	.673	.543	.502	.055
.75	.892	.790	.69	.562	.524	.028
.8	.90	.80	.70	.58	.539	0
.85	.903	.806	.708	.591	.555	.028
.9	.905	.810	.714	.601	.565	.0436
.95	.908	.814	.719	.609	.575	.055
1	.91	.817	.723	.617	.582	.062

The theoretical bandwidth curves are plotted in figure 6.6.-5. The binomial transformer has a very wide bandwidth the reflection being below .01 for λ ranging from 2.7 to 3.6 cm. The linear four section transformer is no better than the two section binomial transformer.

FIG. 6.6-5

THEORETICAL B.W. CURVES FOR FOUR SECTION TRANS.

1. LINEAR TRANS.
2. BINOMIAL TRANS.



CHAPTER 7.

FREE SPACE MATCHING SECTION :

7.1. Theoretical Solution :

The reflection coefficient for a plane dielectric interface is $\frac{\eta - 1}{\eta + 1}$ where η is the index of refraction. For a dielectric constant of 2.56, $\eta = 1.6$ and 5.3% of the incident energy is reflected. By the simple procedure of slotting the interface a quarter-wave section can be produced that will match a dielectric interface to free space. The type of matching section to be considered is illustrated in figure 7.1-1. The electric field is assumed to be polarized parallel to the slots.

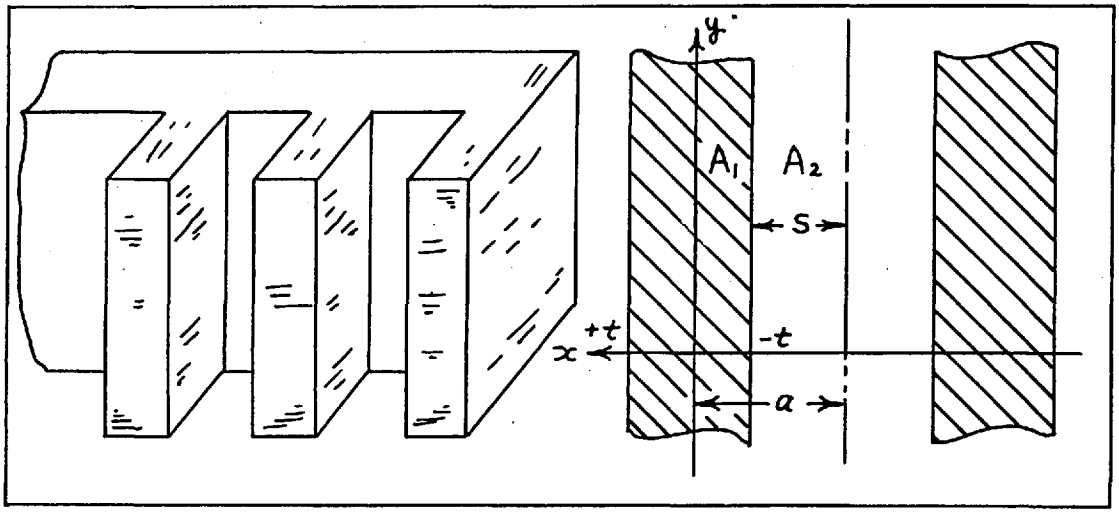


Fig. 7.1-1

For the T.E. waves being considered there are two possible solutions

(1) E_y antisymmetrical about $x = 0$ with a zero average electric field over the aperture.

(2) E_y symmetrical about $x = 0$ with a non-zero average electric field over the aperture.

Solution one is discarded since it cannot be related to the incident plane T.E.M. wave. For the second solution it is easy to see that magnetic walls can be placed at $x = 0, \pm a$ since H_z is zero at these points. The boundary conditions are $H_z = 0$ at $x = 0, \pm a$, and H_z and E_y continuous at $x = \pm t$. Let the incident wave be

$$E_y = e^{-\Gamma_0 z},$$

$$j\omega\mu H_x = -\Gamma_0 E_y = -\Gamma_0 e^{-\Gamma_0 z},$$

$$H_z = 0.$$

In the dielectric section A_1 the fields are

$$E_y = \sum_1^\infty A'_n \cos l_n x \, e^{-\gamma_n z},$$

$$j\omega\mu H_x = \frac{\partial E_y}{\partial z},$$

$$j\omega\mu H_z = \sum_1^\infty A'_n l_n \sin l_n x \, e^{-\gamma_n z},$$

where $\gamma_n^2 = l_n^2 - \kappa k_0^2 = k_n^2 - k_0^2$.

In the section A_2 the corresponding fields are

$$E_y = \sum_1^\infty C_n \cos(k_n x + \theta_n) e^{-\gamma_n z},$$

$$j\omega\mu H_x = \frac{\partial E_y}{\partial z},$$

$$j\omega\mu H_z = \sum_1^\infty C_n k_n \sin(k_n x + \theta_n) e^{-\gamma_n z}.$$

At $x = \pm a$, H_z must vanish and hence $\theta_n = -k_n a$. The continuity conditions at $x = \pm t$ gives

$$A'_n \cos l_n t = C_n \cos k_n (t - a)$$

$$A'_n l_n \sin l_n t = C_n k_n \sin k_n (t - a).$$

Dividing one equation by the other gives

$$l_n \tan l_n t = -k_n \tan k_n s \quad \text{where} \quad s = a - t.$$

This transcendental equation together with the relation $k_n^2 - k_0^2 = l_n^2 - \kappa k_0^2$ determines the wave numbers k_n and l_n.

The constant C_n is given as $C_n = (\cos l_n t \sec k_n s) A_n'$ The solution in the slotted section is therefore as follows :

$$E_y = \begin{cases} \sum_1^\infty A'_n \cos l_n x \, e^{-\gamma_n z}, & |x| \le t, \\ \sum_1^\infty A'_n \dfrac{\cos l_n t}{\cos k_n s} \cos k_n (a-x) e^{-\gamma_n z}, & t \le |x| \le t+2s, \end{cases}$$

$$= \sum_1^\infty A'_n \sqrt{P_n} \, F_n(x) e^{-\gamma_n z} \quad \text{where } P_n \text{ is a}$$

normalization constant.

$$j\omega\mu H_x = -\sum_1^\infty A_n \gamma_n F_n e^{-\gamma_n z} \quad \text{where } A_n = \sqrt{P_n} A'_n.$$

At the aperture there will be a reflected T.E.M. wave given by

$$E_y = R e^{\Gamma_0 z}, \quad j\omega\mu H_x = \Gamma_0 R e^{\Gamma_0 z},$$

where R is the complex reflection coefficient. The higher order modes excited are given by

$$E_y = \sum_1^\infty D_n \cos \frac{n\pi x}{a} e^{\Gamma_n z},$$

$$j\omega\mu H_x = \sum_1^\infty D_n \Gamma_n \cos \frac{n\pi x}{a} e^{\Gamma_n z},$$

where $\Gamma_n^2 = \left(\frac{n\pi}{a}\right)^2 - k_0^2$ and $\Gamma_0^2 = -k_0^2$.

The functions $\phi_n(x)$ will be defined as

$$\sqrt{2/a} \cos \frac{n\pi x}{a} \quad \text{for} \quad n > 0,$$

and $\sqrt{1/a}$ for $n = 0$.

Carrying out a similar procedure to that used in the waveguide problems

the following variational expression is obtained for the junction admittance

$$\frac{1-R}{1+R} = \frac{\sum_{1}^{\infty} \Gamma_n D_n D_n^* + \sum_{m=1}^{\infty} \gamma_m \sum_{n=0}^{\infty} R_{nm} D_n \sum_{n=0}^{\infty} R_{nm} D_n^*}{\Gamma_0 D_0 D_0^*} .$$

The factors R_{nm} are defined by

$$R_{nm} = \int_0^a \phi_n(x) F_m(x) dx , \quad n \geq 0, m \geq 1,$$

and are given by

$$R_{nm} = \frac{1}{2}\sqrt{\frac{2}{a P_m}} \left\{ \left[\frac{\sin(l_m + \frac{n\pi}{a})t}{l_m + \frac{n\pi}{a}} + \frac{\sin(l_m - \frac{n\pi}{a})t}{l_m - \frac{n\pi}{a}} \right] + \frac{\cos l_m t}{\cos k_m s} \left[\frac{\sin(k_m s - \frac{n\pi}{a}t)}{k_m + \frac{n\pi}{a}} + \frac{\sin(k_m s + \frac{n\pi}{a}t)}{k_m - \frac{n\pi}{a}} \right] \right\}$$

and

$$R_{0m} = \frac{1}{\sqrt{a P_m}} \frac{(1-K)k_0^2}{k_m^2 l_m} \sin l_m t .$$

The normalization constants P_m are given by

$$P_m = \frac{1}{2} \left[\frac{2 l_m t + \sin 2 l_m t}{2 l_m} + \frac{\cos^2 l_m t}{\cos^2 k_m s} \left(a - t + \frac{\sin 2 k_m s}{2 k_m} \right) \right].$$

It is desirable that all the higher order modes in the free space region and the solid dielectric region should be attenuated. If some of these modes propagate they will have a considerable effect on the input impedance to the section since part of the transmitted and reflected power will be carried by these higher order modes.

Now $\Gamma_n^2 = (\frac{n\pi}{a})^2 - k_0^2$ in the free space region and $\Gamma_n^2 = (\frac{n\pi}{a})^2 - K k_0^2$ in the solid dielectric region. The latter condition is the more severe of the two and hence 'a' must be chosen so that $a < \frac{\pi}{k_0\sqrt{K}} = \frac{\lambda_0}{2\sqrt{K}}$

for all values of λ_o that are being considered. For the first propagating mode in the slotted section k_1 is imaginary and $l_1 \tan l_1 t = |k_1| \tanh |k_1| s$. Let $l_1 \tan l_1 t = y_1(t)$ and $|k_1| \tanh |k_1| s = y_2(t)$ where $s = a - t$. Now $\frac{dy_1}{dt} = l_1^2 \sec^2 l_1 t$ and $\frac{dy_2}{dt} = -|k_1|^2 \operatorname{sech}^2 |k_1| s$. The two derivatives do not change signs and hence the functions $y_1(t)$ and $y_2(t)$ are monotomically increasing functions and it follows that if a solution for $y_1 = y_2$ exists only one such solution is possible. Such a solution does exist and consequently for some appropriate value of t the wave impedance in the slotted section is the geometric mean of the free space and solid dielectric wave impedances and a quarter-wave matching section can be obtained.

7.2. Numerical Work :

For a mid-band wavelength $\lambda_o = 10$ cm. and a bandwidth of $\pm$ 2 cm. the value of 'a' must be less than $\frac{\lambda_o - 2}{2\sqrt{K}} = 2.54$ for $K = 2.47$. A value of $a = 2$ cm. is chosen as being suitable. The solution for a typical example will be obtained by an application of the Ritz method.

The approximate fields in the slotted section will be taken as

$$E_y = \sum_0^N \alpha_{nm} \phi_n ,$$

$$j\omega\mu H_x = \sum_0^N \alpha_{nm} \gamma_m \phi_n ,$$

$$j\omega\mu H_z = \sum_0^N \alpha_{nm} \frac{d\phi_n}{dx} .$$

The following energy integral will be minimized,

$$\int_o^a \left\{ \left(\sum_0^N \alpha_{nm} \phi_n \right)^2 \beta_m^2 + \left(\sum_0^N \alpha_{nm} \frac{d\phi_n}{dx} \right)^2 \right\} dx - k_o^2 \left\{ \int_o^t K \left(\sum_0^N \alpha_{nm} \phi_n \right)^2 dx + \int_t^a \left(\sum_0^N \alpha_{nm} \phi_n \right)^2 dx \right\}$$

where $\beta_m^2 = |\gamma_m|^2$.

By using a two term approximation ($N=1$) the following result is obtained,

$$\beta_m^2(\alpha_{om}^2+\alpha_{1m}^2)+\alpha_{1m}^2\frac{\pi^2}{a^2}-k_o^2\left\{\left(\alpha_{om}^2\frac{t}{a}+2\alpha_{om}\alpha_{1m}\frac{\sqrt{2}}{\pi}\sin\pi\frac{t}{a}\right.\right.$$

$$\left.+\alpha_{1m}^2\frac{t}{a}+\alpha_{1m}^2\frac{1}{2\pi}\sin 2\pi\frac{t}{a}\right)K+\left(\alpha_{om}^2\frac{a-t}{a}-2\alpha_{om}\alpha_{1m}\frac{\sqrt{2}}{\pi}\sin\pi\frac{t}{a}\right.$$

$$\left.\left.+\alpha_{1m}^2\frac{a-t}{a}-\alpha_{1m}^2\frac{1}{2\pi}\sin 2\pi\frac{t}{a}\right)\right\}.$$

Setting the partial derivatives with respect to α_{nm} equal to zero gives

$$\beta_m^2\alpha_{om}-k_o^2\left\{K\frac{t}{a}\alpha_{om}+K\alpha_{1m}\frac{\sqrt{2}}{\pi}\sin\pi\frac{t}{a}+\alpha_{om}\frac{a-t}{a}-\alpha_{1m}\frac{\sqrt{2}}{\pi}\sin\frac{\pi t}{a}\right\}=0$$

$$\beta_m^2\alpha_{1m}+\alpha_{1m}\frac{\pi^2}{a^2}-k_o^2\left\{K\alpha_{om}\frac{\sqrt{2}}{\pi}\sin\pi\frac{t}{a}+K\alpha_{1m}\frac{t}{a}+K\alpha_{1m}\frac{1}{2\pi}\sin 2\pi\frac{t}{a}\right.$$

$$\left.-\alpha_{om}\frac{\sqrt{2}}{\pi}\sin\pi\frac{t}{a}+\alpha_{1m}\frac{a-t}{a}-\alpha_{1m}\frac{1}{2\pi}\sin 2\pi\frac{t}{a}\right\}=0$$

which can be simplified to give

$$\alpha_{om}\left[\beta_m^2-(K-1)k_o^2\frac{t}{a}-k_o^2\right]-\sqrt{2}\,\alpha_{1m}\left[(K-1)\frac{k_o^2}{\pi}\sin\pi\frac{t}{a}\right]=0$$

$$\alpha_{om}\left[2(1-K)\frac{k_o^2}{\pi}\sin\pi\frac{t}{a}\right]+\sqrt{2}\,\alpha_{1m}\left[\beta_m^2+\frac{\pi^2}{a^2}-k_o^2(K-1)\frac{t}{a}-k_o^2-(K-1)\frac{k_o^2}{2\pi}\sin 2\pi\frac{t}{a}\right]$$

$$=0.$$

Now let

$$\chi_1=\left[(K-1)\frac{t}{a}+1\right]k_o^2,$$

$$\chi_2=(K-1)\frac{k_o^2}{\pi}\sin\pi\frac{t}{a},$$

$$\chi_3=(K-1)\frac{k_o^2}{2\pi}\sin 2\pi\frac{t}{a},$$

and then

$$\alpha_{om}(\beta_m^2-\chi_1)-\sqrt{2}\,\alpha_{1m}\chi_2=0$$

$$-\sqrt{2}\,\alpha_{om}\chi_2+\alpha_{1m}\left(\beta_m^2+\frac{\pi^2}{a^2}-\chi_1-\chi_3\right)=0.$$

The vanishing of the determinant of the coefficients α_{nm} gives the first two values of β_m, thus

$$\beta_m^2 = \frac{2\chi_1 + \chi_3 - \frac{\pi^2}{a^2}}{2} \pm \sqrt{\left(\frac{2\chi_1 + \chi_3 - \frac{\pi^2}{a^2}}{2}\right)^2 + \left(2\chi_2^2 - \chi_1^2 - \chi_1\chi_3 + \chi_1\frac{\pi^2}{a^2}\right)}$$

Table 7.2.-1 gives the calculated values of β_m, χ_j and the other data for the example being worked out in detail.

Table 7.2.-1

$\lambda_0 = 10\,cm$, $a = 2\,cm$, $t = .69\,cm$, $K = 2.47$, $k_0^2 = .395$

$\chi_1 = .595$	$\beta_1^2 = .619$	$\alpha_{01} = .995$	$P_1 = 1.527$
$\chi_2 = .1631$	$\beta^2 = -1.819$	$\alpha_{11} = .0953$	$P_2 = 1.116$
$\chi_3 = .0763$	$\gamma_1 = j.785$	$\alpha_{02} = -.0953$	
$\frac{\pi^2}{a^2} = 2.467$	$\gamma_2 = 1.345$	$\alpha_{12} = .995$	
	$\Gamma_0 = j.629$	$R_{01} = .995$	
	$\Gamma_1 = 1.44$	$R_{11} = .097$	
	$l_1 = .599$	$R_{02} = -.094$	
	$k_1 = j.473$	$R_{12} = .996$	

These values of β_m are within 1% of the correct values as calculated from the transcendental equation given earlier. The β_m are substituted back into the set of homogenous equations and the α_{nm} are solved for subject to the conditions that

$$\alpha_{01}^2 + \alpha_{11}^2 = 1,$$
$$\alpha_{02}^2 + \alpha_{12}^2 = 1.$$

These values of α_{nm} are given in table 7.2.-1 and are seen to be very close to the corresponding values R_{nm}. The variational expression for the junction admittance is now

$$\frac{1-R}{1+R} \approx \frac{\sum_0^1 \Gamma_n D_n D_n^* + \sum_{m=1}^{2} \gamma_m \sum_{n=0}^{1} \alpha_{nm} D_n \sum_{n=0}^{1} \alpha_{nm} D_n^*}{\Gamma_0 D_0 D_0^*}.$$

The partial derivatives with respect to D_n^* are set equal to zero and the resulting equations solved for Dn . Using a two term approximation to the aperture field the following result was obtained,

$$\frac{1-R}{1+R} = 1.25 - j.0065.$$

Now γ_1 / Γ_o = 1.25 and it is seen that the slotted section acts like an ideal transformer of turns ratio $\sqrt{\frac{\gamma_1}{\Gamma_o}}$ and with a negligible junction reactance. This is to be expected since the first mode in the slotted section is almost plane (see figure 7.2-1) and hence the amplitude of the higher order modes that are excited is small and they store a negligible amount of reactive energy.

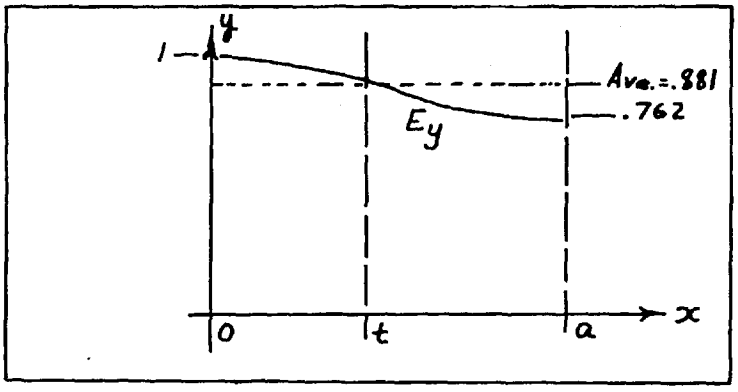


Fig. 7.2-1

As the period $2a$ is made smaller the first mode to propagate in the slotted section becomes closer to a plane wave and the junction reactance decreases.

7.3. Experimental Work :

A matching section was constructed from polystyrene of dielectric constant 2.56 and its properties measured on a 10 cm. strip transmission line. The overall length of the specimen was 50 cm., the thickness of each air slot was 2.64 cm., the thickness of each dielectric section

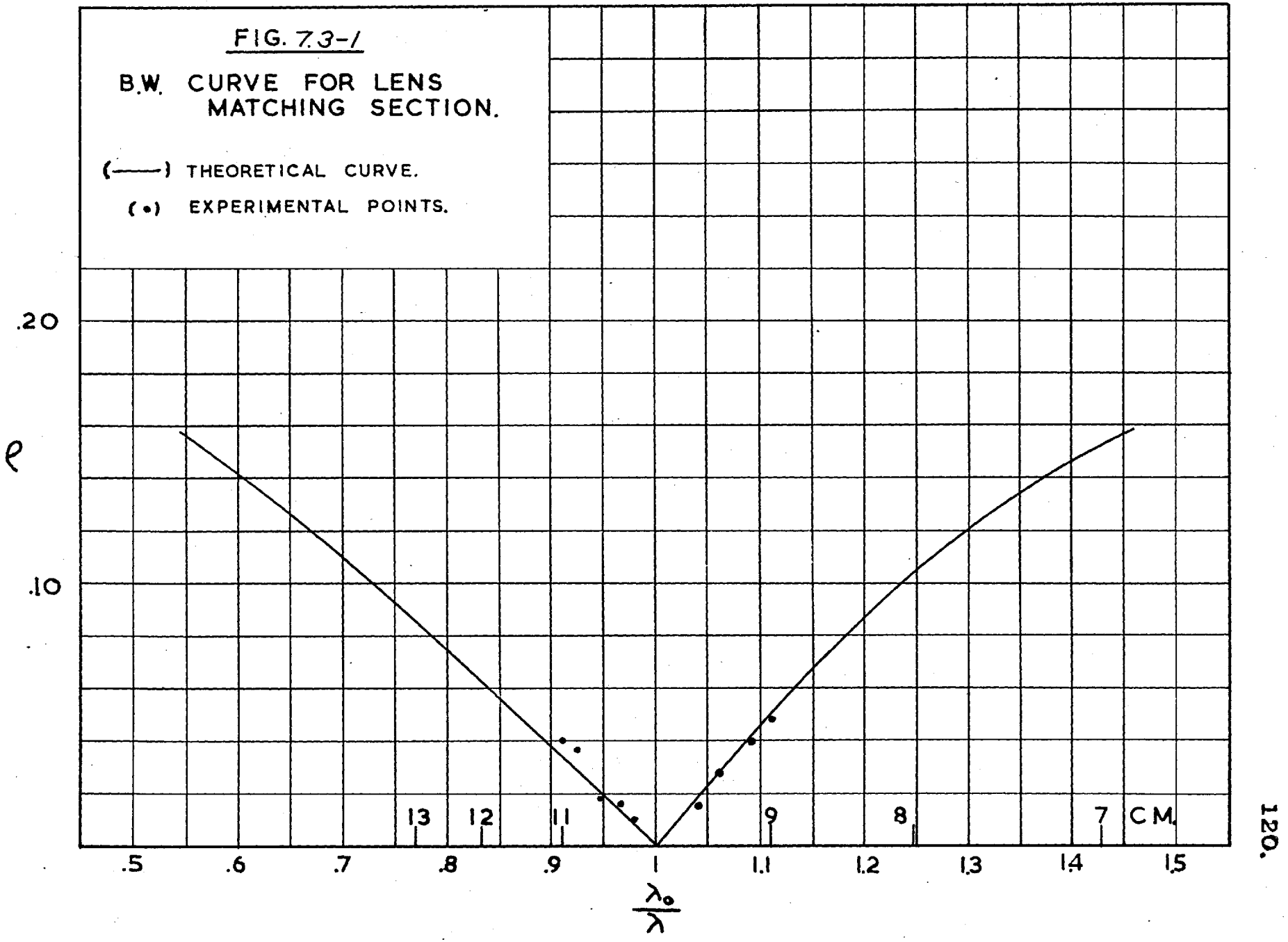
was 1.36 cm., and the length was 1.98 cm. The wavelength in the slotted section was 7.92 cm., for a free space wavelength of 10 cm. Table 7.3.-1 gives the theoretical and experimental values of the reflection coefficient.

Table 7.3.-1

λ_0/λ	.77	.835	.91	.925	.944	.961	.98	1	1.02	1.041	1.062	1.087	1.11	1.25	1.43
λ	13	12	11	10.8	10.6	10.4	10.2	10	9.8	9.6	9.4	9.2	9	8	7
Th. ρ	.085	.063	.035	.028	.022	.014	.007	0	.01	.021	.031	.041	.051	.103	.154
Ex. ρ			.04	.037	.018	.016	.010			.015	.028	.040	.048		
Z_1	.794							.792							.777

The theoretical bandwidth curve and experimental points are plotted in figure 7.3-1. The experimental points seem to indicate that the matching frequency is at approximately 9.9 cm., rather than 10 cm. This is probably due to the fact that the wave in the strip transmission line is closer to a waveguide mode than to a pure T.E.M. wave. For instance with $a \approx 6\,\lambda_0$ the wavelength in the line is about $\frac{1}{15}$% longer than free space wavelength. This discrepancy would shift the theoretical curve along the wavelength axis so that the matching wavelength would fall approximately at 9.95 cm., and a better overall agreement with the experimental points would be obtained. Such a matching section reduces the energy reflection coefficient from 5.3% to 1% over a bandwidth of 6 cm. i.e. λ from 8 to 14 cm.

When the electric field is polarized perpendicular to the slots, the following transcendental equation is obtained for determining the


FIG. 7.3-1
B.W. CURVE FOR LENS MATCHING SECTION.
(——) THEORETICAL CURVE.
(•) EXPERIMENTAL POINTS.
.20
ρ
.10
13
12
11
9
8
7
CM.
.5
.6
.7
.8
.9
1
1.1
1.2
1.3
1.4
1.5
λ₀/λ
120°

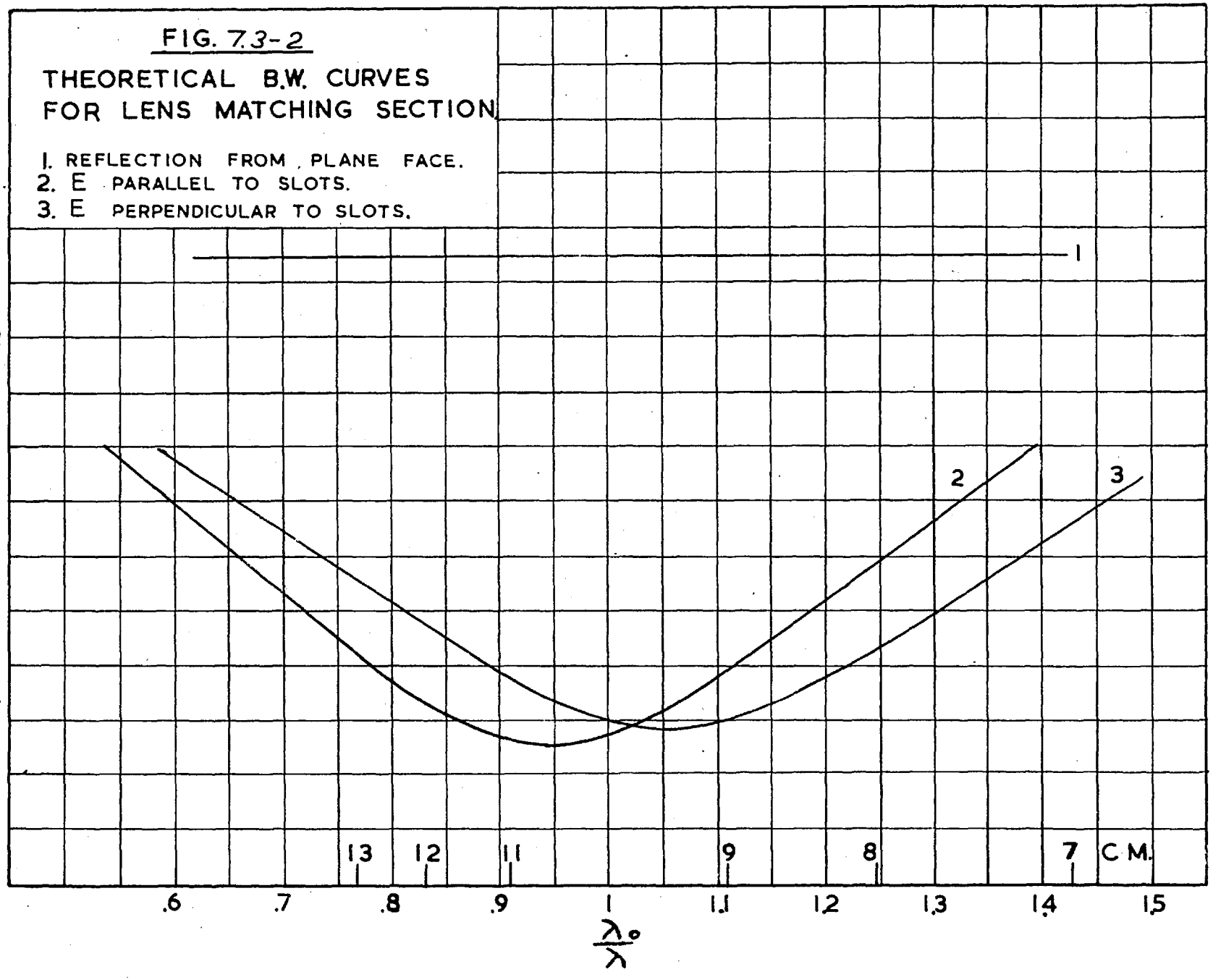
wave numbers k_n and l_n, $l_n \tan l_n t = -K k_n \tan k_n s$. This equation does not have a simultaneous solution with $l_n \tan l_n t = -k_n \tan k_n s$ which is the eigenvalue equation appropriate to the previous case. Thus a matching section designed for one polarization will not work for the other polarization. However by choosing a thickness of slot that is the average of that required for the two polarizations a matching section that gives quite good overall performance for both polarizations can be obtained. Thus for parallel polarization the correct value of $2t$ is 1.36 cm. and the length is 1.98 cm. For perpendicular polarization $2t$ should equal 2.14 cm. and l = 1.98 cm. The section is therefore constructed with a value of $2t$ equal to 1.75 cm. and a length equal to 1.98 cm. The theoretical values of ρ for the two polarizations are given in table 7.3-2. The subscript 'ν' denotes vertical or parallel polarization while 'μ' denotes horizontal or perpendicular polarization. It has been assumed that the junction reactance is negligible for perpendicular polarization also.

These theoretical bandwidth curves are plotted in figure 7.3-2. Although a perfect match is never attained the power reflection coefficient over a band from 8 to 13 cm. is still below 1.4% and the overall performance over the total band is essentially just as good as for the matching section designed for one polarization only. For wider bandwidth applications multi-section quarter-wave transformers can be constructed. Such matching sections can be used for matching a dielectric microwave lens surface to free space. The technique is the equivalent of lens blooming used in optics. For such applications it is essential that no higher order modes propagate since they would increase the side lobe level of the radiation pattern and any gain in

power obtained by matching would be offset by the poorer directivity of the main beam and loss of power in the side lobes.

Table 7.3-2.

λ cm.	λ_0/λ	$\tan\beta_{lV}l$	$\tan\beta_{lH}l$	ρ_V	ρ_H
13	.77	3.25	2.19	.0845	.111
12.5	.80	3.92	2.49	.076	.102
12	.833	5.12	2.89	.0671	.094
11.5	.87	7.54	3.49	.059	.0845
11	.91	14.51	4.455	.0528	.0755
10.5	.952		6.32	.0504	.067
10	1	-12.29	11.63	.0537	.0598
9.5	1.052	-5.85	172	.0635	.0565
9	1.11	-3.67	-12.6	.0785	.0594
8.5	1.178	-2.53	-5.52	.0985	.0697
8	1.25	-1.85	-3.386	.12	.0859
7.5	1.333	-1.36	-2.306	.144	.107
7	1.43	-.989	-1.63	.17	.132


FIG. 7.3-2
THEORETICAL B.W. CURVES
FOR LENS MATCHING SECTION
1. REFLECTION FROM PLANE FACE.
2. E PARALLEL TO SLOTS.
3. E PERPENDICULAR TO SLOTS.
1
2
3
.2
.1
ρ
13
12
11
9
8
7
C M.
.6
.7
.8
.9
1
1.1
1.2
1.3
1.4
1.5
λ₀/λ

CHAPTER 8.

A Rectangular Wave Guide Phase Changer.

8.1. Theory :

During this work on dielectric discontinuities in waveguidesit was noticed that the sum of the propagation constants of an empty and a completely filled guide was less than the sum of the propagation constants for a guide with a dielectric strip in the centre and a guide with two dielectric strips along the sides. It was realised that this property could be utilized for the purpose of producing a phase shift throughout the guide by displacing the central dielectric strip longitudinally with respect to the two side strips which are kept fixed. With reference to figure 8.1-1

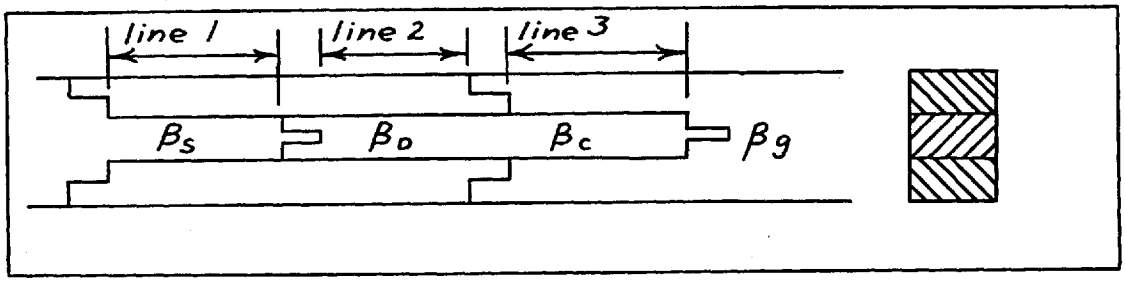
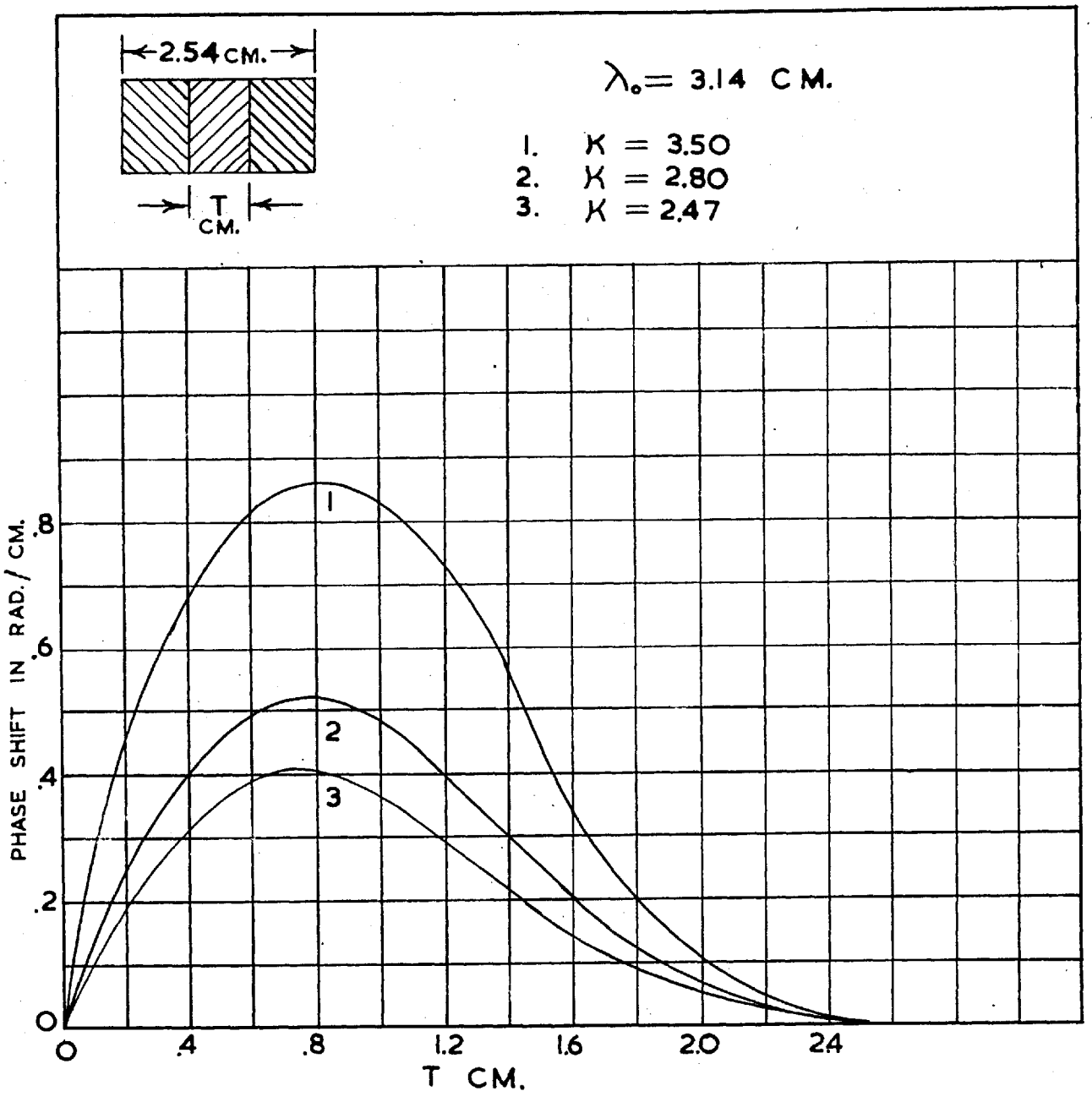


Fig. 8.1-1

it is found that $\beta_c+\beta_s > \beta_D+\beta_g$. In a 3 cm. waveguide and a dielectric constant of 2.54 this difference is of the order of .40 radians per cm. Let this difference be called ϕ , thus $\beta_c+\beta_s-\beta_D-\beta_g = \phi$. Now when the central strip is displaced longitudinally by an amount x cm., the effect is to lengthen the lines 1 and 3 and to shorten the line 2 and the empty wave guide length all by this same amount x . Thus it is readily seen that a phase shift of $x\phi$ radians is produced. The outstanding feature of this type of phase

FIG. 8.1-2


2.54 CM.
T CM.
λ_o = 3.14 CM.
1. K = 3.50
2. K = 2.80
3. K = 2.47
PHASE SHIFT IN RAD./CM.
0
.2
.4
.6
.8
1
2
3
0
.4
.8
1.2
1.6
2.0
2.4
T CM.

changer is its linear characteristics, the phase shift being directly proportional to the displacement. Furthermore if the ends of the dielectric strips can be matched at a given frequency, they are matched for all settings of the phase changer at this frequency. For values of dielectric constant larger than 2.54, the phase shift produced per cm. of movement is greater. Typical values that can be obtained are shown in figure 8.1-2. It is essential to use a dielectric constant less than the value that will allow the H_{03} mode to propagate. The H_{02} mode will not be excited by the structure since it is symmetrical. Also from figure 8.1-2 it can be seen that a maximum phase shift is produced when the central dielectric strip is between a quarter and a third of the guide width 'a'. This thickness is to the first approximation independent of the dielectric constant of the material.

It will be shown that maximum phase shift is obtained when $\beta_c = \beta_s$. The dielectric strips can be matched by quarter wave transformers designed according to the principles given in chapter 6. If a standing wave ratio of less than 1.05 is to be maintained over the desired band then the maximum value of the reflection coefficient for the whole structure must not exceed .025. Since there are four discontinuities and the reflected waves from these four discontinuities are almost certain to add in phase for some particular setting of the phase changer it follows that each discontinuity must be matched so as not to produce a reflection coefficient greater than $\frac{.025}{4}$ or $.006$. This is quite a severe matching condition and it is obvious that a two or three section transformer will be required if a large bandwidth is to be obtained.

It was shown at the end of chapter four that β_s and β_c are given to within a few per cent by the following expressions,

$$\beta_c^2 = k_0^2 \left[K \frac{2t}{a} + \frac{2d}{a} + \frac{K-1}{\pi} \sin 2\pi \frac{t}{a} \right] - \frac{\pi^2}{a^2} \quad (1)$$

$$\beta_s^2 = k_0^2 \left[\frac{2t}{a} + K \frac{2d}{a} - \frac{K-1}{\pi} \sin 2\pi \frac{t}{a} \right] - \frac{\pi^2}{a^2} \quad (2)$$

where $2t$ is the thickness of the centre dielectric strip and $d = \frac{a-2t}{2}$. Although these expressions are not suitable for calculating the phase shift produced per cm. of displacement they are of great value in analysing the overall behaviour of the phase changer. The phase shift produced is a second order quantity and a small error in β_c or β_s produces a much larger error in the calculated phase shift per cm. When the above two equations are added it is seen that

$$\beta_c^2 + \beta_s^2 = k_0^2 (K+1) - \frac{2\pi^2}{a^2} = \text{constant.}$$

To maximize the phase shift per cm. it suffices to maximize $\beta_c + \beta_s$ subject to the condition that $\beta_c^2 + \beta_s^2 =$ Constant. By elementary calculus it is easily shown that the maximum value is obtained if $\beta_c = \beta_s$. Substituting these values of β_c and β_s into equations (1) and (2) and equating the two equations gives

$$\sin 2\pi \frac{t}{a} + 2\pi \frac{t}{a} = \frac{\pi}{2}$$

for the value of $2t$ that maximizes the phase shift. It is seen that this relation is independent of the dielectric constant. The proportion of the waveguide width occupied by the centre strip is the only parameter that fixes the maximum phase shift. The solution to the

above equation is $\frac{2t}{a}$ = .265 which is slightly more than 1/4 of the guide width. However this thickness is not critical and a value of $\frac{2t}{a}$ from .26 to .32 is quite suitable. Actual calculation shows that the above theory is quite closely approximated.

Movement of the central dielectric strip can be obtained by cutting a longitudinal slot in the centre of the broad face of the guide and cementing a short dielectric tongue to the centre dielectric strip, this tongue protruding up through the slot and being fastened to some type of mechanical drive. Although such a slot if it is centrally located and narrow in comparison to the guide width does not cut any current flow lines it can still produce some undesirable effects in the linear characteristics of the phase changer. The phase shift produced is a second order quantity and a small perturbation of the guide wavelength in any one section will produce a considerably larger percentage change in the phase shift per cm. However by a proper design this effect can be made negligible.

8.2. Errors :

If the four discontinuities are perfectly matched then the linear characteristics of the phase changer can be destroyed only by variation in the dielectric constant throughout the strips, non-parallelism of the strips or by the effect of the slot. The first of these can be quite safely dismissed at once since present day manufacturing technique ensures that the dielectric constant of a given sample remains essentially uniform throughout the sample.

The variation in any of the propagation factors due to variation in the dimensions of the centre or side strips can be determined by differentiating the appropriate expressions for the propagation constants with respect to the transverse dimensions of the strips. For an example consider a variation of $\pm .01$ cm. in the thickness of the centre dielectric strip. From equation (1) it is seen that

$$\delta\beta_c = \frac{(K-1)k_o^2}{2\beta_c a}\left(1+\cos 2\pi\frac{t}{a}\right)2\delta t.$$

For $K = 2.56$, $k_o^2 = 3.75$, $\beta_c = 2.26$, β_D 2.76, $\frac{2t}{a} = .265$, $\varphi = .40$ rad./cm. and $2\delta t = .01$ cm. the change in β_c is slightly less than .01 and hence the change in φ is of the order of $2\frac{1}{2}$ per cent. If this change in thickness occurs in the region where the centre strip is moving between the two side strips then the effect on the linear characteristics is very small since the decrease in β_c is almost completely neutralized by the decrease in β_D. The actual change in β_D with gap thickness $\delta S = .005$ as illustrated in figure 8.2-1 is found to be

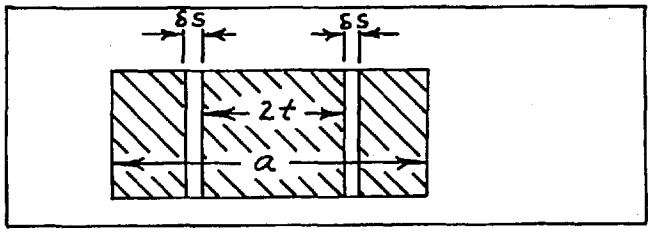


Fig. 8.2-1

$$\delta\beta_D = -\frac{(K-1)k_o^2}{\beta_D a}\left(1+\cos\frac{2\pi t}{a}\right)\delta S = -.0082$$

by an application of the Ritz method similar to that used to obtain equations (1) and (2). The net residual change is of the order of $\frac{1}{2}\%$ in the phase shift produced per cm. At any rate by careful machining

the tolerance on the transverse dimensions can be kept to within $\pm$ .003 cm., so this type of error can be made negligible.

The perturbation in the guide wavelength due to a covered slot can be calculated by considering propagation along the transverse axis of the waveguide. At the cutoff frequency the problem reduces to that of an equivalent parallel plate transmission line with a change in height. Consider a slotted waveguide as in figure 8.2-2.

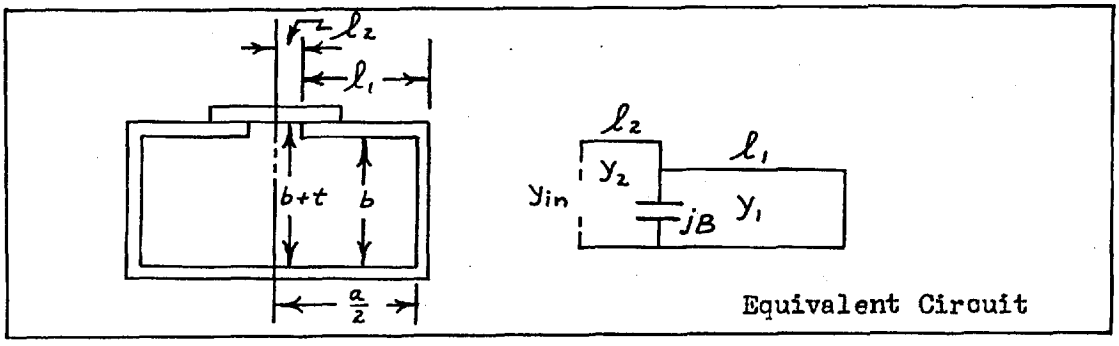


Fig. 8.2-2.

The equivalent circuit consists of two lengths of transmission line with characteristic admittance inversely proportional to the guide height and a capacitive susceptance at the junction. The junction susceptance is given by

$$\frac{B}{Y_1} = \frac{b}{\pi}\frac{k_x}{2}\left[\ln\frac{1-\alpha^2}{4\alpha}\left(\frac{1+\alpha}{1-\alpha}\right)^{\frac{1}{2}(\alpha+\alpha^{-1})}\right]$$

where $\alpha = \frac{Y_2}{Y_1} = \frac{b}{b+t}$ and k_x is the transverse wave number, (see section 6.16 of reference 1.5). For the usual thickness of guide wall the junction susceptance can be neglected. The value of k_x is found from the condition that the admittance at the centre of the guide must be zero. Neglecting the junction susceptance this condition is found to be

$$y_{in} = \frac{j\left(-\cot k_x l_1 + \frac{b}{b+t}\tan k_x l_2\right)}{\frac{b}{b+t} + \cot k_x l_1 \tan k_x l_2} = 0$$

or $\tan k_x l_2 = \frac{b+t}{b} \cot k_x l_1$.

If $l_2 << l_1$ this equation can be approximated by $k_x l_1 \tan k_x l_1 = \frac{l_1}{l_2} \frac{b+t}{b}$. The perturbed propagation constant β_g is obtained from the eigenvalue equation $\beta_g^2 = k_o^2 - k_x^2$. Similar techniques may be used when the guide is partially filled with a dielectric. In this case the transverse wave number is different in the two sections but are related through the condition that the propagation constant along the z axis must be the same over the guide cross section.

8.1-3. A Working Model.

One model was constructed with a 3/32" slot in a .9" x .4" American guide. This slot was centred longitudinally along the guide and a brass slide covered the slot on top along the length of the moving dielectric strip. The centre dielectric strip moved in the slotted section for the first half of the range and in the unslotted waveguide for the last half of the range. It was found that the phase shift produced per cm. of movement was about 5% less when the dielectric strip moved in the slotted section compared to its value when it moved in the unslotted section. A theoretical calculation of the perturbation of the guide wavelength due to the covered slot indicated that the effect was due to the slot. Consequently a slightly modified model was built. This latter model had a 1/16" wide slot located at one end of the guide such that the centre dielectric strip moved in the slotted section for the whole range of movement. A further improvement can be obtained by cutting a longitudinal groove in the broad face of the guide and making

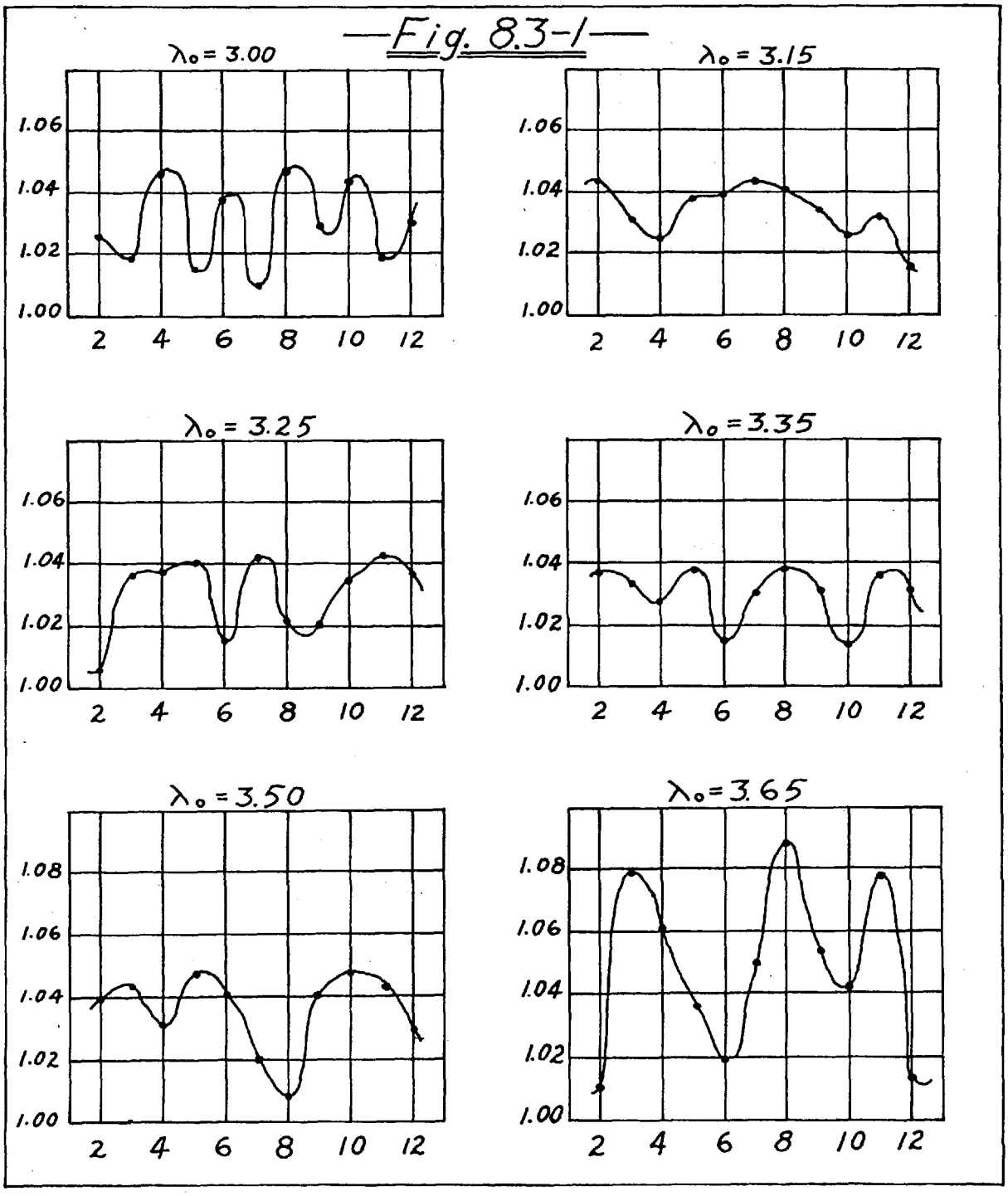
the slide with a projecting tongue which extends down into the groove. Making the groove approximately two thirds the thickness of the guide wall effectively reduces the thickness of the slot to one third of its former value. A drawing of the design followed (with the exception of the tongue and groove which was not made on either model) is included in this thesis. This model was found to give quite good overall performance. The standing wave ratio of the phase changer and the two choke couplings are plotted against phase changer setting for six different wavelengths in figure 8.3-1. Although a good match was never obtained the performance remained quite constant over a band from 3.00 to 3.50 cm. Measurements made on several choke couplings throughout the band showed that as a general rule they produced a standing wave ratio of the order of 1.01 per coupling. In view of this it would seem reasonable to expect that the dielectric strips were matched to produce a voltage standing wave ratio of less than 1.03 in the vicinity of the design wavelength. No doubt the slot had some effect on the matching of the center dielectric strip. By making the slide with a projecting tongue as explained earlier and taking more care with the machining of the dielectric strips it is felt that a better match should be obtained. All the standing wave ratios were obtained from the width of the Wiessfloch curves which were plotted for every setting of the phase changer. At each frequency eleven curves were taken corresponding to one centimetre increments in the phase changer setting.

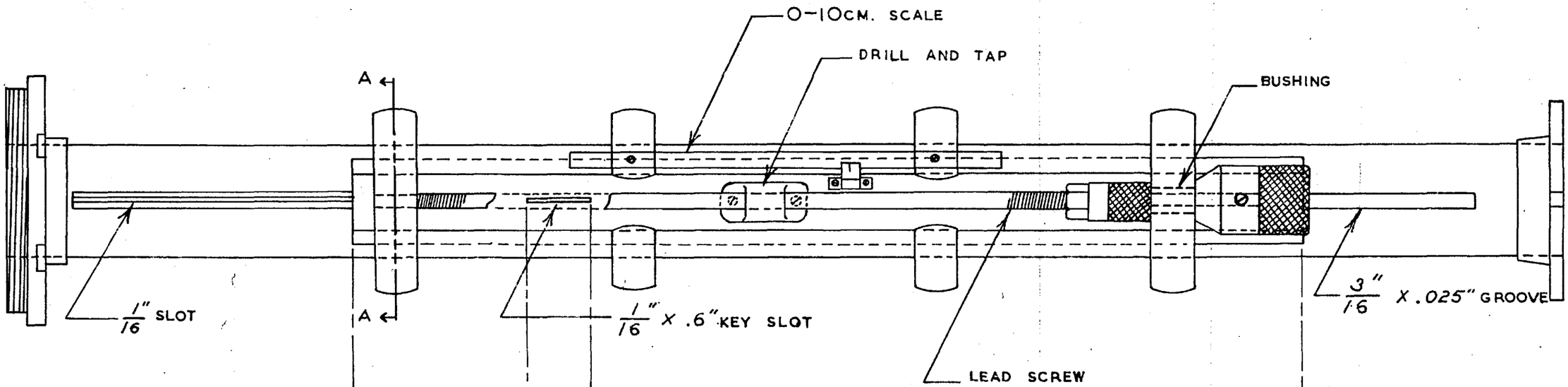
If the phase changer and the two couplings are replaced by an equivalent circuit consisting of two lengths of transmission line and an ideal transformer then it is readily seen that the displacement of the mean centre of the Wiessfloch curve of $\beta_g(1+d)$ vs. $\beta_g 1$ with phase changer setting gives the change in phase of the wave transmitted past the output coupling. The position of the short circuit is located a distance 'l' from the reference plane in the output guide, while a field minimum is located a distance 'd' from the reference plane in the input guide. It was found that the maximum departure from linearity was less than 1° over the whole band. The departure from linearity was probably due mainly to multiple reflections between the ends of the dielectric strips. The mean phase shift per cm. is given in table 8.3-1, below. This mean value was determined so that the sum of the errors over the total range was zero, i.e. $\sum_{n=0}^{10} \beta_g (n d_o - d) = 0$ where $\beta_g d_o$ is the mean phase shift per cm. and β_g is the measured total phase change in the transmitted wave with reference to the initial setting of the phase changer $n = 0$. The mean phase shift produced was a few per cent below the theoretical value and was probably due to the effect of the slot. This model had a total range of 215°. If the dielectric strips were made 6 cm. longer a range of 360° could be covered. This would increase the total length of the phase changer from 36 cm. to 48 cm. The use of a dielectric with a dielectric constant around 3 would reduce this overall length considerably.

Table 8.3-1.

λ_o cm.	3.00	3.15	3.25	3.35	3.50	3.65
$\delta\phi$ $\frac{\text{rad.}}{\text{cm.}}$	.417	.3966	.378	.3745	.371	.368

—Fig. 8.3-1—





X Band Phase Changer.

SCALE : FULL SIZE

DESIGN WAVELENGTH — 3.25 cm.

BANDWIDTH — 3.0 — 3.5 cm.

TOTAL PHASE CHANGE — 180°

APPENDIX 1.

A Note on Weissfloch's Method for Finding Equivalent Circuits.

A general discontinuity in a waveguide can be represented at a single frequency by a four terminal network which requires no more than three parameters to determine it uniquely. There exists a variety of such equivalent circuits. An ideal transformer and two sections of transmission line is one form of equivalent circuit for a lossless structure that lends itself readily to analysis and also has a physical interpretation. Furthermore the parameters of this circuit can readily be determined by plotting the position of a field minimum in the input guide against the position of a movable short circuit in the output guide (A1.1, A1.2, A1.3). Since positions of field minima only are determined any error due to probe reactance, crystal characteristics and so forth are eliminated.

The discontinuity and input and output guides are replaced by an ideal transformer of turns ratio $n:1$ and two lengths of transmission line x and y, of characteristic impedance Z_x and Z_y respectively. The impedances Z_x and Z_y may be freely chosen. In the following analysis they are taken proportional to the usual impedances of the input and output guides, i.e. proportional to the guide wavelengths. The equivalent circuit now assumes the form illustrated in figure 1.

The input impedance at section $a-a$ is

$$Z_a = j Z_y \tan \beta_y (l+y).$$

At section $b-b$ the impedance looking to the right is $n^2 Z_a$.

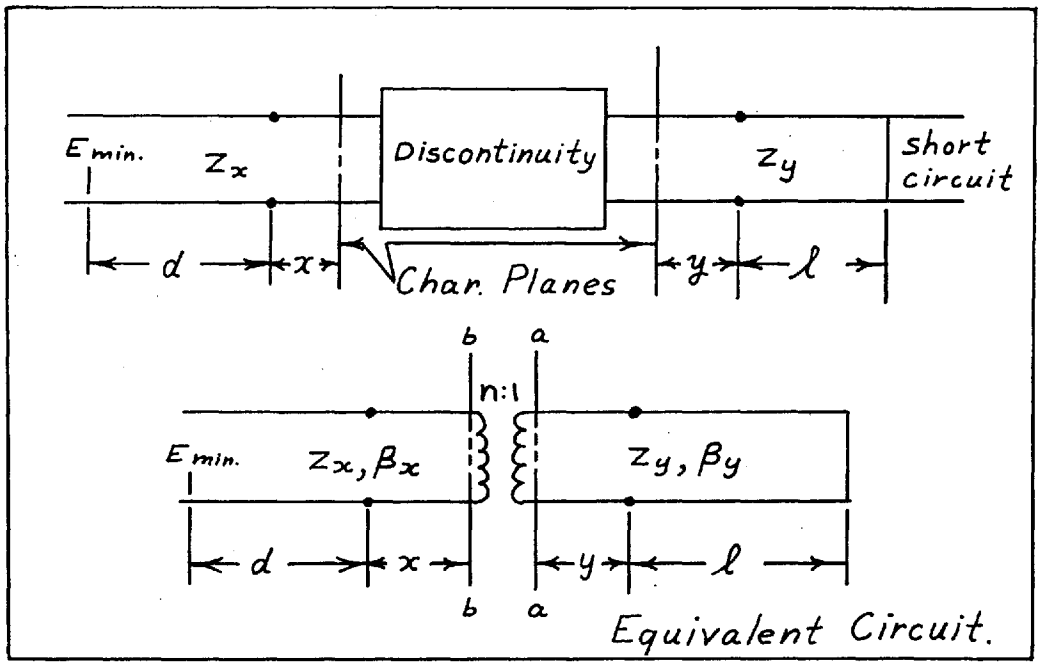


Fig. 1.

At a position of a field minimum the input impedance is zero and hence

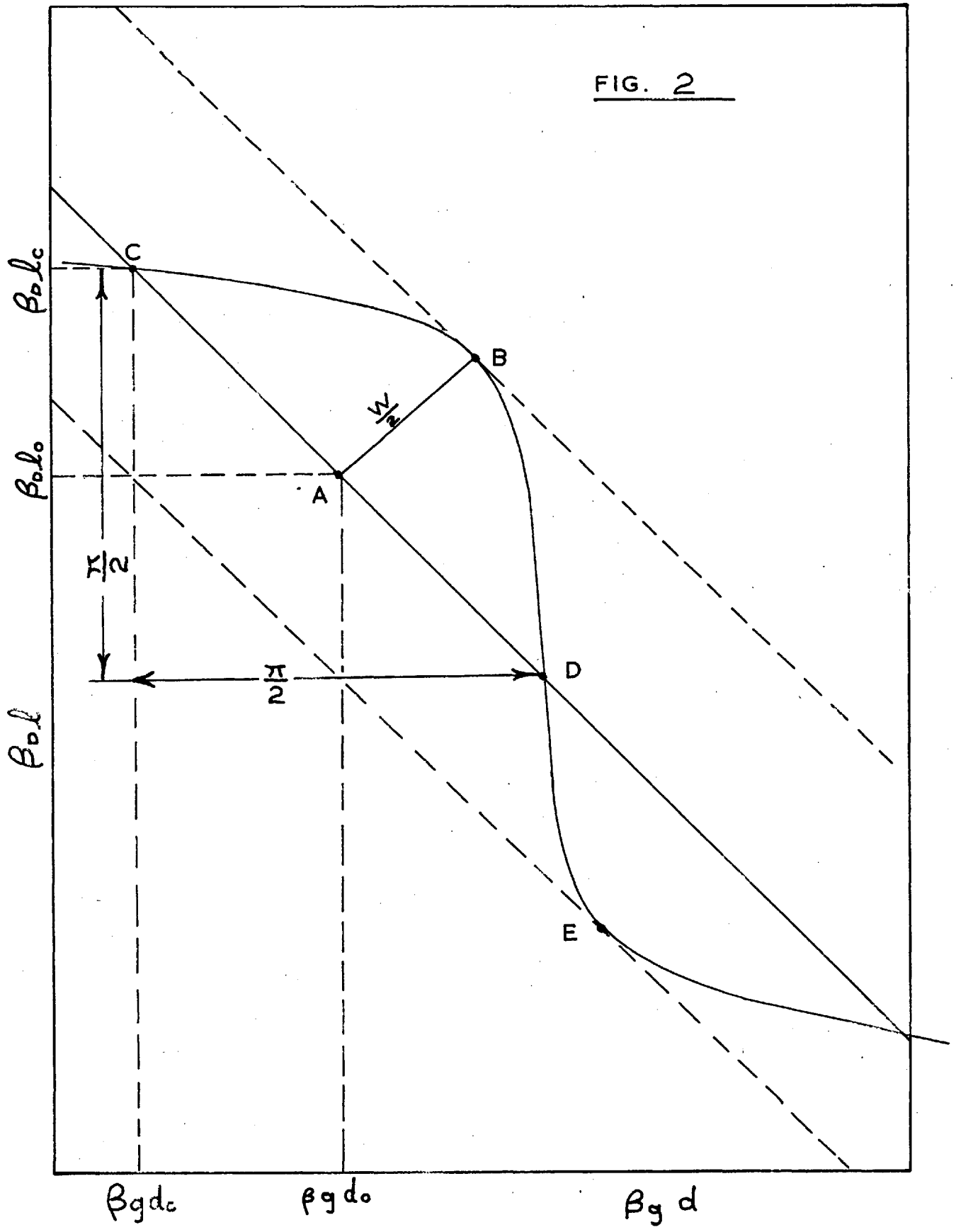
$$\tan \beta_x (x+d) = -n^2 \frac{Z_y}{Z_x} \tan \beta_y (l+y), \quad (1)$$

Let $n^2 \frac{Z_y}{Z_x} = N^2$ and it follows at once that when N^2 equals unity

$$\beta_x (x+d) + \beta_y (y+l) = G\pi + D\pi = n\pi, \quad (2)$$

where G and D are integers. The plot of $\beta_x d$ against $\beta_y l$ is a straight line of slope -1. In general the plot of $\beta_x d$ against $\beta_y l$ is an oscillatory curve about this line. The curve is periodic of period π. The slope of the curve is $\frac{d\,\beta_y l}{d\,\beta_x d} = -\frac{\sec^2 \beta_x (x+d)}{N^2 \sec^2 \beta_y (y+l)}$ and is always negative. When $\beta_x (x+d) = G\pi$ and $\beta_y (y+l) = D\pi$ the slope is $-\frac{1}{N^2}$. When $\beta_x (x+d) = G\pi + \frac{\pi}{2}$ and $\beta_y (y+l) = D\pi - \frac{\pi}{2}$ the slope is $-N^2$. The general type of curve obtained is

FIG. 2


$\beta_D l_c$
$\beta_D l_o$
$\beta_D l$
C
B
A
D
E
$W/2$
$\pi/2$
$\pi/2$
$\beta_g d_c$
$\beta_g d_o$
$\beta_g d$

shown in figure 2. With reference to figure 2 the minimum slope is seen to occur at C and the maximum slope at D. At B and E the slope is -1 so

$$N \sec \beta_y (y+l) = \pm \sec \beta_x (x+d). \quad (3)$$

When equations (1) and (3) are solved for N the result is

$$\frac{1}{N} = \pm \tan \beta_y (l+y). \quad (4)$$

If the positive root is taken then $\beta_y(l+y) = D\pi - \frac{\pi}{2}$ at C since the tangent function is negative when the angle decreases from a multiple of π and is positive when the angle decreases from a multiple of π plus $\frac{\pi}{2}$. In this case the angle $\beta_y(l+y)$ decreases when $\beta_x(x+d)$ increases. It also follows that the slope at C is $-N^2$ and hence N has a value less than unity. When the negative root is taken then $\beta_y(l+y) = D\pi$ with the corresponding slope $-\frac{1}{N^2}$ at C and consequently the value of N obtained will be greater than unity. Both roots lead to a correct equivalent circuit so it is immaterial which one is chosen.

At A, $\beta_y l = \beta_y l_o$ and $\beta_x d = \beta_x d_o$. Also

$$\beta_y (y+l_o) + \beta_x (x+d_o) = n\pi.$$

At B, $\beta_x d = \beta_x d_o + \frac{w}{2\sqrt{2}}$ and $\beta_y l = \beta_y l_o + \frac{w}{2\sqrt{2}}$

where w is the peak to peak width of the curve measured in radians. It follows therefore that at B,

$$\beta_y (l+y) + \beta_x (x+d) = n\pi + \frac{w}{\sqrt{2}}. \quad (5)$$

Now $\tan\left[\beta_y(l+y)+\beta_x(x+d)\right] = \dfrac{\tan\beta_y(l+y)+\tan\beta_x(x+d)}{1-\tan\beta_y(l+y)\tan\beta_x(x+d)}$

$$= \pm\frac{1-\frac{1}{N^2}}{\frac{2}{N}} = \tan\frac{w}{\sqrt{2}}$$

after substituting from equation (5). Furthermore

$$\tan\frac{w}{\sqrt{2}} = \cot\left(\frac{\pi}{2}-\frac{w}{\sqrt{2}}\right) = \frac{1-\tan^2\left(\frac{\pi}{4}-\frac{w}{2\sqrt{2}}\right)}{2\tan\left(\frac{\pi}{4}-\frac{w}{2\sqrt{2}}\right)} = \pm\frac{1-\frac{1}{N^2}}{\frac{2}{N}}.$$

If the positive sign is taken then $N = \cot\left(\frac{\pi}{4}-\frac{w}{2\sqrt{2}}\right)$ and N is greater than unity. The negative sign gives $N = \tan\left(\frac{\pi}{4}-\frac{w}{2\sqrt{2}}\right)$. The two values of N obtainable are reciprocals of each other.

At C, $\beta_y(l_c+y) = D\pi$ or $D\pi-\frac{\pi}{2}$ and $\beta_x(d_c+x) = G\pi$ or $G\pi+\frac{\pi}{2}$. The parameters x and y determine the characteristic planes which have the property that the impedance transformation from a characteristic plane in the input guide to a characteristic plane in the output guide is a real quantity. If the position of the short circuit and E min. is measured from these characteristic planes then the equivalent circuit reduces to an ideal transformer. The new co-ordinates are $d' = d+x$ and $l' = l+y$.

Since the input reactance is proportional to the difference in the magnetic and electric energies stored at the discontinuity, x and y can be interpreted as the lengths of transmission lines that store this equivalent energy. The characteristic planes are located by moving a distance back in the guide such that the energy stored in those sections is equal to the negative of the energy stored at the discontinuity. Short circuits can be placed at the characteristic planes in the two guides and the cavity so formed is resonant at the

frequency for which the equivalent circuit was determined.

The two circuits obtainable are duals of each other. The characteristic planes of one are located a quarter of a wavelength from those of the other and the two turns ratios are reciprocals of one another. The one circuit can be derived from the other by using the properties of quarter wave transformers. That there should be two sets of characteristic planes follows also from the consideration of the general bilinear transformation which has two invariant points (A1.3)

When the width w is very small it is more convenient to plot $\beta_y l + \beta_x d$ against $\beta_x d$ since this removes the slope of the mean centre of the curve. The new width W is equal to $\sqrt{2}\, w$ and hence

$$N = \tan\left(\frac{\pi}{4} - \frac{W}{4}\right)$$

The curve is asymmetrical and the peak occurs closer to D than to C. Since $\tan\beta_x(x+d) = \pm N = \pm\tan\left(\frac{\pi}{4} - \frac{W}{4}\right)$ it follows that $\beta_x(x+d) = \pm\left(\frac{\pi}{4} - \frac{W}{4}\right) + n\frac{\pi}{2}$. Take $\beta_x(x+d) = \frac{\pi}{4} + \frac{W}{4}$ and then since $\beta_x(x+d_c) = G\pi$ at C, $\beta_x(d-d_c) = \frac{\pi}{4} + \frac{W}{4}$. If $\beta_x(x+d_c) = G\pi + \frac{\pi}{2}$ at C then take $\beta_x(x+d) = \frac{3\pi}{4} + \frac{W}{4}$ at B and the same results are obtained. The peak occurs closer to D by an amount $\frac{W}{4}$. It is convenient to know where the peak occurs since it enables one to fit a better curve through the experimental points.

If the output guide is terminated in its characteristic impedance then

$$\frac{Z_{in}}{Z_x} = \frac{N^2 + j\tan\beta_x(x+d)}{1 + jN^2\tan\beta_x(x+d)}$$

for the imput impedance at a point d in the input guide. This input impedance is real whenever $\beta_x(x+d) = \frac{n\pi}{2}$ or at a characteristic plane. At

this point the reflection coefficient ρ is real and hence

$$\frac{1+\rho}{1-\rho} = N^2 \quad and \quad \rho = \frac{N^2-1}{N^2+1} .$$

When W is small it can easily be shown by expanding $\tan\left(\frac{\pi}{4} - \frac{W}{4}\right)$ that $|\rho| \simeq \frac{W}{2}$. The characteristic plane in the output guide is located a distance l_c from the terminal plane in the output guide, where $\beta_y (l_c + y) = \pi$. If the phase of the incident, reflected and transmitted waves are known then l_c may be determined from the following analysis.

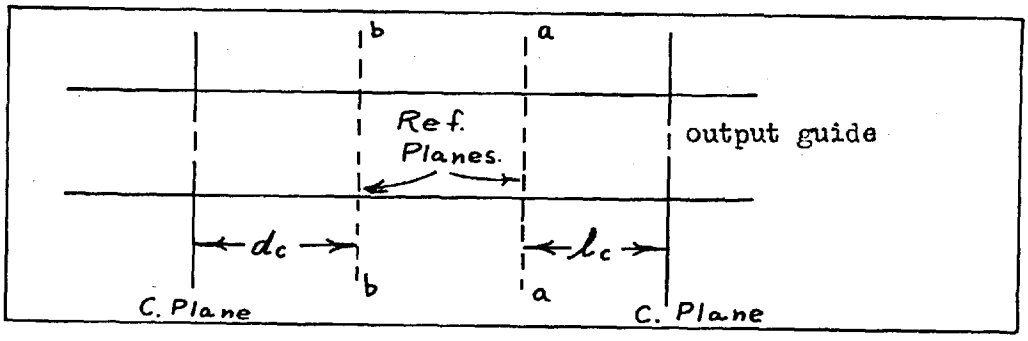


Fig. 3.

Let the phase of the incident wave be zero at plane b-b in figure 3. At the characteristic plane it has increased to $\beta_x d_c$. If the phase of the reflected wave is θ at $b-b$ it will be $\theta - \beta_x d_c$ at the characteristic plane. Now the phase angles of the voltages on either side of the ideal transformer must be the same and hence the phase of the transmitted wave at the characterisric plane in the output guide must be $\psi = \angle \left\{ \rho e^{j(\theta - \beta_x d_c)} + e^{j\beta_x d_c} \right\} = \angle e^{j\beta_x d_c}\left(1+\rho e^{j(\theta - 2\beta_x d_c)}\right)$ The characteristic plane in the input guide is located where $\theta - 2\beta_x d_c = n\pi$ and hence $\psi = \beta_x d_c$. At the reference plane $a-a$ the phase of the transmitted wave is α and hence $\beta_x d_c + \beta_y l_c = \alpha$. Since d_c and α are assumed known this relation determines the unknown

quantity ℓ_c . The input impedance at the characteristic plane is $\frac{e^{j\beta_x d_c} + Re^{-j\beta_x d_c}}{e^{j\beta_x d_c} - Re^{-j\beta_x d_c}} = \frac{1 + Re^{-2j\beta_x d_c}}{1 - Re^{-2j\beta_x d_c}}$ and is real. R is the reflection cofficient referred to the plane $b-b$ and $Re^{-2\beta_x d_c}$ is the equivalent reflection coefficient at the characteristic plane.

APPENDIX II.

Some Properties of Expansions in Terms of Complete Sets of Orthonormal Functions.

A piecewise continuous function $G(x)$ defined over the range $0 \leq x \leq x_0$ can be expanded into a Fourier series by means of a complete set of orthogonal functions which are orthogonal over the range $0 \leq x \leq x_0$. It will be assumed that two such sets of orthogonal functions are available and a few important relationships between them will be derived. Let the two sets of functions be $\sum_1^\infty \varphi_n(x)$ and $\sum_1^\infty F_m(x)$, Further it will be assumed that these functions are normalized so that

$$\int_0^{x_0} \varphi_n \varphi_m \, dx = \int_0^{x_0} F_n F_m \, dx = \delta_{nm}$$ where δ_{nm}

is by definition equal to zero for $n \neq m$ and equal to unity for $n = m$.

Thus by conventional Fourier analysis it follows that

$$G = \sum_1^\infty A_m F_m = \sum_1^\infty B_n \varphi_n$$ where

$$A_m = \int_0^{x_0} G F_m \, dx, \quad B_n = \int_0^{x_0} G \varphi_n \, dx.$$

Now define the quantities R_{nm} by the following relationship

$$R_{nm} = \int_0^{x_0} \varphi_n F_m \, dx.$$

Let $F_m = \sum_1^\infty C_n \varphi_n$ and $\varphi_n = \sum_1^\infty D_m F_m$. Then

$$\int_0^{x_0} \varphi_n F_m \, dx = R_{nm} = \int_0^{x_0} \varphi_n \sum_1^\infty C_n \varphi_n \, dx = C_n.$$

Similarly it is easily seen that $D_m = R_{nm}$. Therefore

$F_m = \sum_{n=1}^{\infty} R_{nm} \phi_n$ and $\phi_n = \sum_{m=1}^{\infty} R_{nm} F_m$. When this series expression for ϕ_n is substituted into the series expansion for F_m as follows

$$F_m = \sum_{n=1}^{\infty} R_{nm} \sum_{j=1}^{\infty} R_{nj} F_j = \sum_{j=1}^{\infty} F_j \sum_{n=1}^{\infty} R_{nm} R_{nj}$$

the conclusion is that $\sum_{n=1}^{\infty} R_{nm} R_{nj} = \delta_{mj}$ where δ_{mj} is defined as above. It may also be shown that $\sum_{m=1}^{\infty} R_{jm} R_{nm} = \delta_{nj}$

Now since

$$\sum_{n=1}^{\infty} B_n \phi_n = \sum_{m=1}^{\infty} A_m F_m = \sum_{m=1}^{\infty} A_m \sum_{n=1}^{\infty} R_{nm} \phi_n$$

$$= \sum_{n=1}^{\infty} \phi_n \sum_{m=1}^{\infty} R_{nm} A_m$$ it follows that

$$B_n = \sum_{m=1}^{\infty} R_{nm} A_m .$$

Similarly $A_m = \sum_{n=1}^{\infty} R_{nm} B_n$.

The transformation from one set of orthogonal functions to another is analogous to the transformation from one orthogonal co-ordinate system to another orthogonal co-ordinate system. The elements of the transformation matrix are the factors R_{nm} . Using matrices this transformation may be written as

$$\{B_n\} = [R_{nm}]\{A_m\}$$ where $\{B_n\}$ and $\{A_m\}$ are the column matrices

$\begin{Bmatrix} B_1 \\ B_2 \\ B_3 \\ \vdots \end{Bmatrix}$ and $\begin{Bmatrix} A_1 \\ A_2 \\ A_3 \\ \vdots \end{Bmatrix}$ and $[R_{nm}]$ is the square matrix

$$\begin{bmatrix} R_{11} & R_{12} & R_{13} & \cdots \\ R_{21} & R_{22} & \cdots & \\ R_{31} & \cdots & & \\ \vdots & & & \end{bmatrix}$$

The inverse transformation is $\{A_m\} = [R_{mn}]\{B_n\}$

It is seen that the matrix of the transformation is an orthogonal matrix.

If the ϕ_n are solutions of the following differential equation

$$\frac{d^2\phi_n}{dx^2} + \lambda_n^2 \phi_n = 0 \quad , \quad \phi(0) = \phi(x_0) = 0$$

where λ_n^2 is a constant then

$$\phi_n = \sqrt{\frac{2}{x_0}} \sin \frac{n\pi x}{x_0}$$ and the eigenvalues

λ_n^2 are $\frac{n^2\pi^2}{x_0^2}$.

If the F_m are solutions of the following Sturm-Liouville boundary value problem over the same range and with the same end conditions

$\frac{d^2F_m}{dx^2} + (k_m^2 + q(x))F_m = 0$ where $q(x)$ is a continuous function of x over the given range with a piecewise continuous derivative, then it is known from the theory of such systems (A2.1) that a discrete set of values k_n exist such that $\lim_{n\to\infty} k_n = \frac{n\pi}{x_0}$ and also that

$$\lim_{n\to\infty} F_n(x) = \phi_n(x).$$

For each value of k_n there exists one solution and the sum of all these solutions forms a complete orthonormal set of functions.

Since F_n approaches ϕ_n as n tends to infinity it follows

that

$$\lim_{m\to\infty} R_{nm} = \lim_{m\to\infty} \int_0^{x_0} \varphi_n F_m \, dx = 0$$

and

$$\lim_{n\to\infty} R_{nn} = \lim_{n\to\infty} \int_0^{x_0} \varphi_n F_n \, dx = 1 .$$

APPENDIX III

Application of the Ritz Method for Finding the Approximate Eigenvalues and Eigenfunctions.

1. Minimum Characterization of the Eigenvalues.

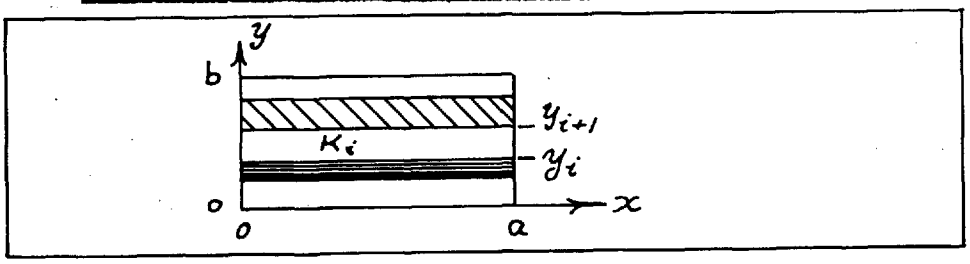


Fig. 1.

Consider a rectangular wave guide inhomogenously filled as in figure 1 with the inhomogenity constant along the x and z axis. The relative dielectric constant K has arbitraty but constant values for any one region $y_i \leq y \leq y_{i+1}$. The fields are derivable from a Hertzian vector $\vec{\pi}$ directed along the y axis by means of the following vector operations

$$\vec{H} = j\omega\epsilon_0 K \nabla \times \vec{\pi} , \qquad \vec{E} = K k_0^2 \vec{\pi} + \nabla\nabla\cdot\vec{\pi} ,$$

thus

$$H_x = -j\omega\epsilon_0 K \frac{\partial \pi}{\partial z} , \quad H_y = 0 , \quad H_z = j\omega\epsilon_0 K \frac{\partial \pi}{\partial x} ,$$

$$E_x = \frac{\partial^2 \pi}{\partial x \partial y} , \quad E_y = K k_0^2 \pi + \frac{\partial^2 \pi}{\partial y^2} , \quad E_z = \frac{\partial^2 \pi}{\partial z \partial y} .$$

The Hertzian vector π satisfies the following wave equation $\nabla^2\pi + K k_0^2 \pi = 0$ where $k_0^2 = \omega^2\epsilon_0\mu_0$. It will now be assumed that variation with x is of the form $\sin\frac{\pi x}{a}$ and variation with respect to z is $e^{-\gamma_m z}$. By virtue of the continuity conditions on E_z and H_z it follows that $K\pi$ and $\frac{\partial \pi}{\partial y}$ are continuous for all y and $\frac{\partial \pi}{\partial y}$ vanishes for $y = 0, b$.

The equation satisfied by π can now be written as

$$\frac{d^2\pi_m}{dy^2} + (\gamma_m^2 - k_x^2 + \kappa_i k_o^2)\pi_m = 0, \quad (1)$$

where π_m is now a function of y only and γ_m^2 is the eigenvalue corresponding to the eigenfunction π_m. Multiply this equation by $\kappa_i \pi_n$ and subtract it from the similar equation obtained by interchanging the subscripts n and m, thus

$$(\gamma_m^2 - \gamma_n^2)\kappa_i \pi_n \pi_m = \kappa_i \pi_m \frac{d^2\pi_n}{dy^2} - \kappa_i \pi_n \frac{d^2\pi_m}{dy^2}.$$

Now integrate over the range $y_i \le y \le y_{i+1}$,

$$(\gamma_m^2 - \gamma_n^2)\int_{y_i}^{y_{i+1}} \kappa_i \pi_n \pi_m dy = \int_{y_i}^{y_{i+1}} \kappa_i \left(\pi_m \frac{d^2\pi_n}{dy^2} - \pi_n \frac{d^2\pi_m}{dy^2}\right) dy$$

$$= \kappa_i \left(\pi_m \frac{d\pi_n}{dy} - \pi_n \frac{d\pi_m}{dy}\right)\Bigg|_{y_i}^{y_{i+1}} \quad \text{by integrating}$$

by parts once. The integrated term is continuous over all y and vanishes on the boundary $y = 0, b$ and hence it follows by summing over all i that if $\gamma_m^2 \neq \gamma_n^2$

$$\int_0^b \pi_n \pi_m \kappa \, dy = 0 \quad \text{for} \quad n \neq m$$

Thus the functions π_j form an orthogonal set over the range $0 \le y \le b$ with respect to the weight function $K(y)$. These functions can be normalized so that

$$\int_0^b K \pi_n \pi_m dy = \delta_{nm}.$$

It will now be shown that a minimization of the integral

$$I = \int_0^b K(y)\left[\left(\frac{d\pi}{dy}\right)^2 - (K k_o^2 - k_x^2)\pi^2\right] dy \quad (2)$$

subject to the conditions that

$$\int_0^b K \pi^2 \, dy = 1, \qquad (3)$$

and $$\int_0^b K \pi \pi_n \, dy = 0 \quad \text{for } n = 1, 2, \cdots m-1. \qquad (4)$$

where π_n is the eigenfunction that satisfies

$$\frac{d^2 \pi_n}{dy^2} + (\gamma_n^2 - k_x^2 + K k_0^2) \pi_n = 0$$

gives an approximation from above to the correct eigenvalue γ_m^2. Due to the properties of the correct eigenfunctions it follows that π can be expanded in terms of them, hence take

$$\pi = \sum_1^\infty C_n \pi_n \qquad \text{with} \qquad C_n = \int_0^b \pi \pi_n K \, dy$$

and $$\frac{\partial \pi}{\partial y} = \sum_1^\infty C_n \frac{\partial \pi_n}{\partial y}. \qquad (5)$$

The normalization condition (3) gives

$$\int_0^b \sum_1^\infty C_n \pi_n K \sum_1^\infty C_s \pi_s \, dy = \sum_1^\infty C_n^2 = 1, \qquad (6)$$

while the $m-1$ orthogonality conditions (4) give $\int_0^b \sum_1^\infty K C_n \pi_n \pi_k \, dy = 0$

$$\text{or} \quad C_k = 0 \quad \text{for } k = 1, 2, \cdots m-1. \qquad (7)$$

Substituting from (5) for one factor in (2) gives

$$I = \int_0^b K \left\{ \frac{d\pi}{dy} \sum_1^\infty C_n \frac{d\pi_n}{dy} + (k_x^2 - K k_0^2) \pi \sum_1^\infty C_n \pi_n \right\} dy$$

$$= \sum_1^\infty C_n \int_0^b K \left\{ \frac{d\pi}{dy} \frac{d\pi_n}{dy} + (k_x^2 - K k_0^2) \pi \pi_n \right\} dy$$

$$= \sum_1^\infty C_n \int_0^b K \left\{ -\pi \frac{d^2 \pi_n}{dy^2} + (k_x^2 - K k_0^2) \pi \pi_n \right\} dy$$

after integrating by parts once. With reference to the wave equation (1) it is seen that this is equivalent to $\sum_1^\infty C_n \int_0^b \gamma_n^2 K \pi \pi_n dy$. Now substitute for π from (5) and it follows that

$$I = \sum_1^\infty C_n \gamma_n^2 \sum_1^\infty C_s \int_0^b K \pi_n \pi_s \, dy = \sum_1^\infty C_n^2 \gamma_n^2 .$$

By virtue of equations (6) and (7) this last factor can be written as $\gamma_m^2 + \sum_{m+1}^\infty C_n^2 (\gamma_n^2 - \gamma_m^2)$. Now it is assumed that all the eigenvalues have been arranged in ascending order so that

$$\gamma_1^2 < \gamma_2^2 < \cdots \gamma_m^2 < \cdots \gamma_n^2 \qquad \text{and consequently} \qquad I \geq \gamma_m^2 .$$

The approximate eigenvalues so calculated will all be too large unless all C_n for $n > m$ are zero, which corresponds to the correct eigenfunction π_m having been chosen. It should be noted that an application of the Euler-Lagrange equations to the integral (2) generates the wave equation (1) as the condition imposed on π.

2. The Approximate Eigenvalues and Eigenfunctions.

For an approximate numerical solution to a problem the infinite series $\sum_1^\infty C_n \pi_n$ is replaced by a finite series $\sum_1^N C_n \phi_n$. It is convenient to choose ϕ_n as the proper functions existing in the empty guide although this is not necessary. The only restrictions on ϕ_n are that they satisfy the boundary conditions on the guide walls and are continuous with piecewise continuous partial derivatives. The m'th approximate eigenfunction will be taken as $\pi_m = \sum_1^N C_{nm} \phi_n$.

The functions π_m will be determined so that they form an orthogonal and normalized set with respect to the weight function $K(y)$ over the guide cross section. When the m'th approximate eigenfunction and

eigenvalue is being determined it is assumed that the first (m-1) functions π_k have already been found.

The normalization condition gives

$$\int_0^b \pi^2 K\,dy = \int_0^b \sum_1^N C_n \phi_n \sum_1^N C_s \phi_s \, K\,dy = 1$$

$$\text{or} \quad \sum_{n,s=1}^{N} C_n C_s \alpha_{sn} = 1 \quad \text{where} \quad \alpha_{sn} = \alpha_{ns} = \int_0^b \phi_n \phi_s K\,dy. \qquad (1)$$

The m-1 orthogonality conditions give

$$\int_0^b \pi \pi_k K\,dy = \int_0^b \sum_1^N C_n \phi_n \sum_1^N C_{sk} \phi_s K\,dy = 0 \quad \text{for } k = 1, 2, \cdots m-1,$$

$$\text{or} \sum_{n,s=1}^{N} C_n C_{ks} \alpha_{ns} = 0 \quad \text{for } k = 1, 2, \cdots m-1. \qquad (2)$$

The following integral is minimized subject to the above conditions,

$$I = \int_0^b K \left\{ \sum_1^N C_n \frac{d\phi_n}{dy} \sum_1^N C_s \frac{d\phi_s}{dy} + (R_x^2 - K k_o^2) \sum_1^N C_n \phi_n \sum_1^N C_s \phi_s \right\} dy. \qquad (3)$$

Define $$T_{sn} = \int_0^b K \left\{ \frac{d\phi_n}{dy} \frac{d\phi_s}{dy} + (R_x^2 - K k_o^2) \phi_n \phi_s \right\} dy \qquad (4)$$

and it follows that $$I = \sum_{n,s=1}^{N} C_n C_s T_{sn}. \qquad (5)$$

To minimize I subject to the conditions (1) and (2) introduce m Lagrange multipliers $-\Gamma_{mm}^2$ and $-\nu_{mk}$ where $k = 1, 2, \cdots m-1$.

Thus $$\sum_{n,s=1}^{N} C_n C_s T_{sn} - \Gamma_{mm}^2 \sum_{n,s=1}^{N} C_n C_s \alpha_{ns} - \sum_{k=1}^{m-1} \nu_{mk} \sum_{n,s=1}^{N} C_n C_{sk} \alpha_{sn} \qquad (6)$$

is minimized. Setting all $\frac{\partial}{\partial C_n}$ equal to zero gives the following set of N homogenous equations in the N unknowns C_n which when solved give the corresponding C_{nm}

$$\sum_{n=1}^{N} \left\{ \sum_{s=1}^{N} C_s T_{sn} - \Gamma_{mm}^2 \sum_{s=1}^{N} C_s \alpha_{sn} - \frac{1}{2} \sum_{k=1}^{m-1} \nu_{mk} \sum_{s=1}^{N} C_{sk} \alpha_{sn} = 0 \right\} \qquad (7)$$

For the actual solutions of the above equations the following results hold

$$\sum_{s=1}^{N}\sum_{n=1}^{N} C_{nm} C_{sj} \alpha_{sn} = \delta_{mj} \qquad (8)$$

by virtue of the normalization and orthogonality conditions that were imposed.

To show that the (m-1) multipliers $-\nu_{mk}$ vanish (Ref. A-3-1) multiply the n'th equation in (7) above by C_{nj} with $j < m$ and sum over all n, thus

$$\sum_{n=1}^{N}\sum_{s=1}^{N} C_{sm} C_{nj} T_{sn} - \Gamma_{mm}^{2} \sum_{n=1}^{N}\sum_{s=1}^{N} C_{sm} C_{nj} \alpha_{ns} - \frac{1}{2}\sum_{k=1}^{m-1} \nu_{mk} \sum_{n=1}^{N}\sum_{s=1}^{N} C_{sk} C_{nj} \alpha_{sn} \qquad (9)$$

where C_{sm} are the actual solutions to (7).

From (8) above it is seen that this reduces to

$$\sum_{n=1}^{N}\sum_{s=1}^{N} C_{sm} C_{nj} T_{sn} = \frac{1}{2}\nu_{mj} \quad \text{since } j < m. \qquad (10)$$

Now for $m=1$ all ν_{1j} are zero since the first eigenfunction is not required to satisfy any orthogonality conditions and hence from (7)

$$\sum_{n=1}^{N} C_{n1} T_{sn} = \Gamma_{11}^{2} \sum_{n=1}^{N} C_{n1} \alpha_{ns} \qquad \text{for all } s .$$

In (10) above let $m=2$, then $j=1$ and

$$\frac{1}{2}\nu_{21} = \sum_{s=1}^{N} C_{s2} \sum_{n=1}^{N} C_{n1} T_{sn} = \sum_{s=1}^{N} C_{s2} \Gamma_{11}^{2} \sum_{n=1}^{N} C_{n1} \alpha_{sn}$$

$$= \Gamma_{11}^{2} \sum_{n=1}^{N}\sum_{s=1}^{N} C_{n1} C_{s2} \alpha_{sn} = 0$$

or the second multiplier vanishes. Thus by the usual process of induction it follows that all the multipliers $-\nu_{mk}$ vanish since the above does hold for $m=1$ which in turn implies that it holds for $m=2$ and so on ad infinitum.

Therefore the set of equations to be solved reduce to

$$\sum_{n=1}^{N}\left[\sum_{s=1}^{N} C_s T_{sn} - \Gamma_{mm}^2 \sum_{s=1}^{N} C_s \alpha_{sn} = 0\right]. \qquad (11)$$

In order for these equations to have a solution the following determinant must vanish,

$$\sum_{n=1}^{N}\left[\sum_{s=1}^{N}\left(T_{sn} - \Gamma_{mm}^2 \alpha_{sn}\right) = 0\right]. \qquad (12)$$

The vanishing of this determinant results in N roots for Γ_{mm}^2. Let Γ_{mm}^2 be the m'th root and assume for the time being that the C_{nm} have been solved for subject to the normalization conditions (1). Multiply the n'th equation in (11) by C_{nm} and sum over all n to get

$$\sum_{n=1}^{N}\sum_{s=1}^{N} C_{nm} C_{sm} T_{sn} = \Gamma_{mm}^2 \sum_{n=1}^{N}\sum_{s=1}^{N} C_{nm} C_{sm} \alpha_{sn} = \Gamma_{mm}^2 .$$

Since the approximate eigenvalue γ_m^2 is given by $I = \sum_{s,n=1}^{N} C_{nm} C_{sm} T_{sn}$ it follows that $\gamma_m^2 = \Gamma_{mm}^2$. Furthermore since the determinant does not depend on the index m it must be concluded that the N roots of Γ_{mm}^2 arranged in ascending order are the first m approximate eigenvalues γ_m^2. Thus for each root γ_m^2 of (12) above a set of coefficients C_{nm} are obtained from (11) above and the m'th approximate eigenfunction is

$$\pi_m = \sum_{n=1}^{N} C_{nm} \varphi_n .$$

It was shown in section 1 that the m'th minimization of the integral **I** with respect to those functions that are orthogonal to the first (m-1) correct eigenfunctions gives an approximation from above to the correct eigenvalue γ_m^2. It does not follow that the same is true for that class of functions which are orthogonal to the first (m-1) approximate eigenfunctions. However it can be shown that this is the

case (A3.1. A3.2).

The above procedure is identical to minimizing the volume integral of the difference between the mean magnetic energy and mean electric energy stored in a given mode. With reference to the field components given at the beginning it will be seen that in the volume integral of the difference between the magnetic and electric energy the integral with respect to z is common to all terms and can be deleted since it will cancel out when the integral is minimized. Similarly the integration with respect to x integrates out to $\frac{a}{2}$ for all components and so it will be necessary to consider the integral over y only, thus

$$W_H \propto \tfrac{1}{2}\mu \int_0^b \omega^2 \epsilon_0^2 \kappa^2 (\beta_m^2 + k_x^2)\pi_m^2 \, dy,$$

$$W_E \propto \tfrac{1}{2}\epsilon_0 \int_0^b \kappa \left[(k_x^2+\beta_m^2)\left(\frac{\partial \pi_m}{\partial y}\right)^2 + (k_x^2+\beta_m^2)\pi_m^2\right] dy,$$

and hence $W_H - W_E \propto \frac{1}{2}\epsilon_0 \int_0^b \kappa \left[(\kappa k_0^2 - k_x^2 - \beta_m^2)\pi_m^2 - \left(\frac{\partial \pi_m}{\partial y}\right)^2\right] dy$

after cancelling the common factor $k_x^2 + \beta_m^2$. A minimization of this integral is seen to be equivalent to a minimization of $I = \int_0^b \kappa \left[\left(\frac{\partial \pi}{\partial y}\right)^2 - (\kappa k_0^2 - k_x^2)\pi^2\right] dy$ subject to $\int_0^b \kappa \pi^2 dy = 1$ if the Lagrange multiplier is identified with $-\beta_m^2$.

Once the approximate eigenfunctions π_m have been found, the field components are obtained by the usual vector operations. These field components may be used in the variational expression for the input admittance or impedance to the inhomogenously filled guide. The y component of the electric field may be taken as $(k_x^2 - \gamma_m^2)\pi_m = (k_x^2 - \gamma_m^2)\sum_1^N C_{nm}\phi_n$. If ϕ_n are the corresponding eigenfunctions for the empty guide then the matrix elements χ_{nm}

used in chapter five may be identified with C_{nm} .

A similar procedure may be used for the H-plane discontinuity discussed in chapter four. In this case the fields are derivable from the scalar component E_y and it suffices to minimize the following integral

$$\int_0^a \left[\left(\frac{\partial E_y}{\partial x}\right)^2 - k k_0^2 E_y^2 \right] dx$$

subject to the normalization condition

$$\int_0^a E_y^2 \, dx = 1$$

and the (m-1) orthogonalization conditions

$$\int_0^a (E_y)(E_y)_k \, dx = 0 \quad \text{for } k = 1, 2, \cdots m-1.$$

Apart from the absence of a weighting factor the same type of analysis and results hold for this case also.

APPENDIX IV

Solutions of the Wave Equation when Guide Wavelength equals Free Space Wavelength.

(1) Asymmetrical Dielectric Strip:

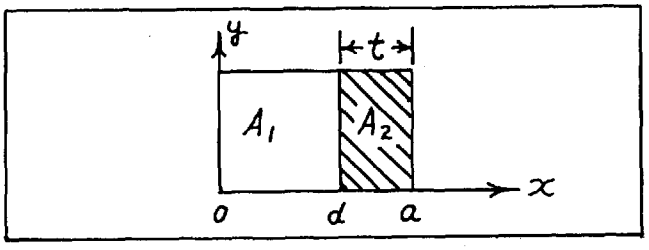


Fig. 1.

When the rectangular guide illustrated in fig. 1 is uniformely filled with a lossless dielectric of dielectric constant K the wavelength of the H_{01} mode is given by

$$\lambda_g = \frac{\lambda_0}{\sqrt{K - \left(\frac{\lambda_0}{2a}\right)^2}}$$

where λ_0 is the free space wavelength. If $K-1 > \left(\frac{\lambda_0}{2a}\right)^2$ then λ_g is less than λ_0. For the empty guide λ_g is greater than λ_0. It is obvious that for some critical thickness t of dieletric the guide wavelength will be equal to the free space wavelength. At this thickness the wave-number k_1 in the x -direction in the section A_1 is zero. The corresponding wave number l_1 in the section A_2 is given by

$$l_1 = \sqrt{K-1}\, k_0 .$$

This relation is obtained by putting γ_1^2 equal to $-k_0^2$ in the eigenvalue equation

$$\gamma_1^2 = l_1^2 - K k_0^2 .$$

The solution of Maxwell's equations takes the following form for the H_{01} mode.

In A_1 –

$$E_y = x\, e^{-\gamma_1 z},$$
$$j\omega\mu H_x = \gamma_1 x\, e^{-\gamma_1 z},$$
$$j\omega\mu H_z = e^{-\gamma_1 z},$$

while in A_2

$$E_y = A \sin l_1 (a-x)\, e^{-\gamma_1 z},$$
$$j\omega\mu H_x = A\gamma_1 \sin l_1 (a-x)\, e^{-\gamma_1 z},$$
$$j\omega\mu H_z = -A l_1 \cos l_1 (a-x)\, e^{-\gamma_1 z}.$$

At $x=d$ the tangential field components must be continuous and hence

$$d = A \sin l_1 t,$$
$$1 = -A l_1 \cos l_1 t.$$

By eliminating the constant A the following transcendental equation is obtained, $\tan l_1 t = -l_1 d$. This equation together with the previously given relation for l_1 determines the critical thickness for which $\lambda_g = \lambda_o$. This later equation could have been obtained by carrying out a limiting process on the relation

$$k_1 \tan l_1 t = -l_1 \tan k_1 d$$

given in chapter 4, section 1.

Thus $$\tan l_1 t = \lim_{k_1 \to 0} -l_1 d \, \frac{\tan k_1 d}{k_1 d} = -l_1 d.$$

For a thickness of dielectric greater than this critical thickness k_1 is imaginary and $\lambda_g < \lambda_o$. The maximum value of E_y occurs in the dielectric since the electric field distribution in A_1 is given by $\sinh |k_1| x$ and is concave upwards. At the critical thickness the electric field distribution in A_1 varies linearly with x .

(2) Symmetrical Dielectric Strip:

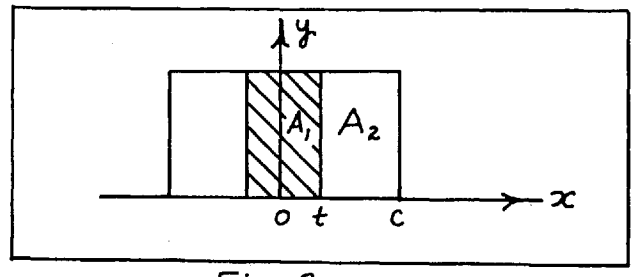


Fig. 2.

When the guide wavelength is equal to the free space wavelength k_1 is zero and l_1 is given by the same expression as for the asymmetrical strip, thus $l_1 = \sqrt{K-1}\, k_0$. In the dielectric filled section A_1 the fields are

$$E_y = \cos l_1 x\, e^{-\gamma_1 z},$$
$$j\omega\mu H_x = \gamma_1 \cos l_1 x\, e^{-\gamma_1 z},$$
$$j\omega\mu H_z = -l_1 \sin l_1 x\, e^{-\gamma_1 z},$$

while in section A_2 they are given by

$$E_y = A(c-x)\, e^{-\gamma_1 z},$$
$$j\omega\mu H_x = A\gamma_1 (c-x)\, e^{-\gamma_1 z},$$
$$j\omega\mu H_z = -A\, e^{-\gamma_1 z}.$$

Equating E_y and H_z at $x=t$ gives

$$\cos l_1 t = Ad$$
$$l_1 \sin l_1 t = A$$

and hence $\cot l_1 t = d$ where $d = c-t$.

The critical thickness for which λ_g equals λ_o is determined by the solution of

$$\cot \sqrt{K-1}\, k_0 t = d.$$

As before this relation could have been obtained from the more general result given in chapter 4, section 2, by a limiting process.

If two dielectric strips are placed along the side of the guide as in fig. 3.

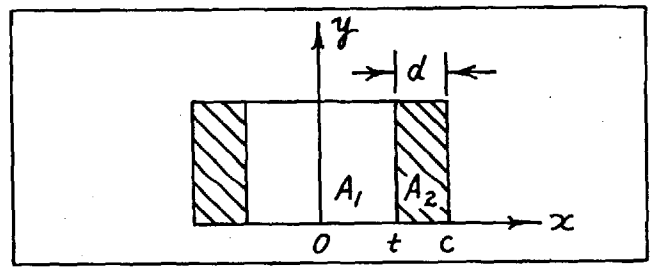


Fig. 3.

then for some critical thickness d the guide wavelength is equal to the free space wavelength and the wave existing in the region A_1 is a pure T.E.M. wave. This is the case when the elementary waves making up the H_{01} mode strike the dielectric-air boundary at a grazing angle. (Ref. 1).

The fields in A_1 are given by

$$E_y = e^{-\gamma_1 z},$$
$$j\omega\mu H_x = \gamma_1 e^{-\gamma_1 z},$$
$$H_z = 0,$$

while in A_2 they are

$$E_y = A \sin l_1(c-x) e^{-\gamma_1 z},$$
$$j\omega\mu H_x = \gamma_1 A \sin l_1(c-x) e^{-\gamma_1 z},$$
$$j\omega\mu H_z = -A l_1 \cos l_1(c-x) e^{-\gamma_1 z}.$$

At $x = t$, H_z must equal zero and hence

$\cos l_1 d = 0$ or $l_1 d = \frac{\pi}{2}$. After substituing for l_1 the following equation is obtained for the critical thickness d,

$$d = \frac{\pi}{2k_0\sqrt{K-1}} = \frac{\lambda_0}{4\sqrt{K-1}}.$$

For values of d greater than this the electric field distribution

reaches a maximum in the dielectric because the distribution in section A_1 is given by $\cosh l_1 x$ and is concave upward.

It is impossible to have the condition of a T.E.M. wave existing in the dielectric strip placed in the centre of the guide since this implies that l_1 is zero and k_1 is imaginary and such a solution is impossible. For a solution to exist at least one of the transverse wave numbers must be real.

(3) Asymmetrical E-Plane Dielectric Strip:

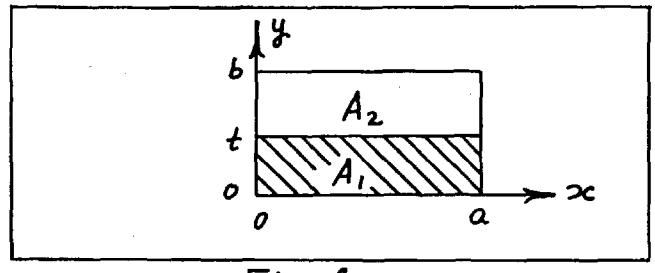


Fig. 4.

It was shown in chapter 5 that the fields existing in the partially filled guide illustrated in figure 4 are derivable from a Hertzian vector $\vec{\pi}$ directed in the y direction through the following equations

$$\vec{H} = j\omega\epsilon_0 K \nabla \times \vec{\pi},$$

$$\vec{E} = \nabla\nabla\cdot\vec{\pi} + K k_0^2 \vec{\pi}.$$

The Hertzian vector $\vec{\pi}$ is taken as

$$\vec{\pi} = \vec{i}_y \cos k_y y \sin k_x x \, e^{-\gamma_1 z}.$$

In the section A_1 let the wave number along the y axis be l_1 for the first propagating mode. The electric and magnetic field components are then

$$H_x = j\omega\epsilon_0 K \gamma_1 \sin k_x x \cos l_1 y \, e^{-\gamma_1 z},$$

$$H_y = 0,$$

$$H_z = j\omega\epsilon_0 K k_x \cos k_x x \cos l_1 y \, e^{-\gamma_1 z},$$

$$E_x = -k_x l_1 \cos k_x x \sin l_1 y \, e^{-\gamma_1 z},$$

$$E_y = (K k_0^2 - l_1^2) \sin k_x x \cos l_1 y \, e^{-\gamma_1 z},$$

$$E_z = \gamma_1 l_1 \sin k_x x \sin l_1 y \, e^{-\gamma_1 z},$$

where $k_x = \frac{\pi}{a}$.

Since λ_g is taken equal to λ_0 it follows that $k_y^2 + k_x^2 = 0$ in the region A_2. Thus the wave number in the y direction in A_2 is $j\frac{\pi}{a}$. The fields are derivable from the following Hertzian vector

$$\vec{\pi} = C \vec{i}_y \sin k_x x \cosh \tfrac{\pi}{a}(b-y) \, e^{-\gamma_1 z}.$$

The field components are

$$H_x = j\omega\epsilon_0 C \gamma_1 \sin k_x x \cosh \tfrac{\pi}{a}(b-y) \, e^{-\gamma_1 z},$$

$$H_y = 0,$$

$$H_z = j\omega\epsilon_0 C k_x \cos k_x x \cosh \tfrac{\pi}{a}(b-y) \, e^{-\gamma_1 z},$$

$$E_x = C k_x \tfrac{\pi}{a} \cos k_x x \sinh \tfrac{\pi}{a}(b-y) \, e^{-\gamma_1 z},$$

$$E_y = C (k_0^2 + \tfrac{\pi^2}{a^2}) \sin k_x x \cosh \tfrac{\pi}{a}(b-y) \, e^{-\gamma_1 z},$$

$$E_z = -C \gamma_1 \tfrac{\pi}{a} \sin k_x x \sinh \tfrac{\pi}{a}(b-y) \, e^{-\gamma_1 z}.$$

From the continuity conditions for the tangential field components the following transcendental equation is obtained,

$$K \tfrac{\pi}{a} \tanh \tfrac{\pi}{a} d = l_1 \tan l_1 t \qquad \text{where } d = b - t.$$

Now $\beta_g^2 = k_0^2 = K k_0^2 - k_x^2 - l_1^2$ and consequently

$l_1 = \left(\overline{K-1} \, k_0^2 - \frac{\pi^2}{a^2} \right)^{1/2}$. These equations can be solved for the critical thickness at which the guide wavelength equals free space wavelength. For a dielectric constant of 2.56, and a free space wavelength of 3.14 cm., this thickness is approximately 1/3 the guide height for standard 1/2" by 1" British waveguide.

When the wavelength in the partially filled guide is equal to the wavelength of an H_{01} mode in the empty guide the y -axis wave number in section A_2 must be zero. The fields in section A_2 are then derivable from the following Hertzian vector

$$\vec{\pi} = C \hat{i}_y \sin k_x x \, e^{-\gamma_1 z},$$

thus

$$H_x = j\omega\epsilon_0 C \gamma_1 \sin k_x x \, e^{-\gamma_1 z},$$

$$H_y = 0,$$

$$H_z = j\omega\epsilon_0 k_x \cos k_x x \, e^{-\gamma_1 z},$$

$$E_x = 0,$$

$$E_y = C k_0^2 \sin k_x x \, e^{-\gamma_1 z},$$

$$E_z = 0.$$

The continuity of tangential components at $y = t$ gives

$$K \cos l_1 t = C,$$

$$\sin l_1 t = 0 \quad \text{or} \quad l_1 t = \pi.$$

Since k_1 is zero l_1 is given by $\sqrt{K-1}\, k_0$. The critical thickness is given by $t = \frac{\lambda_0}{2\sqrt{K-1}}$ as obtained by replacing $\frac{2\pi}{\lambda_0}$ for k_0 . The wave in the section A_2 or empty part is a pure H_{01} mode while in the dielectric filled section it is a longitudinal section E wave. For a rectangular guide of dimension 2.54 cms. by 1.27 cms. this critical thickness is $\lambda_0/2.50$ for a dielectric with a relative permitivitty of 2.56. Thus only for wavelengths less than 3.17 cm. can a mode propagate with a wavelength equal to the wavelength of an H_{01} mode in the empty guide. This mode is actually the second propagating mode since one mode with an imaginary wave number in section A_2 exists.

Appendix 5.

Theoretical Solution for E- Plane Dielectric Step.

For a rectangular guide partially filled as in figure 1 with a lossless dielectric of relative dielectric constant K two independent solutions of Maxwell's equations exist. For one set H_y is zero and the modes are called longitudinal section E waves. For the other set E_y is zero and the modes are referred to as longitudinal section H waves.

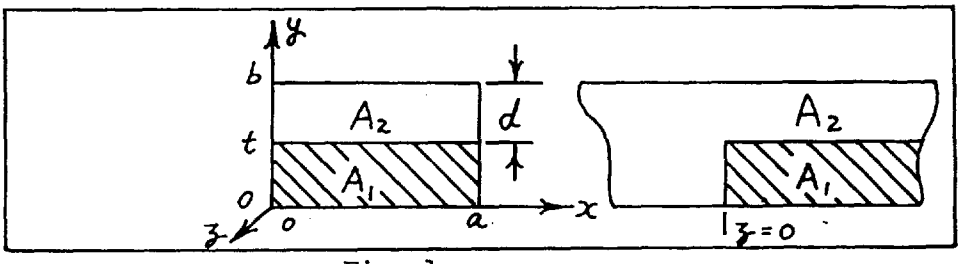


Fig. 1.

The L.S.E. waves are derivable from an electric type Hertzian vector $\overrightarrow{\pi}_1$ directed along the y-axis while the L.S.H. waves are derivable from a magnetic type Hertzian vector $\overrightarrow{\pi}_2$ directed along the y-axis. (See chapter 5, section 1.) . The various field components are given by the following expressions -

$$E_x = \frac{\partial^2 \pi_1}{\partial x \partial y} + j\omega\mu \frac{\partial \pi_2}{\partial z}, \qquad H_x = -j\omega\epsilon_0 K \frac{\partial \pi_1}{\partial z} + \frac{\partial^2 \pi_2}{\partial x \partial y},$$

$$E_y = \frac{\partial^2 \pi_1}{\partial y^2} + K k_0^2 \pi_1, \qquad H_y = \frac{\partial^2 \pi_2}{\partial y^2} + K k_0^2 \pi_2,$$

$$E_z = \frac{\partial^2 \pi_1}{\partial z \partial y} - j\omega\mu \frac{\partial \pi_2}{\partial x}, \qquad H_z = j\omega\epsilon_0 K \frac{\partial \pi_1}{\partial x} + \frac{\partial^2 \pi_2}{\partial z \partial y},$$

where both π_1 and π_2 satisfy the following wave equation

$$\nabla^2 \pi_i + K(y) k_0^2 \pi_i = 0,$$

with $K(y)$ equal to K in A_1, and unity in A_2.

At the junction between the empty and partially filled guide both types of waves must be included in order to satisfy all boundary conditions. It is easily verified by taking the curl of the transverse electric and magnetic field in the aperture plane that H_z and KE_z are continuous respectively if the transverse field components are. The appropriate forms for the Hertzian vectors $\vec{\pi}_1$ and $\vec{\pi}_2$ are found by a consideration of the boundary conditions that the fields derived from them must satisfy. In the following analysis variation of the field components with x will be restricted to either $\sin k_x x$ or $\cos k_x x$ where $k_x = \frac{\pi}{a}$.

With an H_{01} wave incident on the step the appropriate forms of π_1 and π_2 in the input guide are -

$$\pi_1 = (\phi_0 e^{-\Gamma_0 z} + R\phi_0 e^{\Gamma_0 z}) \sin k_x x + \sum_1^\infty A_n \phi_n \sin k_x x \, e^{\Gamma_n z},$$

$$\pi_2 = \sum_1^\infty B_n \psi_n \cos k_x x \, e^{\Gamma_n z},$$

where the functions ϕ_n and ψ_n are given by

$$\phi_0 = \sqrt{\frac{1}{b}}, \quad \phi_n = \sqrt{\frac{2}{b}} \cos \frac{n\pi}{b} y, \quad \psi_n = \sqrt{\frac{2}{b}} \sin \frac{n\pi}{b} y,$$

and $\Gamma_n^2 = \left(\frac{n\pi}{b}\right)^2 + k_x^2 - k_0^2$.

In the output guide it is found by matching the tangential fields at $y=t$ that suitable forms for π_1 and π_2 are -

$$\pi_1 = \sum_{m=1}^{\infty} C_m \frac{F_m(y)}{K(y)} \sin k_x x \, e^{-\gamma_m z},$$

where $$\frac{F_m(y)}{K(y)} = \frac{1}{\sqrt{P_m}} \begin{cases} \cos l_m y, & 0 \le y \le t, \\ K \dfrac{\cos l_m t}{\cos k_m d} \cos k_m (b-y), & t \le y \le b, \end{cases}$$

with P_m a normalization constant determined so that

$$\int_0^b \frac{F_m^2(y)}{K(y)} \, dy = 1.$$

The propagation constants γ_m are given by

$$\gamma_m^2 = l_m^2 + k_x^2 - K k_0^2 = k_m^2 + k_x^2 - k_0^2 \qquad \text{where}$$

$$l_m \tan l_m t = -K k_m \tan k_m d \qquad \text{and} \qquad d = b - t.$$

$$\pi_2 = \sum_{m=1}^{\infty} D_m W_m(y) \cos k_x x \, e^{-\beta_m z} \qquad \text{where the}$$

functions $W_m(y)$ are given by

$$W_m(y) = \frac{1}{\sqrt{Q_m}} \begin{cases} \sin h_m y, & 0 \le y \le t, \\ \sin h_m t \csc g_m d \sin g_m (b-y), & t \le y \le b, \end{cases}$$

and Q_m is a normalization constant such that

$$\int_0^b W_m^2(y) \, dy = 1.$$

The propagation constants β_m are given by

$$\beta_m^2 = h_m^2 + k_x^2 - K k_0^2 = g_m^2 + k_x^2 - k_0^2 \qquad \text{and}$$

$$g_m \tan h_m t = -h_m \tan g_m d.$$

Since π_1 and π_2 are not continuous in the z direction across the aperture plane $z = 0$ it is found to be more convenient to relate the

fields to the total electric and magnetic field in the y direction at the aperture. This is equivalent to specifying π_1 and π_2 since π_1 and π_2 can be uniquely determined from E_y and H_y respectively. The transverse field components are derived from π_1 and π_2 by means of the previously given expressions. Equating the transverse fields at the aperture gives -

$$E_x = k_x \sum_1^\infty A_n \frac{d\phi_n}{dy} + j\omega\mu \sum_1^\infty B_n \Gamma_n \psi_n =$$

$$k_x \sum_1^\infty C_m [K(y)]^{-1} \frac{dF_m}{dy} - j\omega\mu \sum_1^\infty D_m B_m W_m ,$$

$$E_y = k_0^2(1+R)\phi_0 + \sum_1^\infty A_n(k_x^2-\Gamma_n^2)\phi_n = \sum_1^\infty C_m(k_x^2-\gamma_m^2)\frac{F_m(y)}{K(y)} = G_1(y),$$

$$H_x = j\omega\epsilon_0\left[(1-R)\Gamma_0\phi_0 - \sum_1^\infty A_n\Gamma_n\phi_n\right] - k_x\sum_1^\infty B_n\frac{d\psi_n}{dy} =$$

$$j\omega\epsilon_0 \sum_1^\infty C_m\gamma_m F_m - k_x\sum_1^\infty D_m\frac{dW_m}{dy},$$

$$H_y = \sum_1^\infty B_n(k_x^2-\Gamma_n^2)\psi_n = \sum_1^\infty D_m(k_x^2-B_m^2)W_m = (j\omega\mu)^{-1}G_2(y),$$

where the common functions of x appearing on both sides of the equations have been cancelled out. G_1 and G_2 are complex functions of the real variable y and all the unknown coefficients can be determined from them by means of the orthogonality relations given in chapter 2, section 1.

Thus $(1+R)k_0^2 = \int_0^b G_1\phi_0\,dy$, $A_n(k_x^2-\Gamma_n^2) = \int_0^b G_1\phi_n\,dy$,

$$C_m(k_x^2-\gamma_m^2) = \int_0^b G_1F_m\,dy,\quad j\omega\mu B_n(k_x^2-\Gamma_n^2) = \int_0^b G_2\psi_n\,dy,\quad j\omega\mu D_m(k_x^2-B_m^2) = \int_0^b G_2W_m\,dy.$$

Continuity of E_y and H_y is obvious since these components are equal to

G_1 and $(j\omega\mu)^{-1} G_2$ respectively at the aperture plane. Substituting the above integral expressions for the unknown coefficients and introducing $(1+R)$ it is seen that the continuity equations for H_x and E_x can be written as -

$$H_x = j\omega\epsilon_0 \left[\frac{1-R}{1+R}\frac{\Gamma_0}{k_0^2}\phi_0 \int_0^b G_1\phi_0\,dy - \sum_1^\infty \frac{\Gamma_n\phi_n}{k_x^2-\Gamma_n^2}\int_0^b G_1\phi_n\,dy\right] - \frac{k_x}{j\omega\mu}\sum_1^\infty \frac{\psi_n'}{k_x^2-\Gamma_n^2}\int_0^b G_2\psi_n\,dy =$$

$$j\omega\epsilon_0 \sum_1^\infty \frac{\gamma_m}{k_x^2-\gamma_m^2} F_m \int_0^b G_1 F_m\,dy - \frac{k_x}{j\omega\mu}\sum_1^\infty \frac{W_m'}{k_x^2-\beta_m^2}\int_0^b G_2 W_m\,dy, \quad (1)$$

$$E_x = k_x \sum_1^\infty \frac{\phi_n'}{k_x^2-\Gamma_n^2}\int_0^b G_1\phi_n\,dy + \sum_1^\infty \frac{\Gamma_n\psi_n}{k_x^2-\Gamma_n^2}\int_0^b G_2\psi_n\,dy =$$

$$k_x \sum_1^\infty \frac{\kappa^{-1}(y)}{k_x^2-\gamma_m^2} F_m' \int_0^b G_1 F_m\,dy - \sum_1^\infty \frac{\beta_m W_m}{k_x^2-\beta_m^2}\int_0^b G_2 W_m\,dy, \quad (2)$$

where the prime (') indicates $\frac{d}{dy}$.

The fields derived from π_1 and π_2 are independent solutions of Maxwell's equations and hence the general orthogonality relations applicable to a lossless structure given in chapter 2 section 1, yields -

$$\int_a \left[(E_{x_1}^* + E_{x_2}^*)H_{y_2} - E_{y_1}^*(H_{x_1} + H_{x_2})\right] da =$$

$$\int_a E_{x_2}^* H_y\,da - \int_a E_y^* H_{x_1}\,da, \quad (3)$$

$$\text{and} \quad \int_a E_{x_1}^* H_y\,da = \int_a E_y^* H_{x_2}\,da, \quad (4)$$

The subscripts '1' and '2' refer to the partial fields derived from π_1 and π_2 respectively and the star donates the conjugate complex field. In particular these relations hold between the field components at the aperture. Threfore integrating the cross product of the total transverse conjugate electric field with the total transverse magnetic field over

the aperture gives, $\frac{1-R}{1+R}\Gamma_0\int_0^b G_1^*\phi_0\,dy\int_0^b G_1\phi_0\,dy =$

$$k_0^2\left\{\sum_1^\infty \frac{\Gamma_n}{k_x^2-\Gamma_n^2}\int_0^b G_1^*\phi_n\,dy\int_0^b G_1\phi_n\,dy + \sum_1^\infty \frac{\gamma_m}{k_x^2-\gamma_m^2}\int_0^b G_1^*F_m\,dy\int_0^b G_1F_m\,dy\right\} -$$

$$\left\{\sum_1^\infty \frac{\Gamma_n}{k_x^2-\Gamma_n^2}\int_0^b G_2^*\psi_n\,dy\int_0^b G_2\psi_n\,dy + \sum_1^\infty \frac{\beta_m}{k_x^2-\beta_m^2}\int_0^b G_2^*W_m\,dy\int_0^b G_2W_m\,dy\right\}. \quad (5)$$

This expression clearly shows that the input admittance is equal to the power transmitted past the aperture plus the difference between the mean stored magnetic and electric energy in the evanescent modes. It is readily shown that highly evanescent L.S.E. waves store an excess of electric energy while L.S.H. waves store an excess of magnetic energy.

For modes that are close to propagating i.e. β_m^2 and γ_m^2 less than k_x^2, this characteristic is reversed.

Integrating the product of the conjugate electric field in the x direction with $(j\omega\mu)^{-1}G_2$ over the aperture and using relation (4) gives

$$\sum_1^\infty \frac{\Gamma_n}{k_x^2-\Gamma_n^2}\int_0^b G_2^*\psi_n\,dy\int_0^b G_2\psi_n\,dy + \sum_1^\infty \frac{\beta_m}{k_x^2-\beta_m^2}\int_0^b G_2^*W_m\,dy\int_0^b G_2W_m\,dy =$$

$$\sum_1^\infty \frac{k_x}{k_x^2-\Gamma_n^2}\int_0^b G_1^*\psi_n'\,dy\int_0^b G_2\psi_n\,dy - \sum_1^\infty \frac{k_x}{k_x^2-\beta_m^2}\int_0^b G_1^*W_m'\,dy\int_0^b G_2W_m\,dy. \quad (6)$$

Equation (6) shows that if the functions ψ_n and W_n are almost identical then the quadratic expression involving G_2 in equation(5) will be small since it is given by the difference of two quantities which are almost identical. For small values of K or t/b, ψ_n and W_n are indeed almost identical and a good approximation to the input admittance can be obtained by taking G_2 identically zero. For the symmetrically positioned E-plane step this approximation is better

still. The functions ψ_1 and W_1 are plotted in figure 2 for the particular example worked out in detail in chapter 5. W_1 is seen to be almost identical with ψ_1 for this case. For values of $n>1$, W_n approaches ψ_n even closer.

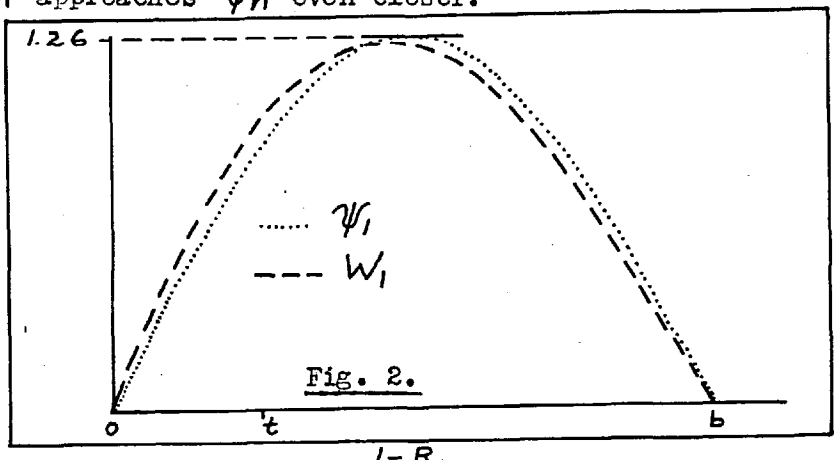


Fig. 2.

It can be shown that $\frac{1-R}{1+R}$ is stationary with respect to arbitrary variations of G_1^* and G_2^* that satisfy equations (4) and (6). Consequently it follows that a first order approximation to G_1^* and G_2^* will give a second order approximation to $\frac{1-R}{1+R}$. An approximation to G_1 and G_2 is most readily obtained from equations (1) and (2). Approximate G_1 by $\sum_{n=0}^{N} A_n \varphi_n$ and G_2 by $\sum_{n=1}^{M} B_n \psi_n$. There is no loss in generality by taking A_0 equal to unity since all the other coefficients can be divided by A_0. Multiplying equation (1) by φ_n for $n=1,\cdots N$ and integrating over y gives the following set of equations to be solved -

$$\sum_{n=1}^{N}\left\{k_0^2\left(\frac{\Gamma_n}{k_x^2-\Gamma_n^2}A_n+\sum_{s=0}^{N}A_s\sum_{m=1}^{\infty}\frac{\gamma_m}{k_x^2-\gamma_m^2}f_{nm}f_{sm}\right)=\right.$$

$$\left.k_x\left(\frac{n\pi/b}{k_x^2-\Gamma_n^2}B_n-\sum_{s=1}^{M}B_s\sum_{m=1}^{\infty}\frac{w'_{nm}w_{sm}}{k_x^2-\beta_m^2}\right)\right\}, \qquad (7)$$

where $$\int_0^b \varphi_n F_m \, dy = f_{nm},$$

$$\int_0^b \psi_n W_m \, dy = w_{nm},$$

$$\int_0^b \psi_n \frac{d W_m}{dy} \, dy = w'_{nm}.$$

Similarly multiplying equation (2) by ψ_n for $n = 1, 2 \cdots M$ gives the following set of equations to be solved -

$$\sum_{n=1}^{M} \left\{ k_x \left(\frac{n\pi/b}{k_x^2 - \Gamma_n^2} A_n - \sum_{s=0}^{N} A_s \sum_{m=1}^{\infty} \frac{f'_{nm} f_{sm}}{k_x^2 - \gamma_m^2} \right) = \right.$$

$$\left. \left(\frac{\Gamma_n}{k_x^2 - \Gamma_n^2} B_n + \sum_{s=1}^{M} B_s \sum_{m=1}^{\infty} \frac{\beta_m}{k_x^2 - \beta_m^2} w_{nm} w_{sm} \right) \right\} \qquad (8)$$

where $$- \int_0^b \psi_n K^{-1}(y) \frac{d F_m}{dy} \, dy = f'_{nm}.$$

The set of equations (7) and (8) together give $N + M$ equations which when solved give the $N + M$ unknowns A_n and B_n. These approximate values for G_1 and G_2 may then be used in equation (5) to get a second order approximation to the input admittance $\frac{1-R}{1+R}$. Although the summations over m are not terminated the matrix elements f_{nm}, f'_{nm}, w_{nm}, and w'_{nm} converge to zero quite rapidly for $m > n$.

Bibliography

1.1. Saxon, D. – "Notes on lectures by J.Schwinger". Unpublished.

1.2. Lewin, L. – "Advanced theory of waveguides". Iliffe & Sons,Ltd., London.

1.3. Miles, J.W. – "The equivalent circuit of a plane discontinuity in a cylindrical waveguide". Proc. I.R.E. V34, #10, pp.728-742.

1.4. Marcuwitz,N. – "Waveguide Handbook". R.L.S. Vol. 10. McGraw Hill.

1.5. Montgomery, Dicke, Purcell – "Principles of microwave circuits". R.L.S. Vol.8, ibid.

1.6. Stratton, J. – "Electromagnetic theory" McGraw Hill.

1.7. Ramo and Whinney – "Fields and Waves in Modern radio". Wiley and Sons, Ltd.

2.1-1. Adler, R.B. – "Properties of guided waves on inhomogenous cylindrical structures". M.I.T. Report # 102, May 1949.

2.2-1. Livens, G.H. – "Variational principle for the electromagnetic field". Phil. Trans of the Roy.Soc. of London, V220, June 1920.

2.2-2. Pipes. – "Applied mathematics for engineers and physicists". McGraw Hill.

2.5-1. Chambers,G. – "Compilation of the propagation constants of an inhomogenously filled waveguide". Brit.Journ. of Appl.Phys., V.3. #1, Jan. 1952.

3.1.-1. Kharadli – "An investigation of certain types of artificial dielectrics". Univ. of London, Ph.D. Thesis, 1953.

4.4.-1. Klopfenstein,R.W. - "Impedance matching with transformer sections".
R.C.A. Review and Tech.Journ. V14 1, Mar. 1953.

5.1.-1. Pincherle,L. - "Electromagnetic waves in metal tubes filled longitudinally with two dielectrics".
The Phys.Rev. V66, 1944, p.118.

5.1-2. Van Bladel,J.- "Field expandibility in normal modes for a multilayered rectangular or circular waveguide".
Journ. Franklin Inst. V253, 1952, #4, p.313.

6.1-1. Southworth - "Principles and applications of waveguide transmission".
D. Van-Nostrand, 1950.

6.1-2. Slater - "Microwave transmission".
McGraw Hill.

6.1-3. Fubini and Rockett - "Bandwidth of quarter-wave sections".
Electronics, Oct.1952, p.138.

6.1-4. Collin and Brown - "Properties of a matching system using two quarter-wave transformers".
To be published in Wireless Engineer.

A1.1. Weisfloch - Hochfreq. u. electro. Vol. 60, 1942,p.67.

A1.2. Barlow and Cullen- "Microwave Measurements". (Section on Feenberg's method).

A1.3. Slater - "Microwave electronics".
D. Van-Nostrand Co. Ltd.

A2.1. Churchill - "Modern Operational Mathematics in Engineering".
Chap. 9, McGraw Hill.

A3.1. Weinstock - "Calculus of Variations". Ch.9.
McGraw Hill.

A3.2. Courant and Hilbert - "Methoden der Mathematischen.Physick".
Julius Springer, Berlin, 1931.

See Also :

Chambers,G. - "An approximate method for the calculation of propagation constants for inhomogenously filled waveguides".
To be published.

A4.1. Woodward,Alice M.- "Wireless Engineer, July, 1947.